

University of South Bohemia in České Budějovice
Faculty of Science

**Characterization of metabolic changes in hemocytes during
the immune response in *D. melanogaster***

Master thesis

Bc. Gabriela Krejčová

Supervised by Mgr. Adam Bajgar, PhD

České Budějovice, 2018

Krejčová, G., 2018: Characterization of metabolic changes in hemocytes during the immune response in *D. melanogaster*. Mgr. thesis, in English. - 97 p., Faculty of Science, University of South Bohemia, České Budějovice, Czech Republic.

ANNOTATION

The aim of this thesis is to characterize metabolic changes in hemocytes during the immune response in *D. melanogaster* using *in vivo* markers as well as by measuring gene expression. The impact of the transcription factor HIF1 α on the gene expression of glycolytic enzymes and its impact on the systemic metabolism was evaluated. The importance of HIF1 α and LDH in the process of fighting against *S. pneumoniae* infection was tested as well.

DECLARATION

I hereby declare that I worked on this master thesis on my own and used only the resources mentioned in the bibliography.

I hereby declare that, in accordance with Article 47b of Act No. 111/1998 in the valid wording, I agree with the publication of my master thesis, in full to be kept in the Faculty of Science archive, in electronic form in publicly accessible part of the STAG database operated by the University of South Bohemia in České Budějovice accessible through its web pages.

Further, I agree to the electronic publication of the comments of my supervisor and thesis opponents and the record of the proceedings and results of the thesis defense in accordance with aforementioned Act No. 111/1998. I also agree to the comparison of the text of my thesis with the Theses.cz thesis database operated by the National Registry of University Theses and a plagiarism detection system.

České Budějovice, 18. 4. 2018

.....

Bc. Gabriela Krejčová

ACKNOWLEDGEMENTS

First of all, I would like to express my deepest gratitude to Dr. Adam Bajgar for supervising this thesis, for his friendly approach, exceptional empathy, help, time and effort he invested in my education. He sincerely shared my happiness from work well done and he was always there for me during tough times. I am thankful for his infinite patience, for sharing his knowledge and for his realistic view of research. I highly appreciate everything he has done for me and I have been amazingly fortunate to be supervised by him.

I am indebted to doc. Tomáš Doležal for giving me the opportunity to work in his laboratory, for his advice, thought-provoking debates, willingness to discuss my results and for reading and commenting on this thesis.

I would like to thank to all my lab mates and to other student members of the neighbouring laboratories for creating kind and friendly environment, especially to Pablo, who had to face many random questions every time he walked in our lab and showed me how to do things more easily.

I have greatly benefited from the Department of Medical Biology where I was sorting my samples and from the Institute of Entomology where my confocal images were captured.

Many thanks to my family for providing me with their endless support and love throughout my years of study. This accomplishment would have not been possible without them.

Special thanks to Petr for his interest, support and unbiased thoughts. Thank you for listening and taking care of me.

ABBREVIATIONS

2-NBDG 2-(N-(7-Nitrobenz-2-oxa-1,3-diazol-4-yl)Amino)-2-Deoxyglucose

Acetyl-CoA Acetyl coenzyme A

Act Actin

AMPs Antimicrobial peptides

ATP Adenosin triphosphate

BSA Bovine serum albumin

CFUs Colony forming units

Cis Citrate synthase

CG10219 *Drosophila* homolog of succinate dehydrogenase

CRE Cyclic AMP responsive element

CTL Cytotoxic T lymphocyte

DAMPs Damage associated molecular patterns

DEPC Diethyl pyrocarbonate

d/e/i/nNOS *Drosophila*/endothelial/inducible/neuronal nitric oxide synthase

Eno Enolase

ETC Electron transport chain

FACS Fluorescence activated cell sorting

Fga Fatiga (*Drosophila* homolog of prolyl hydroxylase dehydrogenase)

Gapdh1 Glyceraldehyd 3 phosphate dehydrogenase A

GFP Green fluorescent protein

Hex Hexokinase A

HIF1 α/β Hypoxia inducible factor 1 α/β

HDAC Histone deacetylase

HDMs Histone demethylases

Hml Hemolectin

HMTs Histone methyltransferases

HRE Hypoxia response element

Igfbp Insulin-like growth factor-binding protein

Imd Immune deficiency

IFN γ Interferone γ

ImpL2 Ecdysone-inducible gene L2

ImpL3 Ecdysone-inducible gene L3

LDH Lactate dehydrogenase
LPS Lipopolysaccharide
NO Nitric oxide
ODD Oxygen-dependent degradation domain
OXPHOS Oxidative phosphorylation
PAMPs Pathogen associated molecular patterns
PBS Phosphate buffered saline
Pfk Phosphofructokinase
Pgi Phosphoglucose isomerase
PHDs Prolyl hydroxylase domain proteins
PPP Pentose phosphate pathway
PRRs Pathogen recognition receptors
RNAi Ribonucleic acid interference
ROS Reactive oxygen species
Rp49 Ribosomal protein L32
Scs α Succinyl coenzyme A synthetase α subunit
Sima Similar (*Drosophila* homolog of HIF1 α)
SL2 Schneider cells, line 2
Sp *Streptococcus pneumoniae*
TCA Tricarboxylic acid cycle
TET Ten-eleven translocation
Tgo Tango (*Drosophila* homolog of HIF1 β)
Th1/2 Type 1/2 T helper
TLRs Toll-like receptors
Tpi Triose phosphate isomerase
VHL Von Hippel-Lindau
X-gal 5-bromo-4-chloro-3-indolyl β -D-galactopyranoside

CONTENT

1. INTRODUCTION.....	1
1.1. General introduction.....	1
1.2. Energetic demands of the immune system.....	2
1.3. Characteristic progress of immune response.....	3
1.4. Macrophage function in the immune system	4
1.5. Metabolic switch in immune cells during immune response	6
1.6. Metabolic reprogramming is crucial for activation of macrophages	7
1.7. The role of HIF1 α in metabolic reprogramming.....	8
1.8. Metabolic intermediates play a role in epigenetic landscape of macrophages	10
1.9. Arginin plays a crucial role in macrophage polarization	11
1.10. M1/M2 macrophage balance in disease	14
1.11. Macrophage polarization in cancer	15
1.12. Immune system of <i>D. melanogaster</i>	15
1.13. Model organism <i>D. melanogaster</i>	16
1.14. Selfish immune system theory	19
2. AIMS OF THE THESIS	21
3. MATERIALS AND METHODS	22
3.1. <i>Drosophila</i> techniques.....	22
3.2. <i>Drosophila melanogaster</i> strains	23
3.3. Crosses	24
3.4. Infections.....	27
3.5. Colony forming units (CFUs)	29
3.6. Metabolites measurement.....	30
3.7. X-gal staining.....	32
3.8. Fluorescence-activated cell sorting (FACS).....	32
3.9. Isolation of RNA	36
3.10. Reverse transcription.....	36
3.11. qPCR	36
3.12. NBDG	38
3.13. Confocal microscopy	38
3.14. Statistics and data processing.....	39
4. RESULTS	40

4.1. Activated macrophages show temporarily increased expression of glycolytic enzymes.....	40
4.2. Metabolic changes of <i>Drosophila</i> macrophages <i>in vivo/in situ</i>	43
4.3. Transcription factor HIF1 α plays an important role in macrophage polarization..	47
4.4. Enzyme lactate dehydrogenase and HIF1 α protein are necessary for effective elimination of bacterial infection	53
4.5. The regulation of ImpL2 gene in immune response in <i>D. melanogaster</i>	57
5. DISCUSSION	60
5.1. Activated macrophages show temporarily increased expression of glycolytic enzymes.....	61
5.2. Metabolic changes of <i>Drosophila</i> macrophages <i>in vivo/in situ</i>	63
5.3. Transcription factor HIF1 α plays an important role in macrophage polarization..	64
5.4. Enzyme lactate dehydrogenase and HIF1 α protein are necessary for effective elimination of bacterial infection	66
5.5. The regulation of ImpL2 gene in immune response in <i>D. melanogaster</i>	67
6. CONCLUSION	69
7. SUPPLEMENTARY DATA	70
7.1. Introduction	70
7.2. Materials and methods	71
7.3. Results.....	72
7.3.1. Gene expression of HIF1 α isoforms in macrophages of <i>D. melanogaster</i> : Efficiency of Sima KK RNAi.....	72
7.3.2. Efficiency of Sima TRiP RNAi and ImpL3 RNAi	81
8. REFERENCES.....	84

1. INTRODUCTION

1.1. General introduction

The aim of this thesis is to elucidate whether the immune cells of model organism *Drosophila melanogaster* exhibit similar metabolic shift as it was described in mammalian system. If this metabolic switch would be proven to take place also in the immune system of *D. melanogaster*, experimental model for macrophage polarization studies would be further characterized. This model organism for immune cell metabolism studies would be of a great importance since targeting metabolism in immune cells may be a novel therapeutic strategy for treatment of diseases associated with macrophage polarization. Fruit flies would have provide us with an opportunity to elucidate particular details of this conserved regulation since it allows to use many tools and approaches of forward and reverse genetics. It would enable us to reveal new regulators of the metabolism during immune response, which may have a homologous molecule also in mammalian system. Furthermore, we would like to characterize processes important for interorgan communication, particularly the impact of immune system on systemic metabolism. Detailed understanding of ongoing processes could help us to understand the motivation of immune cells to release signal molecules which have an impact on the whole organism.

Identification of metabolic switch in macrophages and its role in immune response with impact on the systemic metabolism covers several distant and important topics. The next paragraphs present and summarize the most important recent knowledge covering and connecting the systemic outcomes of bacterial infection (**1.2. Energetic demands of the immune system, 1.3. Characteristic progress of immune response, 1.4. Macrophage function in immune system**) with cellular metabolic changes of macrophages and their importance and regulation (**1.5. Metabolic switch in immune cells during immune response, 1.6. Metabolic reprogramming is crucial for activation of macrophages, 1.7. The role of HIF1 α in metabolic reprogramming, 1.8. Metabolic intermediates play a role in epigenetic landscape of macrophages, 1.9. Arginin plays a crucial role in macrophage polarization**) together with outcomes of such a process. The impact of the polarization dysregulation in case of disease is also mentioned to emphasize the importance of further study of this issue (**1.10. M1/M2 macrophage balance in disease, 1.11. Macrophage polarization in cancer**). Following chapter covers basic information about the immune response in *Drosophila* necessary for understanding of the experimental logic used

(**1.12. Immune system of *D. melanogaster***) and how this model organism can be used for gaining of novel data (**1.13. Model organism *D. melanogaster***), for example for further evaluation of the concept of "selfish immune system" (**1.14. Selfish immune system theory**).

1.2. Energetic demands of the immune system

Adequate immune response and control of pathogen growth requires fast activation of immune system. Effective immune response is a very complex process requiring adaptation of many cellular processes which involve large increases in cellular proliferative, biosynthetic, and secretory activities (Wolowczuk et al., 2008), resulting in remodeling of overall cellular metabolism (Frauwirth and Thompson, 2004). Quiescent cell needs to shift to highly active phenotype within hours after infection (Wolowczuk et al., 2008). Activated immune cells need to feed phagocytosis, antigen processing/presentation, cytoskeletal remodeling, mobility, phosphorylation, differentiation and effector responses besides feeding housekeeping and sustenance processes (Krauss et al., 2001; Buttgereit et al., 2000). These changes place large bioenergetic demands on all immune cells leading to high energy consumption which makes the immune response energetically costly (Fong et al., 1990; Straub et al., 2010). Parallel systemic metabolic adaptation of the whole organism is therefore necessary. Infection, no matter how mild, have adverse effects on systemic metabolism. Sickness behaviour, e.g. increased fatigue, drowsiness, low mood, anorexia, decreased interest in pleasurable pursuits such as food, socializing, and sex, is disease associated process serving one purpose - conserve the energy for immune system (Larson and Dunn, 2001), which is the main goal of the afflicted organism. Sickness behaviour is initialized mostly by cytokines of the host, not by infectious agent, and is conserved during evolution (Adamo, 2006). The reallocation of energy is not over even when the pathogen is destroyed. The energy is still needed for healing processes and recovery of the homeostasis.

Quiescent immune cells, especially those of the adaptive arm, contain little glycogen stores, which makes them dependent on imported glucose to satisfy metabolic needs (Doughty et al., 2006). Glucose is considered the most quantitatively important fuel for immune cells in addition to glutamine or fatty acids (Wolowczuk et al., 2008). Lymphocytes increase the number of glucose transporter GLUT1 in order to increase glucose transport across the plasma membrane upon infection (Jacobs et al., 2008). However, a balance must exist and immune cell metabolism needs to be tightly regulated in order to protect the host and resume homeostasis. The energy usurpance is beneficial as long as it is only for short

period of time, otherwise the overall fitness is decreased. For example, overexpression of GLUT1 leads to hyperactive lymphocytes and immune pathologies although its expression is crucial for lymphocyte activation (Jacobs et al., 2008).

In case of adequate immune response, the activation and resolution of inflammation is delicately controlled process and the characteristic progress can be proposed.

1.3. Characteristic progress of immune response

Immune system is artificially divided into two parts eventhough it functions as a whole and all its components extensively communicate with each other. The first part is innate immunity: innate because the defense mechanisms are germline encoded, they have been selected over evolutionary time and passed down from generation to generation with only minor improvements (Litman and Cooper, 2007). The second part is adaptive immunity, which is specific, diverse and capable of formation of long-term memory. Adaptive immunity is a privilege of vertebrates and consists of B and T lymphocytes (Thompson, 1995).

Innate immune system alerts the adaptive part and it also delays the need for an adaptive immune response since it needs four to seven days to generate the clonal expansion and differentiation (Janeway et al., 2001). Innate immunity represents first line of defence against invading pathogens. This conserved part of immune system is responsible for detection of harmful substances and initiation of inflammatory response, which consists of several phases. The first phase is headed towards pathogens destruction, while dead, dying or damaged cells are removed in the second phase (Rock and Kono, 2008). The inflammatory response is terminated with the recovery phase in which tissues are being repaired resulting in re-establishment of tissue integrity. Inflammation is stimulated by chemical substances released from injured cells and it is initiated by immune cells, that are already there, i.e. resident macrophages, dendritic cells, Kupffer cells and mast cells (Davies at al., 2013). Inflammatory response is mediated by cytokines produced by macrophages and other innate immunity cells. Anaphylatoxins stimulate mast cells to release histamine, prostaglandins and serotonin resulting in vasodilation and increased permeability, which allows migration of immune cells into affected tissues (Ley et al., 2007).

Innate immune recognition of invading pathogens relies on a limited number of germline-encoded PRRs (pathogen recognition receptors), which play a major role in recognition of phylogenetically conserved PAMPs (pathogen associated molecular patterns, e.g. LPS, lipoproteins, peptidoglycans) and thus in initiation of immune response

(Medzhitov, 2007). PRRs are involved in opsonization, activation of complement, phagocytosis, activation of coagulation cascade, proinflammatory signaling pathways and induction of apoptosis. Innate immune or germline-encoded recognition receptors bearing cells are macrophages, dendritic cells, mast cells, neutrophils, eosinophils and NK (natural killer) cells (Janeway and Medzhitov, 2002). However, PRRs are also responsible for recognition of DAMPs (damage associated molecular patterns) (Takeuchi and Akira, 2010), which are expressed on surface of damaged, apoptotic or senescent cells. Innate immunity thus also maintains tissue homeostasis. TLRs represent the best described group of PRRs. Recognition is usually followed by phagocytosis, which is major mechanism of macrophages, neutrophils, eosinophils and dendritic cells in pathogen elimination. Processing and presentation of foreign molecules associated with MHC II follows if the phagocyte happens to be also APC (antigen presenting cell) (Greenberg and Grinstein, 2002).

Strikingly, the concept that only adaptive immunity can build immunological memory has recently been challenged since innate immune system shows enhanced responsiveness when they reencounter pathogens. This phenomenon is called trained immunity and has not been fully understood yet (Netea et al., 2016). It is evident that innate immune cells, especially macrophages, play much more important role in the regulation of infection and tissue homeostasis than it was assumed.

1.4. Macrophage function in the immune system

The mononuclear phagocyte system (MPS), which consists of bone marrow precursors, circulating monocytes, resident macrophages and dendritic cells, plays a vital role in inflammation activities (Taylor and Gordon, 2003). Monocytes originate in the bone marrow and represent key players during immune challenge. Recruited monocytes phagocytose pathogens, produce ROS, nitric oxide, myeloperoxidase and inflammatory cytokines (Serbina et al., 2008). Monocytes may also contribute to angiogenesis and atherogenesis (Avraham-Davidi et al., 2013). Monocytes can differentiate and polarize into macrophages.

Macrophages occur in all animals whether they have T cells or not (Mills et al., 2015), which is a fact of a great importance not only for this thesis. Tissue resident macrophages are embryonically derived and maintained by in situ proliferation (Geissmann et al., 2010; Schulz et al., 2012) whilst macrophages that develop from monocytes recruited from the bone marrow during inflammation have hematopoietic origin (Geissmann et al., 2010). Their basic function was described using abbreviation SHIP (sample, heal, inhibit and present (antigen)) (Mills et al., 2014). Macrophages "sample" based on "self" and "nonself"

signals in their surroundings (Dzik, 2010). Healing phenotype is called M2 response, whereas ability to inhibit pathogens is possessed by M1 cells. M1 cells are induced by ligands of TLRs (e.g. LPS) in combination with IFN γ cytokine, which is produced by Th1 cells (Murray et al., 2014). M1 macrophages secrete proinflammatory cytokines and also produce ROS in order to ensure efficient microbial killing via process called respiratory burst (West et al., 2011). M2 macrophages promote tissue repair, replace lost or depleted tissues to maintain homeostasis and they also reduce M1-driven inflammation (Mills et al., 2015). M1 or M2 phenotype is T cell independent. Moreover, it stimulates either Th1 cells and CTL response, or Th2 lymphocytes to further stabilize the predominant immune phenotype in positive feed-back loop (Mills and Ley, 2014).

The fourth ability, present, means that macrophages present the molecules of invading pathogen to T cells in order to activate them (Mills et al., 2015).

Macrophages also produce chemokines, which recruit other cells to the site of infection. The recruitment of inflammatory monocytes to inflammatory sites is mediated by the chemokine CCL2 (C-C motif ligand 2) (Tsou et al., 2007). Tissue resident macrophages maintain tissue homeostasis and have an important role in resolution of inflammation, which takes only few days and then the recovery phase follows. However, this inflammation also represents a potential harm not only for the pathogen, but also for the host. Therefore it needs to be tightly regulated in order to prevent inordinate tissue damage (Nathan, 2002).

Macrophages are also involved in pathophysiology such as in cancer, autoimmunity, metabolic, and fibrotic disorders (Mills et al., 2015). Acute infection may deteriorate into chronic inflammation if the cause of inflammation is persistent. Macrophages and T lymphocytes play a primary role since they produce cytokines and enzyme causing more ongoing damage to the tissues. Tissue damage and destruction manifests as tissue fibrosis. Disordered fibroblast behaviour is considered to be the cause of chronic inflammation since they fail to switch off their inflammatory programme and thus leukocytes are retained within inflamed tissues. Persisting circulating proinflammatory mediators cause the state of global catabolism (Rosenthal and Moore, 2015). Inflammation also plays a role in promoting insulin resistance and dysfunction of pancreatic β -cell (Westwell-Roper et al. 2014; Bendtzen et al., 1986). Apoptosis of β -cells is induced by pro-inflammatory cytokine IL-1 β (Bendtzen et al., 1986), which therefore participates in type II diabetes (Donath, 2014; Larsen et al., 2007). Infection is also linked with insulin resistance (Straub, 2014; Dandona et al., 2004), the most energy saving process.

Hallmark of uncontrolled infection is considered to be cachexia (Andersen et al.,

2004). Increased level of lactate, hyperlactatemia, is commonly found in people who are unwell, e.g. those with chronic medical condition, severe infection with sepsis or systemic inflammatory response (Garcia-Alvarez, 2014). Ongoing hyperglycemia increases inflammatory processes and if it persists it has a negative impact on the innate immune system (Collier et al., 2008). Number of polarized macrophages as well as the duration of polarization, thus, has an effect on the general fitness of the whole organism.

1.5. Metabolic switch in immune cells during immune response

In quiescent cells, the resulting molecule of glycolysis, pyruvate, is mainly directed to the TCA cycle via acetyl-CoA. Krebs cycle then generates NADH, which subsequently donates electrons to the electron transport chain located in mitochondria. Even though some pyruvate is converted to lactate, OXPHOS is the main metabolic source of energy (Kelly and O'Neill, 2015).

In 1927 Otto Warburg described a metabolic profile of tumor cells. Despite the normoxic conditions here, glycolysis is the predominate pathway for energy production eventhough oxygen is available for oxidative metabolism (Warburg et al., 1927). Pyruvate is converted to lactate instead of being fed into the TCA cycle for subsequent generation of NADH. This lactate is also an inducer of arginase expression in TAM (tumor associated macrophages) and these M2 macrophages then promote tumor growth (Colegio et al., 2014). The important role of arginase in function of macrophages is discussed later in this thesis.

The concept of Warburg effect reappeared in 1950s with the discovery that neutrophils depending on aerobic glycolysis and having only few mitochondria (Sbarra and Karnovsky, 1959). These cells also exhibited high glucose and low oxygen consumption. Later discoveries revealed that activated macrophages exhibit increased glycolysis since they increase the expression of hexokinase and glucose-6-phosphate dehydrogenase (Newsholme, 1986; Hard, 1970). It was also shown that most of the glucose consumed by mouse macrophages was converted to lactate, while only a little was used for OXPHOS (Newsholme et al., 1987). Conversion of pyruvate into lactate is essential for regeneration of NAD⁺ which is necessary for maintenance of the glycolytic flux through the glycolysis since OXPHOS is not very active and thus NAD⁺ cannot be regenerated via malate aspartate shuttle (Locasale and Cantley, 2011). Metabolism of activated immune cell is thus similar to metabolism of tumor cells. While TCA cycle activity is decreased, flux through the PPP is increased (Haschemi et al., 2012). Purines and pyrimidines are produced from PPP and they can be used for synthesis of biomolecules necessary for effective immune response (Kelly

and O'Neill, 2015). PPP also provides NADPH which is then used by NADPH oxidase for generation of mitochondrial ROS (Bedard and Krause, 2007) for bacterial killing (West et al., 2011). NADPH is also required for NO synthesis (Aktan, 2004). The importance of NO for macrophage function is discussed later in this thesis as well. Production of ROS is also connected with reduced mitochondrial respiration. Mitochondria of LPS activated macrophages are recruited to phagolysosomes, ROS are transferred inside and used for killing of phagocytosed bacteria (West et al., 2011).

Otto Warburg assumed that tumor cells rely on glycolysis since their mitochondria are impaired. However, some scientist believe the opposite: increased glycolysis leads to the reduction of mitochondrial activity. Sidney Weinhouse found, that cancer cells use glycolysis also under normoxic conditions (Weinhouse et al., 1951) and he argued the opposite: reduced mitochondrial activity of cancer cells is a consequence of increased glycolytic flux. This phenomenon is called Crabtree effect (Crabtree, 1929). However, the field has not been able to reach a decision on this issue to this day. There are still many questions concernig also immune cell activation: What is the first impuls for immune cell metabolism modification? Is it mitochondrial dysfunction, lack of ATP or activation of glycolysis by extracellular signals? Does the metabolism determine the function of macrophages or does the function determine the metabolism?

1.6. Metabolic reprogramming is crucial for activation of macrophages

Mammalian immune cells undergo metabolic reprogramming in order to be activated. Metabolism has been determined as a key factor in polarization of macrophages. It was shown that inhibition of glycolysis with 2-deoxyglucose, which cannot be metabolized, decreased the inflammatory response and inhibition of mitochondrial respiration have no such effect, supporting the theory that oxidative metabolism is shut down under inflammatory conditions (Kellett, 1996). It was also shown that 2-deoxyglucose inhibits activation of hypoxia inducible factor 1 α (HIF1 α), which is discussed later in this thesis (Tannahill, 2013). While glycolytic pathway is essential for M1 macrophage activation, OXPHOS promotes M2 macrophage phenotype (Ganeshan and Chawla, 2014). It was shown that blocking of oxidative metabolism blocks the M2 phenotype. Furthermore, it drives M2 macrophages into M1 phenotype and similarly, forcing oxidative metabolism in M1 macrophages leads to M2 phenotype (Rodríguez-Prados et al., 2010; Vats et al., 2006). Recent proteomic analysis identified glucose-6-phosphate dehydrogenase, fructose-1,6-bisphosphatase 1, alpha enolase and fructose bisphosphate aldolase A to be differentially

expressed in human M1/M2 macrophages (Reales-Calderon et al., 2014).

One of the outcomes of metabolic reprogramming is fragmented TCA cycle and complete change of its intermediate metabolites. This effect leads to the establishment of special condition that can be called pseudohypoxia resulting in aerobic stabilization of HIF1 α .

1.7. The role of HIF1 α in metabolic reprogramming

Since transition between quiescent and activated state requires the dispense of nutrients into different pathways (Pearce and Pearce, 2013), there is an interest in how metabolic pathways are regulated and how they direct functional changes. Recently, the mechanisms behind these metabolic changes have been studied.

The HIF signaling cascade described in hypoxic conditions in tumors plays also an important role in activated macrophages under normoxic conditions (Blouin, 2003). Stabilization of HIF1 α in physiological oxygen concentrations results in pseudohypoxia (Mohlin et al., 2017). HIF is a heterodimeric protein consisting of α and β subunits. There are two HIF α isoforms: HIF1 α has been associated with induction of M1 phenotype, whilst HIF2 α has been recently linked to M2 phenotype (Mills et al., 2015). HIF1 α expression is driven through PI3K/AKT/mTOR pathway (Burns and Manda, 2017), which is activated by LPS. mTOR is a serine/threonine protein kinase, which is active when nutrients are in abundance, i.e. in proliferating cells and metabolically demanding situations, e.g., after TLR stimulation (Byles et al., 2013).

TLR signaling activates NF- κ B and its subunits then bind and activate HIF1 α gene. NF- κ B also controls expression of inflammatory cytokines (Kawai and Akira, 2007). In normoxic conditions and in the presence of Fe²⁺ and α -ketoglutarate, HIF1 α is ubiquitously produced, but it is still hydroxylated by PHDs and thus ubiquitinated by VHL and consequently degraded by the proteasome. In hypoxic conditions molecular oxygen is lacking and since it serves for PHDs as a co-substrate, PHDs cannot hydroxylate HIF1 α and VHL thus cannot bind HIF1 α which leads to stabilization of HIF1 α . Subsequently, HIF1 α is translocated to the nucleus, dimerizes with HIF β , binds to HRE and the expression of target genes is promoted (Fig. 1). HIF1 α target genes are LDH, glycolytic genes, proinflammatory cytokines, GLUT1 or PDK, which phosphorylates and thereby inhibits pyruvate dehydrogenase, that converts pyruvate into acetyl CoA (Imtiyaz and Simon, 2010).

HIF1 α is a crucial transcription factor for metabolic reprogramming of macrophages. It was shown that HIF1 α ^{-/-} macrophages exhibit impaired capability to clear both gram

positive and gram negative bacteria (Peyssonnaud et al., 2005). HIF1 α knockout macrophages have decreased expression of iNOS after IFN γ stimulation (Takeda et al., 2010).

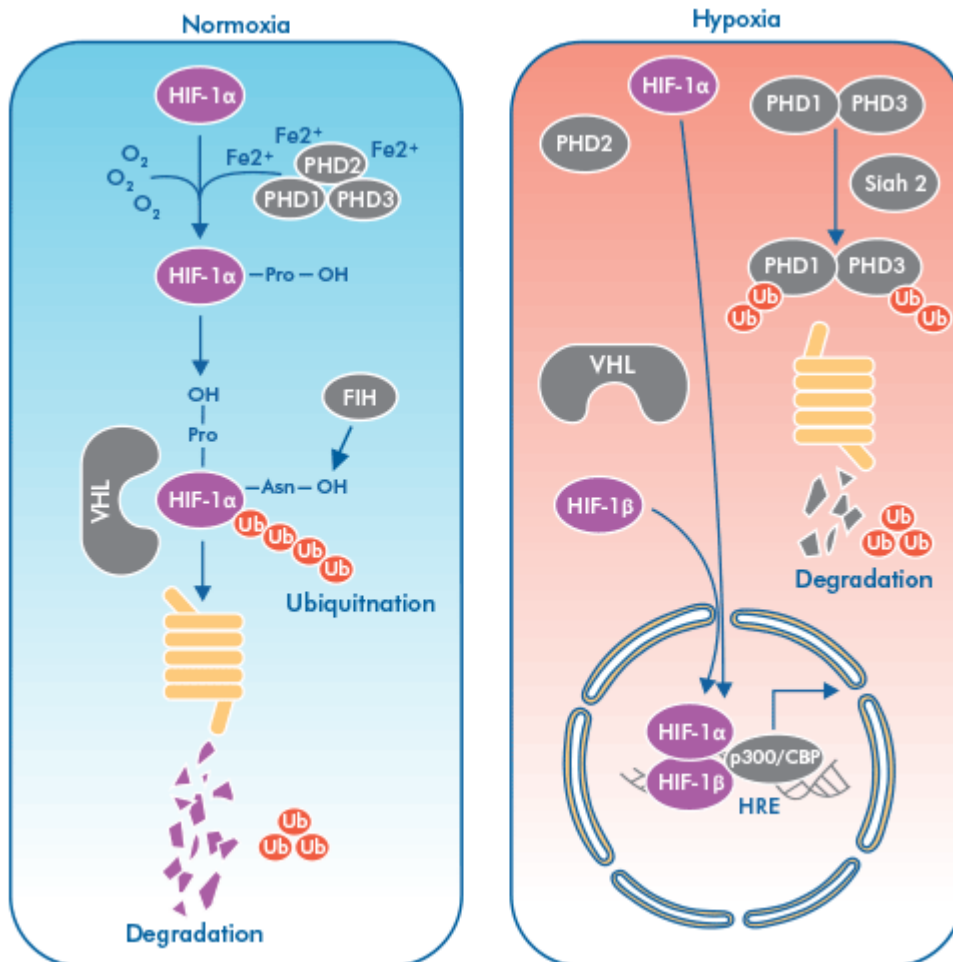


Figure 1: Adopted from Novus Biologicals. Abbreviations: CBP, CREB (cAMP-response element-binding protein) binding protein; Siah 2, seven in absentia homolog 2; Pro, proline; Asn, asparagine; FIH, factor inhibiting hif.

TCA cycle in M1 macrophages is fragmented (O'Neill, 2015) (Fig. 2). Metabolomic studies of M1 macrophages showed that isocitrate dehydrogenase, enzyme converting citrate to α -ketoglutarate, was decreased 7-fold compared to quiescent macrophages leading to increased level of citrate which was used for production of itaconic acid (Jha et al., 2015). Itaconic acid has been showed to have antimicrobial effect (Michelucci et al., 2013). Citrate is also used for fatty acid production, another hallmark of M1 response. There is also increased amount of 2-hydroxyglutarate (former oncometabolite), which is produced from α -

ketoglutarate (Jha et al., 2015). Increased amount of succinate, TCA cycle intermediate, has been found in activated macrophages. Succinate inhibits the activity of PHDs and therefore stabilizes HIF1 α and promotes the metabolic switch to glycolysis (Kelly and O'Neill, 2015). Succinate is converted to fumarate, which is then converted to malate. Highly increased level of malate was also found since arginino-succinate shunt was enhanced. Arginino-succinate shunt also produces NO (O'Neill, 2015). The outcome of such a complex metabolic rearrangement is an atypical concentration of several metabolites, which are used as a signaling factor serving for further stabilization of the polarization.

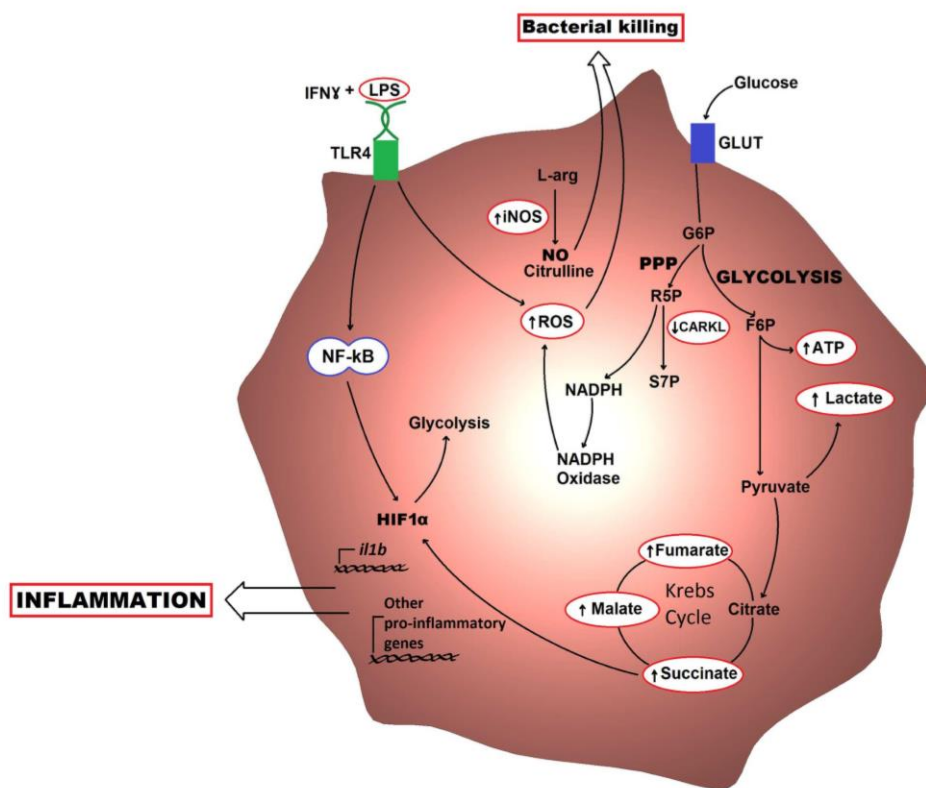


Figure 2: Metabolic profile of M1 macrophages. Adopted from Galvan-Pena and O'Neill, 2014. Abbreviations: G6P, glucose-6-phosphate; F6P, fructose-6-phosphate; R5P, ribulose-5-phosphate; S7P, sedoheptulose phosphate; L-arg, L-arginine; i11b, interleukin 1b.

1.8. Metabolic intermediates play a role in epigenetic landscape of macrophages

The accumulation of metabolic TCA intermediates is linked to proinflammatory function of M1 macrophages and it also affects the epigenetic machinery. Chromatin modifying enzymes sense metabolic status of macrophages and are regulated by the

availability of acetyl-coenzyme A, α -ketoglutarate, nicotinamide adenine dinucleotide or polyamines (Baardman et al., 2015). Epigenetic mechanisms then control macrophage activity. HMTs, enzymes responsible for histone methylation, are α -ketoglutarate-, iron- and oxygen-dependent. HDMs, enzymes responsible for histone demethylation, are inhibited by succinate, fumarate and ROS. Lactate represent an HDAC inhibitor resulting in inhibition of closed chromatin state. α -ketoglutarate, iron and oxygen are required cofactors of TET proteins while succinate and fumarate inhibit TET (Baardman et al., 2015).

Macrophages are also crucial for systemic iron homeostasis since they recycle iron for processes like erythropoiesis (Ganz, 2012). It was shown that M1 macrophages exhibit decreased iron export and thus increased iron storage leading to restriction of growth and pathogenicity of extracellular pathogens (Ganz, 2012). M2 macrophages demonstrate recycling of iron contrary to M1 cells (Zhu et al., 2015). Differential management of iron can also affect methylation state of macrophages since α -ketoglutarate-dependent demethylases require iron as a cofactor. Altered metabolism can therefore affect the epigenetic landscape and function of macrophages (Baardman et al., 2015), however, certain type of metabolism, such as metabolism of arginine, is also connected with bactericidal function of macrophages.

1.9. Arginin plays a crucial role in macrophage polarization

Macrophages show high plasticity thus they exhibit a whole spectrum of polarization states (Mosser and Edwards, 2008), which basically means the ability to acquire different functional phenotypes. It was proposed that similarly to primary colours, macrophage populations can blend into various other "shades", resulting in different phenotypes, where M1 and M2 macrophages are the extremes (Mosser and Edwards, 2008; Xue et al., 2014). M1 macrophages respresent kill/inhibit type of response, whereas M2 cells exhibit repair/heal phenotype (Mills, 2012).

Different function of M1/M2 macrophages is associated also with L-arginine besides the changes in the metabolic pathways for ATP production. Arginin is metabolized to either growth inhibiting NO and citrulline or growth promoting ornithine and urea (Mills, 2001). Tissue macrophages, macrophages of healing wounds or macrophages in growing tumors are those which metabolize arginine primarily to ornithine via enzyme arginase. They were named type M2. Arginase was found to be developed not only in mammals, but also is some fish species e.g. rainbow trout *Oncorhynchus mykiss* (Sigh et al., 2004; Chettri et al., 2011) or Atlantic salmon *Salmo salar L.* (Skugor et al., 2008). M1/M2 differentiation has not yet been detected in invertebrates. Macrophages producing NO via iNOS (inducible nitric oxide

synthase) for killing many pathogens or cancer cells were named M1 (Albina et al., 1990; Nathan and Hibbs, 1991; Mills et al., 1992).

iNOS incorporates molecular oxygen, releases NO from the terminal guanidino nitrogen group of arginine and generates citrulline as a byproduct (MacMicking et al., 1997) (Fig. 3). iNOS can also synthesize superoxide in the absence of arginine and BH4 (tetrahydrobiopterin). This superoxide can then react with NO to form peroxynitrite (Mills et al., 2015). Physiological role of NO is to generate cGMP via stimulation of guanylate cyclase, however, NO also reacts with a variety of molecules to create RNS such as dinitrogen trioxide, peroxynitrite or nitronium ion in the presence of oxygen radicals (Ignarro, 1990) or it leads to creation of nitrosylated proteins. Many metabolic enzymes were found to be nitrosylated on cysteine residues by NO, including glycolytic enzymes, enzymes of TCA cycle and fatty acid metabolism (Doulias et al., 2013). Cysteine nitrosylation is likely to affect the enzymatic activity. Upregulated iNOS expression and resulting increased production of NO leads to nitrosylation and inhibition of ETC proteins and consequent dampening of OXPHOS (Kelly and O'Neill, 2015). Experimental inhibition of iNOS restored normal mitochondrial respiration suggesting, that NO is the mediator or mitochondrial functional collapse and increased glycolysis (Everts et al., 2012). iNOS is calcium/calmodulin dependent in contrast with other NOSs (nNOS, eNOS) and it is regulated via its transcription. iNOS transcription can be induced by a variety of proinflammatory cytokines, microbial products or hypoxia, whilst antiinflammatory cytokines suppress its transcription (Modolell et al., 1995).

It was shown that *Drosophila* NOS (dNOS) activity is dependent on calcium and calmodulin as well, however, the activity is very low compared to other NOSs (Sengupta et al., 2003). dNOS shows the highest homology with mammalian nNOS (Regulski et al., 1995). Nonetheless, this low amount may be sufficient for functioning as a signaling molecule in plasticity (Ghosh et al., 1997). dNOS was upregulated after infection in *Drosophila* larvae and inhibition of dNOS increased larval sensitivity to gram negative bacterial infection (Foley and O'Farrell, 2003). NO plays a role also in the development of nervous system and imaginal disc (Kuzin et al., 1996) and response to hypoxia (Wingrove and O'Farrell, 1999). Although NO and arginases are primitive innate responses it remains unknown whether invertebrate analogs of IFN γ are able to produce LPS-induced NO. However, Dzik claims that the ability of M1 macrophages to produce NO in response to infection is a vertebrate evolutionary invention (Dzik, 2014).

The second arginine pathway in macrophages is driven by arginase I (Fig. 3).

Although arginase is known as an enzyme of the hepatic ornithine cycle since 1932, it is expressed in many different types of cells. Transcription of arginase is mediated by Th2 cytokine (Pauleau et al., 2004). Polyamines are synthesized from ornithine via ornithine decarboxylase. They regulate DNA replication, cell growth and cell differentiation (Pegg, 2009). Proline, a molecule essential for synthesis of collagen, is synthesized from ornithine via ornithine aminotransferase (Kelly and O'Neill, 2015). Ornithine is thus important in tissue remodeling processes. Increased level of arginase was found in allergic asthma (Maarsingh et al., 2011; Zimmermann et al., 2003) and fibrotic lung disease (Kitowska et al., 2008).

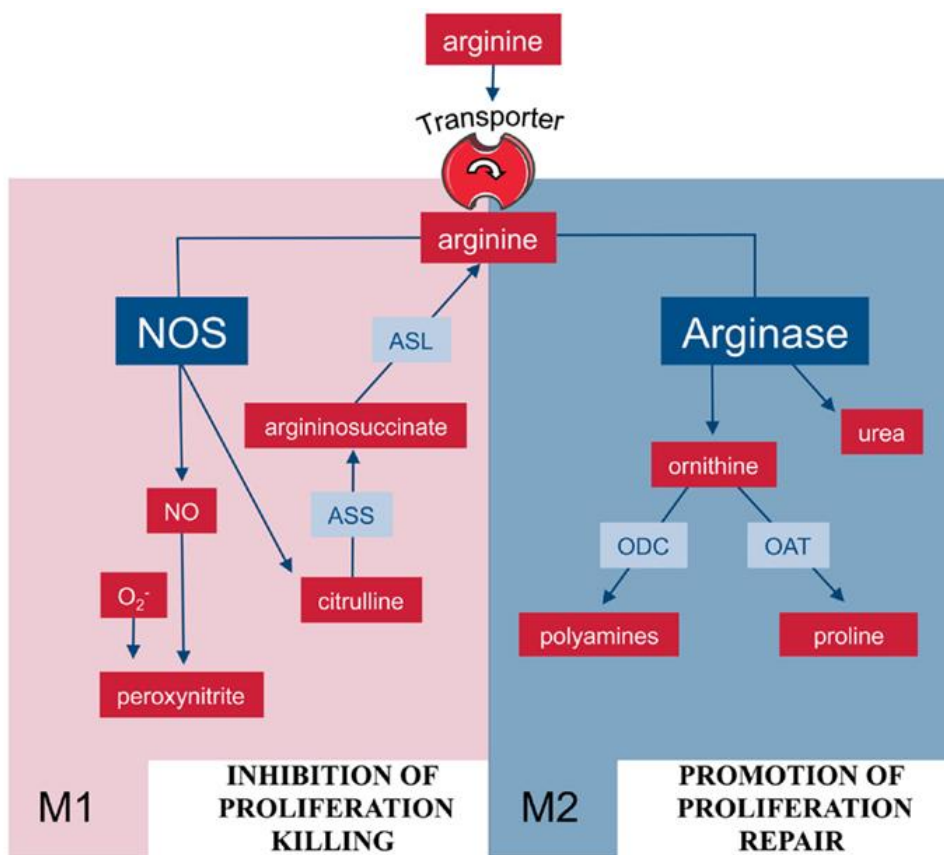


Figure 3: Arginine metabolism at the center of the M1/M2 polarization of macrophages. Abbreviations: ASL, argininosuccinate lyase; ASS, argininosuccinate synthase; OAT, ornithine aminotransferase; ODC, ornithine decarboxylase. Adopted from Mills et al., 2015.

1.10. M1/M2 macrophage balance in disease

The negative side of primarily protective role of M1 response is caused by dysregulation of polarization and is often associated with chronic inflammatory states. There is a connection between chronic M1 response and occurrence of many systemic (hard to be understood and treated) diseases. It was shown that M1/M2 cells are found during foam cell formation, which is a hallmark of atherosclerosis (Thomas and Mattila, 2014). Progression of atherosclerosis is associated with M1 and regression with M2 cells (Peled and Fisher, 2014). The role of macrophages in COPD (chronic obstructive pulmonary disease) was also reviewed (Vlahos, 2014). There is an accumulation of alveolar macrophages of which transcriptome indicated M2 polarization. This phenotype suggests defective phase of inflammation resolution. Macrophage polarization was discussed also in type II diabetes and obesity (Kraakman et al., 2014), where M1 macrophages are enhanced compared to M2 phenotype. Patients with chronic venous ulcer suffer from chronic inflammation since M1 macrophages fail to switch to M2 phenotype (Sindrilaru et al., 2011). The role of macrophage polarization was also investigated in normal and complicated pregnancies. It was shown that increased number of M1 cells is associated with adverse outcomes (Mills et al., 2015). The importance of M1/M2 imbalance in various diseases is indisputable. There is therefore an interest how to therapeutically intervene macrophage polarity to restore health. M1/M2 phenotypes have been revealed to be shaped by members of protein family SOCS (suppressor of cytokine signaling) in several disease settings (Wilson, 2014). Macrophage polarization is also influenced by MSP (macrophage stimulating protein) (Chaudhuri, 2014) and MCSF (macrophage colony stimulating factor). GM-CSF (granulocyte-macrophage colony stimulating factor) shapes the responsiveness to stimuli directing macrophage polarization (Hamilton et al., 2014). The knowledge about how is the acquisition of M1/M2 functions regulated will allow to fine-tune the polarization of macrophages to restore health.

Macrophages also play an important role in the destruction of beginning cancer since they remove dead or "strange" cells in the organism. Innate immune system thus destructs many cancerous deposits every day and it was already documented that malign cells can overcome this defense mechanism by modification of macrophage polarization phenotype (Brenot et al., 2018).

1.11. Macrophage polarization in cancer

Increasing our knowledge of macrophage polarization in cancer and its modulation is of a great importance. M2 macrophages have been shown to dominate in poor-prognosis tumors (Komohara et al., 2014; Weigert and Brune, 2008). There is an evidence indicating that decreasing number of M2 and increasing number of M1 macrophages can slow or even reverse tumor growth (Beatty et al., 2011; Mills et al., 1992). Furthermore, antitumor effects recently observed seems to be primarily mediated by macrophages, not T lymphocytes (Beatty et al., 2011), since macrophages stimulate T cells to Th1 response. Th1 cells and CTL further amplify M1 macrophages (Mills and Ley, 2014). Altering macrophage polarization thus represents a promising approach in cancer treatment. Clinical manipulation of polarization has its first results. Administration of $INF\gamma$, a classical M1 activator, has beneficial effects on ovarian carcinomas (Allavena et al., 1990; Colombo et al., 1992). However, in order to manipulate something, it is necessary to understand it properly and model organism *Drosophila melanogaster* may significantly contribute to understanding of this issue if the metabolic switch would prove to be true also for *Drosophila* macrophages.

1.12. Immune system of *D. melanogaster*

Drosophila innate immunity consists of two main components: cellular and humoral. Mechanisms of cellular responses are phagocytosis, formation of nodules and encapsulation of pathogens (Ratner and Vinson, 1983). Some of the immune responses are stage-specific, for example production of lamellocytes for encapsulation of parasitoid wasp egg is larval-specific (Neyen et al., 2014). Larval immune system consists of circulating hemocytes (plasmatocytes, crystal cells and lamellocytes), sessile cells and antimicrobial peptides. Plasmatocytes are professional phagocytes.

Some components of *Drosophila* innate immunity are very similar to mammalian innate immunity (Govind, 2008), for instance antimicrobial peptides (AMPs), which are produced by leukocytes in vertebrates and in the fat body and plasmatocytes of *Drosophila*. *Drosophila* hemocytes show many similarities with mammalian monocytes and macrophages. They are involved in wound healing, phagocytosis and removal of apoptotic bodies (Madera and Godson, 2003).

In *Drosophila*, systemic immune responses take place in the body cavity and involves hemocytes, hemolymph and the fat body. Humoral response includes antimicrobial peptides and melanisation (Neyen et al., 2014). Local immune response on the other hand takes place

in barrier epithelia (e.g. gut, tracheae) (Ferrandon, 1998).

Expression of AMPs is induced upon infection. AMP genes are regulated via two pathways, Imd and Toll (Lemaitre et al., 1995). Imd pathway responds to gram negative bacteria and controls the expression of antibacterial peptide genes via activation of Relish protein (*Drosophila* NF- κ B). The Toll pathway on the other hand is activated by gram positive bacteria and fungi and starts by the cleavage of the cytokine Spätzle. It triggers nuclear translocation of NF- κ B and it controls the expression of AMPs with antifungal activity. Even though Toll and Imd are two distinct pathways, they usually work in synergy. Direct injection of microbes into the haemocoel activates both pathways, but at different levels, since it depends on the type of microorganism injected (Lemaitre et al., 1997).

Subset of *Drosophila* immune response genes is regulated by the JAK/STAT pathway, which does not regulate AMPs but it is associated with the stress and tissue damage response (Agaisse et al., 2003).

Besides an active fight, hemocytes play also an important role in dealing with the consequences of bacterial infection since sepsis can induce an overwhelming systemic inflammatory response, resulting in organ damage (Singer et al., 2016).

Contrary to the systemic response, epithelia must tolerate some bacteria since the digestive tract is often associated with an indigenous microbes. This suggest a tight regulation of immune activation and bacterial tolerance. *Drosophila* can orally ingest infectious bacteria which can persist in the gut and induce a local immune response. There are two mechanisms for controlling bacterial persistence and infection in the gut - generation of ROS and local production of AMPs. ROS are synthesized in the gut by NADPH oxidase called dDuox. Experiments with microbe-contaminated food showed that knockdown of dDuox resulted in increase in mortality (Ha et al., 2005). The cells in the gut detect the pathogen and activate hemocytes via an NO-dependent signal. The hemocytes then activate immune inducible gene expression in the fat body by a signal that is still unknown (Foley and O'Farrell, 2005).

1.13. Model organism *D. melanogaster*

Drosophila research highly benefits from an easily manipulated genome or a variety of transgenic tools. Even though *Drosophila* immune system lacks its adaptive part, it shares many characteristics of the vertebrate innate immune system. Given the evolutionary conservation of many signaling pathways and transcription factors that control metabolism and immunity, it represents an ideal model organism for study of innate immunity

(Padmanabha and Baker, 2014; Lemaitre and Hoffmann 2007). *Drosophila* immune response depends on many physiological factors, e.g. the type of pathogen, developmental stage, the tissue affected or genotype. Physiological processes interfere with host survival of infection since an immune response requires reallocation of resources and it competes with other vital processes (McKean et al., 2008; Short and Lazzaro, 2013). *Drosophila* is infected by parasites (e.g. parasitoid wasps), viruses, protozoans (e.g. trypanosomes), fungi or bacteria. Each of these pathogens triggers distinct overlapping immune pathways (Neyen et al., 2014). Embryos and pupae are often used for studying wound healing reactions, while larvae and adults serve for research of humoral and cellular immunity. Maturation of immune response is dependent on steroid hormone ecdysone (Regan et al., 2013; Rus et al., 2013), while immune pathways in adult individuals are less affected by developmental timing. Immune response can be affected by mutations in many genes and even the genetic background can have an impact on observed phenotypes (Neyen et al., 2014). *Drosophila* immune system can be challenged by various types of bacteria. However, different bacterial strains from the same bacterial species differ in virulence factors and they may thus behave differently. The most common route of access of the pathogen is by oral infection to the digestive system or by tracheal system in wild insects. Microorganisms can be also introduced via cuticular injuries. Systemic infection is experimentally induced by pricking of anaesthetized adults into the thorax or abdomen with a thin needle dipped in a concentrated bacterial pellet. Individuals then quickly recover and the site of wound is melanised within a few hours. However, certain experiments require a more precise dosage and a defined volume of bacteria is microinjected using a thin glass capillary (Tzou et al., 2002). Nonetheless, capillaries tend to cause larger wounds, stronger melanisation and longer recovery time. Injected microbes grow within the host leading to complex immune response. Injected individuals should be counted at two hours after infection and dead flies should be removed from the experiment. Eye injection, genitalia infection (Gendrin et al., 2009) or placing flies with cut-off tarsal part of legs on contaminated media represent alternative methods.

Survival to infection is widely used for assessment of immune response defects. It is necessary to consider certain technical issues: usage of females may require more frequent flipping in first few days of the experiment since larvae will hatch in the diet. On the other hand, vials containing only males need to be flipped every two or three days since they tend to grow sticky with bacteria quicker. Infections can be performed with lethal or sublethal dose depending on the question addressed.

Infected host has two options to defend against pathogen. The first one, resistance,

means, that the host clears the pathogen. The second one is tolerance (Ayres and Schneider, 2012). To determine, whether the flies died due to low resistance or low tolerance, counting of colony forming units per fly at given times after infection can be used. CFUs determine the efficiency of an immune response. For this assay, flies are mashed in media, supernatant is serially diluted, plated on agar with added antibiotics and incubated until colonies are visible.

Streptococcus pneumoniae infection, in a form used in this thesis, is not natural as a high number of bacteria are injected directly into the body and thus mechanisms of epithelial immunity are not employed (Lemaitre and Hoffman, 2007; Govind, 2008). However, this use of bacterial infection serves as an ideal sepsis model and a model of uncontrollable bacterial propagation in an organism. After the penetration of *S. pneumoniae* into the body it immediately proliferates and immune response is activated with certain delay (Wang, et al., 2014). In this time period the level of colony forming units (CFUs) rises. Innate immunity comprises the main part of *Drosophila* immune reaction. Plasmatocytes phagocyte and kill the pathogen and thus serve as an analog of mammalian M1 macrophages (Govind, 2008; Novak and Koh, 2013). Phagocytosis of bacteria starts with the recognition of bacterial PAMPs with PRRs on the surface of the immune cell resulting in cytoskeletal remodeling, which allows the internalization of foreign substance. This substance is then degraded via lysosomal enzymes (Lemaitre and Hoffman, 2007). Simultaneously, the humoral immunity is activated and antimicrobial peptides are produced in fat body as well as in hemocytes (Wang et al., 2014). Even though antimicrobial peptides play more of a supporting role, when the cooperation of both components is not efficient enough, the fly perishes (Lemaitre and Hoffman, 2007). Effective immune response results in decrease in CFUs.

Besides *Drosophila* being very useful model organism for innate immunity studies, it possesses many unique features facilitating the understanding of underlying mechanisms. One of the widely used tools is RNAi together with its site and time controlling system UAS-Gal4 (Brand and Perrimon, 1993). These tools enable us to analyze the effect of gene of interest in specific tissue very easily. Besides regulation of gene expression, there is a plenty of already developed tools for detection of gene specific expression, which is often marked with fluorescent proteins (e.g. GFP, RFP). Another gene expression visualizing compound is blue indigo, which is produced by β -galactosidase (X-gal staining of P[LacZ]-expressing individuals). This is only a small fraction of possibilities. All the tools kindly shared by the whole *Drosophila* community makes *Drosophila* to be an ideal model organism

for forward and reverse genetics applications and for analysis of complicated processes *in vivo*.

In our laboratory, we have already proved that *D. melanogaster* can be used for studying such complex questions since we have used it for studying of adenosine signaling pathway in the "selfish immune system" theory.

1.14. Selfish immune system theory

The human brain possesses the characteristics of being "selfish" since it allocates the most energy to itself. Prof. Achim Peters established Selfish brain theory paradigm for the regulation of energy supply within the organism meaning, that the brain regulates its own ATP concentration as a matter of priority, while the peripheral energy supply is of second importance (Peters et al., 2004). Strikingly, immune system exhibits similar behaviour.

After the fly consumes glucose, it is transferred into fat body and stored here in a form of glycogen under regular conditions. Glycogen serves as an energy reservoir (Arrese and Soulages, 2010). This conversion of glucose into glycogen enables the enzyme called glycogen synthase. In case of higher energy demand, e.g. upon infection, glycogen is decomposed back to glucose and trehalose via glycogen phosphorylase and thus serves as a prompt energy source for other tissues (Reyes-DelaTorre et al., 2012). This trehalose is utilized for phagocytosis, production of AMPs or tissue repair after infection (Govind, 2008). It is necessary to decrease the energy consumption of nonimmune tissues in order to have sufficient amount of energy for immune processes. The need of the whole organism is superior to the needs of particular tissues at this point and it is essential to behave "selfishly" concerning the interorgan communication. Owing to this fact, hemocytes cause insulin resistance of nonimmune tissues so the glucose can not enter the cells and stays in hemolymph available for the immune cells (Bajgar et al., 2015). Insulin resistance can be therefore seen as an immune system supporting program. The level of glycogen decreases while the level of circulating glucose as a freely available energy source increases (Bajgar et al., 2015). Dolezal group found that adenosine, purine nucleoside released from immune cells, is responsible for reallocation of the energy, which would be otherwise used for development, to differentiating immune cells. This switch is crucial for an effective immune response since preventing adenosine signaling reduces host resistance. Adenosine is the crucial molecule that secures more energy for immune cells at the expense of other tissues (Bajgar et al., 2015). Recently, a similar role of extracellular adenosine was proved also in adult flies (Bajgar and Dolezal, accepted). In 2017 Sokcevicova showed in her MSc. thesis another

"selfish" signal molecule, which is released from immune cells and that induced systemic metabolic changes - ImpL2 (Sokcevicova, MSc. thesis 2017 [in Czech]). ImpL2 is known to bind insulin-like peptides extracellularly and thus causing insulin resistance in *Drosophila*. Hemocyte specific production of ImpL2 is responsible for dramatic metabolic rearrangement of systemic metabolism as well as for survival of infection (Sokcevicova, MSc. thesis 2017 [in Czech]). ImpL2 was described to be produced in *Drosophila* cancer cells where it affects insulin sensitivity as well as general fitness of many organs and tissues by inducing systemic cachexia (Figueroa-Clarevega and Bilder, 2015).

In this thesis, I would like to describe whether systemic bacterial sepsis induces metabolic changes also in *Drosophila* macrophages and how this rearrangement influences the general ability to overcome the infection. To identify the dynamicity of the process, the phenotypes were analyzed in the first five days since that is how long it takes to the macrophages to clear the pathogen. Furthermore, I would like to characterize the regulation of this metabolic shift and how is it interconnected with the systemic metabolism.

2. AIMS OF THE THESIS

To map the macrophage specific gene expression of metabolic genes during infection

To characterize the macrophage metabolism using *in vivo* markers

To test the importance of metabolic changes in resistance to infection

To identify the role of transcriptional factor HIF1 α in metabolic shift in macrophages during infection

3. MATERIALS AND METHODS

3.1. *Drosophila* techniques

Flies in stocks were raised in glass vials with cotton plugs on a cornmeal diet with 5 % glucose (Tab. 1) and kept in incubators with natural light/dark periods at 18 °C or 25 °C. When higher numbers were needed, flies were raised in plastic bottles since they provide larger area for laying eggs (also cornmeal diet). Infected males selected for survival experiments and for qPCR analyses were kept in plastic vials on 0 % glucose experimental cornmeal diet (Tab. 2). Infected flies were kept in incubators at 29 °C due to the temperature sensitivity of *Streptococcus pneumoniae* and induction of temperature sensitive genetic construct. During the experiments, vials were transferred from 18 °C to 29 °C depending on tissue and time specific RNAi using Gal4Gal80^{Ts} construct. Humidity in incubators oscillated between 52-57 %.

Table 1: Stock diet with 5 % glucose

Water	1500 mL
Cornmeal	120 g
Agar (Amresco, J637)	15 g
Instant yeast	60 g
Saccharose	75 g
Cook for 12 min at 100 °C, then 50 min at 90 °C, then cool to 60 °C	
10% Methylparaben/EtOH	25 mL

Table 2: Experimental diet with 0 % glucose

Water	1500 mL
Cornmeal	80,3 g
Agar <i>Drosophila</i> Type II. (Apex – 66-103)	9,3 g
Instant yeast	42,3 g
Cook for 12 min at 100 °C, then 50 min at 90 °C, then cool to 60 °C	
10% Methylparaben	25 mL

3.2. *Drosophila melanogaster* strains

In this section, there are listed strains of *D. melanogaster*, that were used for this thesis. The first designation represents the appellation by which individual strains are named in this work.

HmlGal4 TubGal80^{Ts} - w*; HmlΔ-Gal4*; P{tubPGal80ts}*

HmlGal4>GFP - w; HmlΔ-Gal4 UAS-GFP (kindly provided by Bruno Lemaitre)

Sima TRiP - BL-26207: y[1] v[1]; P{y[+7.7] v[+1.8]=TRiP.JF02105}attP2

Sima KK - VDRC- v106504: P{KK110834}VIE-260B

UAS GFP-RNAi - BL-9331: w[1118]; P{w[+mC]=UAS-GFP.dsRNA.R}143

RNAi KK control - VDRC-60100, y, w[1118]; P{attP,y[+],w[3`]}

ImpL3 RNAi - BL-33640, y[1] v[1]; P{y[+7.7] v[+1.8]=TRiP.HMS00039}attP2

HRE-LacZ reporter (Fig. 4) - used as a reporter line for visualization of HIF1 α transcription factor activity. This construct clearly identifies the cells in which HIF1 α is translocated into the nucleus and activates gene expression under HRE promoter. Kindly provided by Pablo Wappner.

LDH mCherry (Fig. 5) - used as a reporter line for visualization of sites of LDH expression. Kindly provided by Jason Tennessen (unpublished).

w¹¹¹⁸

HRE-LacZ reporter

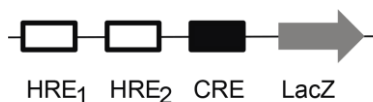


Figure 4: HRE-LacZ construct (De Lella Ezcurra et al., 2016).

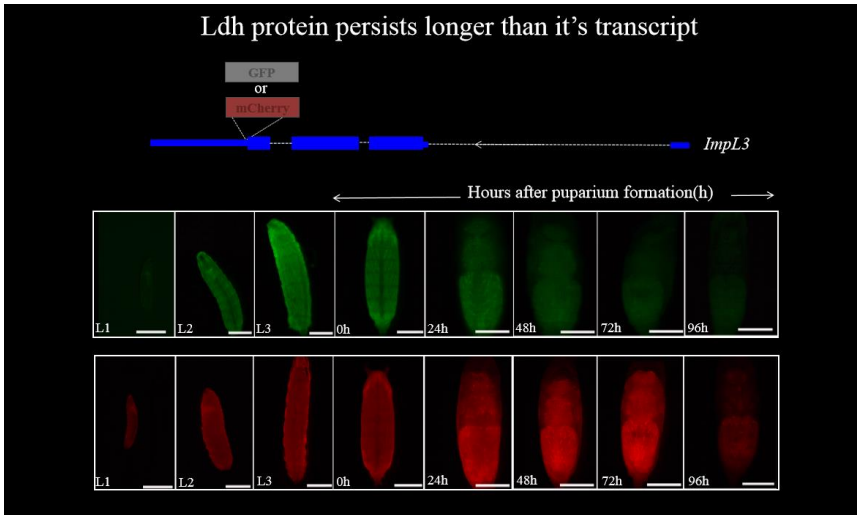


Figure 5: LDH mCherry construct. Adapted from Jason Tennesen - unpublished description of the genetic construct and its basal expression during the development.

3.3. Crosses

Crosses described below were performed in order to obtain flies with desired combination of certain characteristics. For collecting virgins and males, flies were anaesthetized using CO₂ Flowbuddy Flow Regulator (Genesee Scientific, 7l/min).

Cross no1: Experimental line *HmlG4>GFP* x LDH mCherry

$$P: \frac{w}{w}; \frac{Hml\Delta-Gal4GFP}{Hml\Delta-Gal4GFP}; \frac{+}{+} \quad \times \quad \frac{w}{l}; \frac{ImpL3-mCherry}{ImpL3-mCherry}; \frac{+}{+}$$

$$F1: \frac{w}{w}; \frac{Hml\Delta-Gal4GFP}{ImpL3-mCherry}; \frac{+}{+} \quad \times \quad \frac{w}{l}; \frac{+}{CyO}; \frac{+}{+}$$

$$F2: \frac{w}{l}; \frac{Hml\Delta-Gal4GFP \ ImpL3-mCherry}{CyO}; \frac{+}{+} \quad \times \quad \frac{w}{w}; \frac{Hml\Delta-Gal4GFP \ ImpL3-mCherry}{CyO}; \frac{+}{+}$$

$$F3: \frac{w}{w}; \frac{Hml\Delta-Gal4GFP \ ImpL3-mCherry}{Hml\Delta-Gal4GFP \ ImpL3-mCherry}; \frac{+}{+}$$

Cross no2: Experimental line HmlG4>GFP x UAS Sima RNAi KK

$$P: \frac{w}{w}; \frac{Hml\Delta-Gal4GFP}{Hml\Delta-Gal4GFP}; \frac{+}{+} \quad \times \quad \frac{w}{l}; \frac{+}{+}; \frac{UAS\ Sima\ RNAi\ KK}{UAS\ Sima\ RNAi\ KK}$$

$$F1: \frac{w}{l}; \frac{Hml\Delta-Gal4GFP}{+}; \frac{+}{UAS\ Sima\ RNAi\ KK}$$

Cross no3: Control line HmlG4>GFP x RNAi KK control

$$P: \frac{w}{w}; \frac{Hml\Delta-Gal4GFP}{Hml\Delta-Gal4GFP}; \frac{+}{+} \quad \times \quad \frac{w}{l}; \frac{RNAi\ KK\ control}{RNAi\ KK\ control}; \frac{+}{+}$$

$$F1: \frac{w}{l}; \frac{Hml\Delta-Gal4GFP}{RNAi\ KK\ control}; \frac{+}{+}$$

Cross no4: Experimental line HmlG4G80 x UAS Sima RNAi KK

$$P: \frac{w}{w}; \frac{HmlGal4}{HmlGal4}; \frac{P\{tubPGal80ts\}}{P\{tubPGal80ts\}} \quad \times \quad \frac{w}{l}; \frac{+}{+}; \frac{UAS\ Sima\ RNAi\ KK}{UAS\ Sima\ RNAi\ KK}$$

$$F1: \frac{w}{l}; \frac{HmlGal4}{+}; \frac{P\{tubPGal80ts\}}{UAS\ Sima\ RNAi\ KK}$$

Cross no5: Control line HmlG4G80 x RNAi KK control

$$P: \frac{w}{w}; \frac{HmlGal4}{HmlGal4}; \frac{P\{tubPGal80ts\}}{P\{tubPGal80ts\}} \quad \times \quad \frac{w}{l}; \frac{RNAi\ KK\ control}{RNAi\ KK\ control}; \frac{+}{+}$$

$$F1: \frac{w}{l}; \frac{HmlGal4}{RNAi\ KK\ control}; \frac{P\{tubPGal80ts\}}{+}$$

Cross no6: Experimental line HmlG4G80 x UAS Sima RNAi TRiP

$$P: \frac{w}{w}, \frac{HmlGal4}{HmlGal4}, \frac{P\{tubPGal80ts\}}{P\{tubPGal80ts\}} \quad \times \quad \frac{w}{l}, \frac{+}{+}, \frac{UAS\ Sima\ RNAi\ TRiP}{UAS\ Sima\ RNAi\ TRiP}$$

$$F1: \frac{w}{l}, \frac{HmlGal4}{+}, \frac{P\{tubPGal80ts\}}{UAS\ Sima\ RNAi\ TRiP}$$

Cross no7: Control line HmlG4G80 x UAS GFP-RNAi

$$P: \frac{w}{w}, \frac{HmlGal4}{HmlGal4}, \frac{P\{tubPGal80ts\}}{P\{tubPGal80ts\}} \quad \times \quad \frac{w}{l}, \frac{GFP\ RNAi\ TRiP\ control}{GFP\ RNAi\ TRiP\ control}, \frac{+}{+}$$

$$F1: \frac{w}{l}, \frac{HmlGal4}{GFP\ RNAi\ TRiP\ control}, \frac{P\{tubPGal80ts\}}{+}$$

Cross no8: Experimental line HmlG4G80 x UAS ImpL3 RNAi

$$P: \frac{w}{w}, \frac{HmlGal4}{HmlGal4}, \frac{P\{tubPGal80ts\}}{P\{tubPGal80ts\}} \quad \times \quad \frac{w}{l}, \frac{+}{+}, \frac{UAS\ ImpL3\ RNAi}{UAS\ ImpL3\ RNAi}$$

$$F1: \frac{w}{l}, \frac{HmlGal4}{+}, \frac{P\{tubPGal80ts\}}{UAS\ ImpL3\ RNAi}$$

Cross no9: Control line w x UAS ImpL3 RNAi

$$P: \frac{w}{w}, \frac{+}{+}, \frac{UAS\ ImpL3\ RNAi}{UAS\ ImpL3\ RNAi} \quad \times \quad \frac{w}{l}, \frac{+}{+}, \frac{+}{+}$$

$$F1: \frac{w}{l}, \frac{+}{+}, \frac{UAS\ ImpL3\ RNAi}{+}$$

Drosophila mating schemes were created according to Root and Prokop (2013).

3.4. Infections

For survival and qPCR assays, newly emerged male flies were collected and transferred on 0 % glucose experimental diet, where they were kept for at least 7 days so their immune system gets stabilized after the emergence. Since flies for survival experiments beared HmlGal4Gal80^{Ts} construct, they were stored at 18 °C. 24 hours before infections males were transferred at 29 °C in order to induce degradation of Gal80 protein and consequently trigger RNAi. Concerning flies for qPCR assays, flies only with HmlGal4 construct were used, so they were kept at 25 °C. All the experimental and control groups in one particular experiment always underwent the same temperature treatment.

Streptococcus pneumoniae (EJ1 strain, kindly provided by David Schneider, referred as *Sp*) was stored in microtubes in Tryptic Soy Broth media (TSB) (Sigma) with 16% glycerol at -80 °C. The upper layer was scraped off using a disposable inoculation loop (Biologix) and spreaded on a Petri dish, which was prepared as follow (Tab. 3):

Table 3: Recipe for TSB agar for Petri dishes.

dH2O	400 mL
Tryptic Soy Broth (Sigma) 3 %	12 g
Agar (Amresco, J637) 1,5 %	6 g
Boil for 1 min in microwave oven. Autoclave for 20 min at 121 °C, let it cool down to 50 °C.	
Streptomycin sulfate salt (Sigma) 0,0075 %	0,03 g

This Petri dish was then left in an incubator at 37 °C, (5 % CO₂) overnight.

Simultaneously, TSB liquid media was prepared as follow (Tab. 4):

Table 4: Recipe for TSB liquid media.

dH2O	100 mL
Tryptic Soy Broth (Sigma) 3 %	3 g
Boil for 1 min in microwave oven. Autoclave for 20 min at 121 °C, let it cool down to 50 °C. Afterwards, bacterial filter (Ø 0,20 µm) was used.	

Three glass tubes with TSB liquid media were prepared: One of them was used for *S. pneumoniae* inoculation from plate, second for *S. pneumoniae* inoculation to fresh media next day and third was used as a blank (Fig. 6). Three milliliters of TBS liquid media was then placed in each glass tube and 100 µl of streptomycin (Sigma) and 100 µl of catalase (Sigma) was also added. Next day in the morning, one colony from the Petri dish was placed in the first glass tube. This tube was then placed into incubator at 37 °C, 5 % CO₂. After 24 hours 100 µl from this first tube was pipetted into the second glass tube. This process ensured, that, at the time of infections, the growth curve of *S. pneumoniae* was in exponential phase.

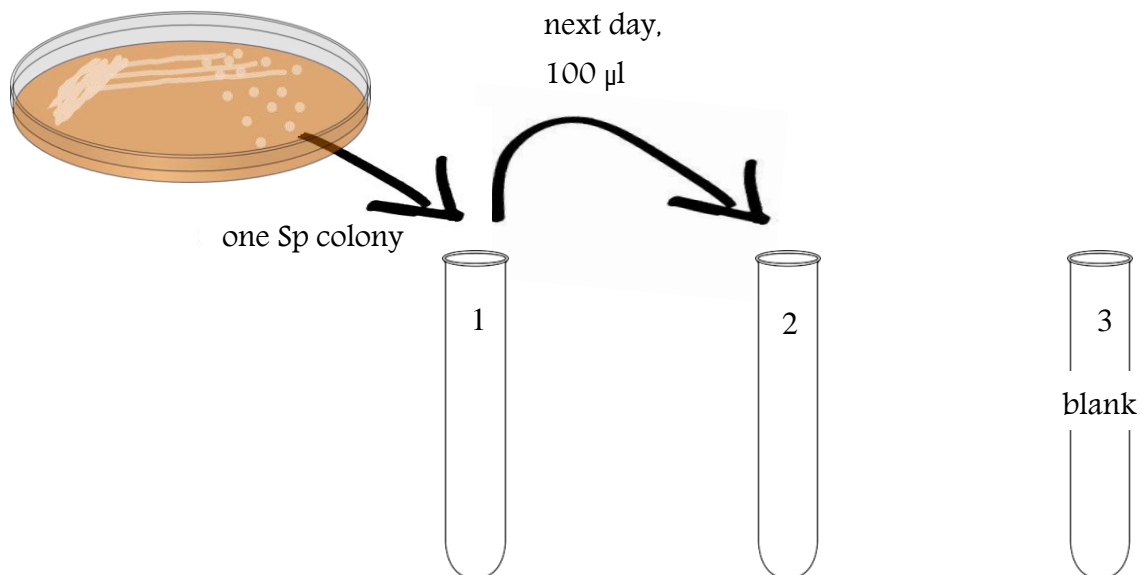


Figure 6: Schematic representation of *S. pneumoniae* preparation for infections.

Bacterial density was then measured using disposable cuvette (BRAND®) at OD600 with spectrophotometer Optizen 1412V, centrifuged and dissolved in PBS so the final OD reached $A = 2,4$. During the process of infection *S. pneumoniae* culture was kept on ice.

Flies were infected with 20 000 bacteria of *S. pneumoniae* in 50 nL of buffer using Eppendorf Femtojet Microinjector. End (approximately 3 mm) of a glass needle was broken using tweezers and 50 nL of buffer with *S. pneumoniae* was injected into this infection glass needle using an extra long pipette tip. For calibration small dish with oil was laid down under binocular microscope (Olympus SZ51) and the glass needle was placed into this oil. An enlargement of 4 ensured that a small grating of the microscope was visible. Using this small grating a drop of size of 21 units was created based on a combination of time and pressure. Such 50 nL drop contained 20 000 bacteria. Flies were injected on the CO₂ Flowbuddy Flow Regulator's plate (Genesee Scientific, 7l/min). Control flies were injected with 50 nL of PBS. After infections flies were transferred into plastic vials with 0 % glucose diet. To be sure that all flies survived the process of infection, it was necessary to check if all infected flies woke up afterwards. If not, these flies were excluded from the experiment. Since *S. pneumoniae* is temperature sensitive, infected flies were kept at 29 °C. Infected males were transferred into fresh vials every second day in order to ensure good condition of the food. This transfer was performed without using CO₂ as it could have negatively influenced *Drosophila's* mortality. The number of dead flies transferred from an old vial was recorded on the new vial so it will not be counted/included twice. The number of dead individuals was counted/recorded every day for at least 23 days (or until all flies were dead). Flies which were lying on their back and when dabbed/patted on the vial they were not assigned any movement were considered dead. Subsequently, these data were statistically evaluated using standard survival analysis. Flies which died in account of unskilled manipulation or flies which stuck to the food layer were excluded from the experiment. Statistical processing of the resulting data is stated in 3.14. Statistics and data processing. Experimental design was adopted from Linford et al., 2013.

3.5. Colony forming units (CFUs)

To determine bacterial growth rate in *Drosophila* after infection, CFUs were performed at 18 and 24 hours post infection (hpi). To define if the distribution of bacteria among individuals was even, the number of bacteria per fly was also evaluated immediately after infection (0hpi). Each randomly chosen infected fly was anaesthetized using CO₂ and placed in microtube containing 200 µL of PBS. All microtubes were kept on ice. The fly was then homogenized using a pestle motor mixer (VWR) and 20 µL of this homogenate was transferred in one well of 96-well plate and 180 µL of PBS was added. This sample was then

diluted twice. Afterwards, 20 μL of the diluted *Sp* culture was plated on the TSB Agar Petri dish (Fig. 7) and thus the dilution factor was $1/10^4$.

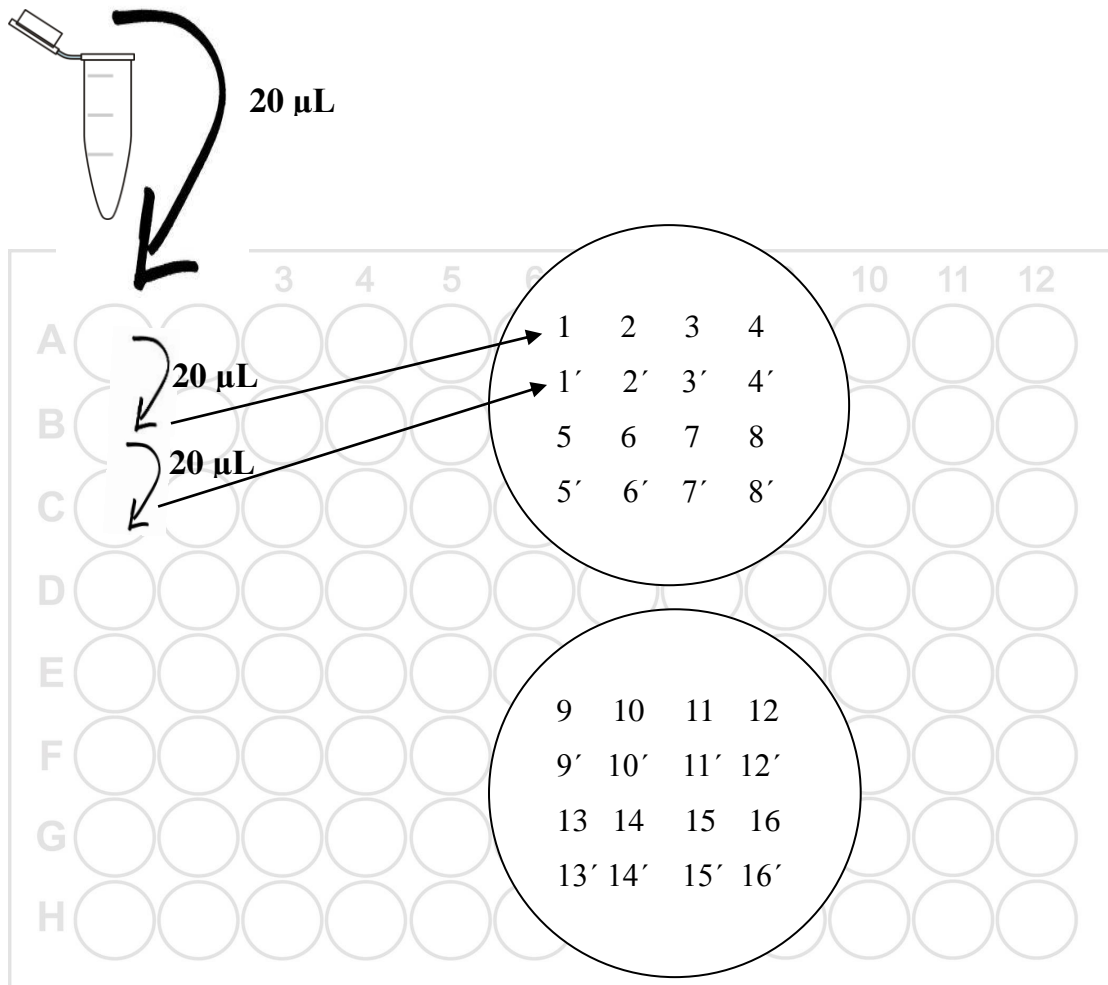


Figure 7: Schematic representation of CFUs.

After the drops got dry, the dish was transferred into incubator at 37 $^{\circ}\text{C}$. Sixteen flies per one genotype were analysed. After 48 - 72 hours the number of colonies (which reflect the number of cultivated bacterial units in each *Drosophila*) was counted using binocular microscope. These data were entered/recorded in a table and processed afterwards (see 3.14 Statistics and data processing)

3.6. Metabolites measurement

Three quantities were measured - free glucose, glycogen and proteins, which served for standardization of possible deviations caused by different sizes of individual flies.

Infected males were collected at 0, 12 and 24hpi. For sample preparation five individuals per one microtube were homogenized in 200 μ L of PBS and centrifuged (3 min, 4 $^{\circ}$ C, 8000 RPM). Samples intended for proteins quantification were transferred at/to -80 $^{\circ}$ C, while samples for glucose and glycogen measurement were denaturated at 75 $^{\circ}$ C for 10 minutes and transferred at/to -80 $^{\circ}$ C as well afterwards.

BCA kit (Sigma) was used for proteins quantification. 1 part of sample was mixed with 20 parts of solution (50 parts of bicinchoninic acid + 1 part of reagent B). Simultaneously, standard curve of specific range (0; 1 μ g/mL; 10 μ g/mL; 0,1 mg/mL; 0,5 mg/mL; 1 mg/mL) was created using BSA (New England Biolabs). Protein concentration was deduced from absorption at 562 nm (Sunrise - Absorbance microplate reader, Tecan).

GAGO-20 kit (Sigma) was used for glucose measurement. 45 μ L of sample was mixed with 100 μ L of Assay reagent (glucose oxidase-peroxidase reagent + o-dianisidine). Afterwards, this solution was incubated at 37 $^{\circ}$ C for 30 minutes. To stop the reaction, 100 μ L of 12N H₂SO₄ was added. Simultaneously, standard curve of specific range (0; 0,03 mg/mL; 0,067 mg/mL; 0,125 mg/mL; 0,25 mg/mL; 0,5 mg/mL; 1 mg/mL) was created using D-Glucose (Sigma). Absorption was measured at 540 nm.

For glycogen quantification, 25 μ L of sample was mixed with 5 μ L of amyloglucosidase (Sigma), 15 μ L of PBS and 100 μ L of Assay reagent (glucose oxidase-peroxidase reagent + o-dianisidine, Sigma). This solution was also incubated at 37 $^{\circ}$ C for 30 minutes. Thereafter, 100 μ L of H₂SO₄ was added. Since glycogen was cleaved by this process into glucose, the same standard curve as for glucose was also used for glycogen evaluation and therefore the absorption was also measured at 540 nm. In order to get the precise amount of glucose originated by cleavage of glycogen, the glucose amount measured for the sample was subtracted from the overall glucose amount.

For better understanding of the experimental scheme, following timescale was created (Fig. 8).

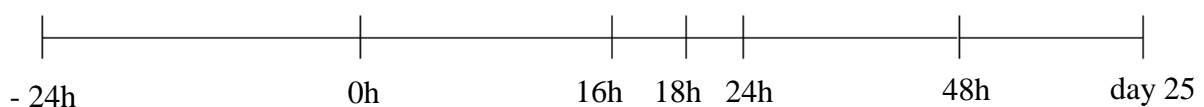


Figure 8: Schematic timescale of the experiments.

-24hpi: transfer of males from 18 $^{\circ}$ C to 29 $^{\circ}$ C

0hpi: infection, CFUs - T0, collection of individuals for metabolites measurement

16hpi: collection of individuals for metabolites measurement

18hpi: CFUs - T1

24hpi: CFUs - T2

48hpi: collection of individuals for metabolites measurement, CFUs - T3

25 days post infection: end of daily counting of dead individuals

3.7. X-gal staining

X-gal staining was performed using *Sp* infected HRE-LacZ reporter adults. PBS injected HRE-LacZ adults were considered as a control. In order to make the adult flies non-hydrophobic, adult flies were dipped in 75% EtOH for one second. Flies were impaled on thin needles attached to Sylgard (ELCHEMCo) which was poured in Petri dish. Thorax and abdomen were gently opened in PBS and fixation was performed with 2,5% glutaraldehyde/PBS on LabRoller rotator for 7 minutes at room temperature. Adults were then washed three times in PBS on rotator at room temperature. Next two washings were performed using a PT solution (1 mL 10xPBS (Ambion), 100 μ L 1M MgCl₂ x 6H₂O, 300 μ L 10% Triton, 8 mL dH₂O, 320 μ L 0,1M K₄[Fe(CN)₆], 320 μ L K₃[Fe(CN)₆]) for 10 minutes. Lastly, PT solution was changed again and few grains of X-gal (Invitrogen) were added and this mixture was well mixed. Adult samples in microtubes were placed in thermoblock at 37 °C and occasionally mixed and the colorimetric reaction was monitored. After the blue color developed, reaction was stopped at the same time for all samples. Final three washings were performed using PBS. Pictures (Fig. 18) were taken using stereo microscope (Olympus SZX12).

3.8. Fluorescence-activated cell sorting (FACS)

Following sample preparation steps were performed at 0, 6, 24, 72 and 120 hpi. Approximately 200 flies per each sample were anaesthetized with CO₂ and divided into three microtubes with 200 μ L of PBS, which were kept on ice. Subsequently, adults were homogenized using a pestle (without motor mixer as it could damage the cells). Homogenate

from all three microtubes was sieved through nylon cell strainer (\varnothing 40 μm). To make sure that nothing was left in the microtubes, microtubes were washed with 200 μL of PBS, which was then added to the homogenate. Samples were centrifuged (3 min, 6 $^{\circ}\text{C}$, 3500 RPM), supernatant was removed and 1 mL of PBS was added to the pellet and resuspended. This centrifugation process was then repeated twice.

Flow cytometry gate was established using positive (Hml GFP bearing individuals) and negative (w^{1118}) control flies (Fig. 9). Prior to sorting, quality control was performed using ten drops of Pro Line Universal Calibration Beads (Bio-Rad). Gating strategy is shown in figure 9 and laser and additional settings of S3TM Cell Sorter (Bio-Rad) are shown in figure 10.

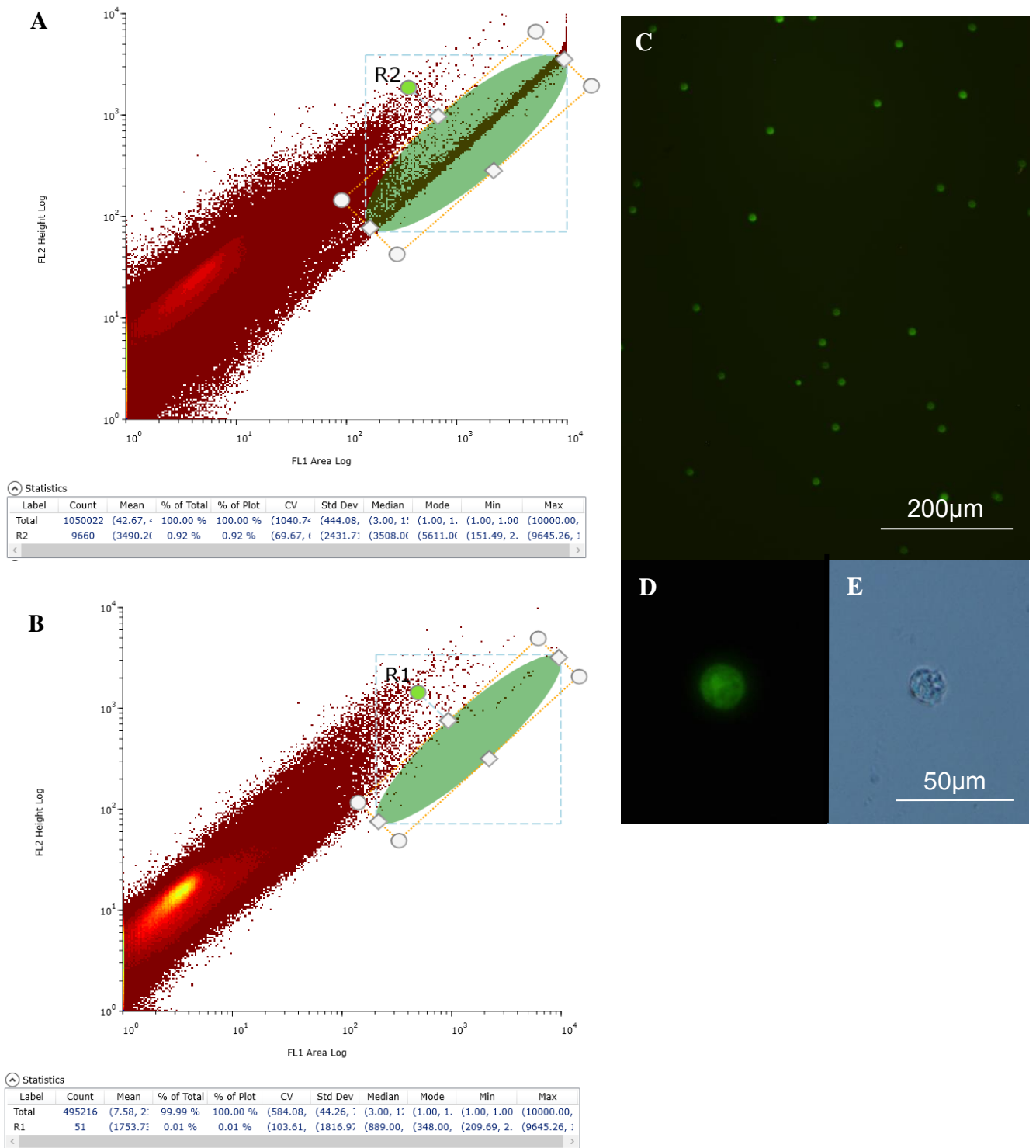


Figure 9: Example of a positive (A) and negative (B) control. Fluorescent image of sorted cells (C), detailed image of one of the sorted cells (D and E) captured by inverted microscope.

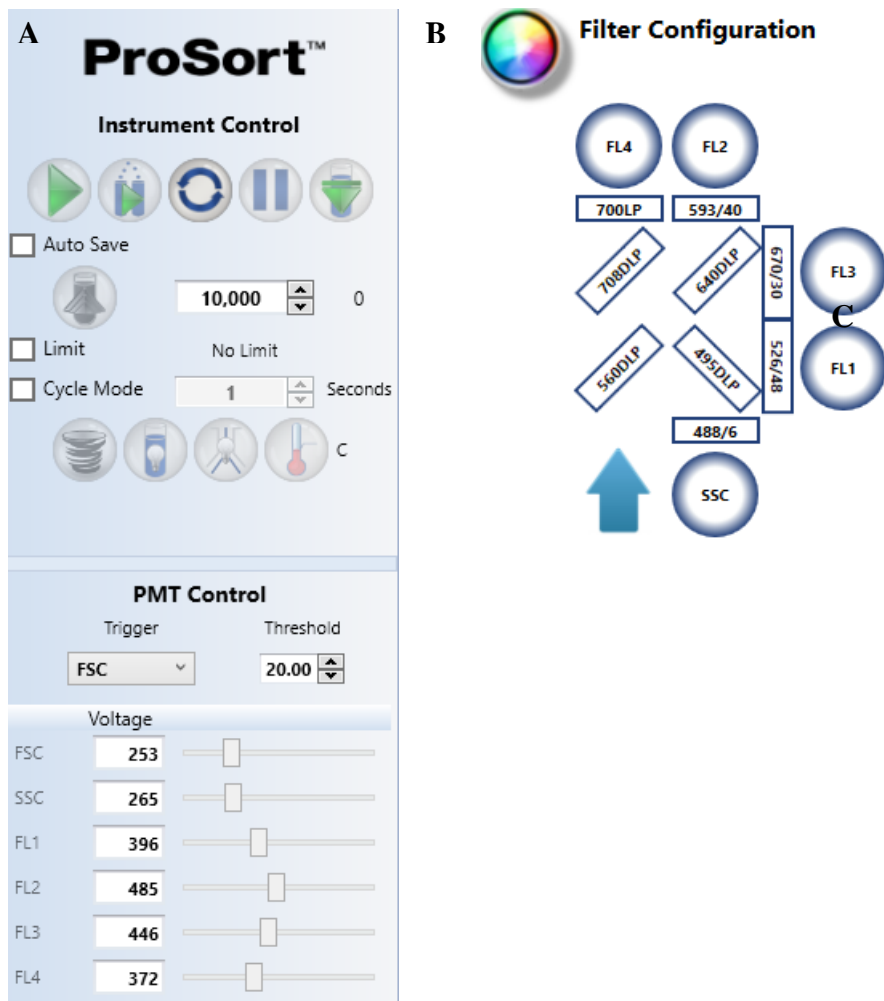


Figure 10: Laser voltage (A) and filter configuration (B) used.

Samples were transferred to polystyren FACS tubes using disposable bacterial filter (\emptyset 50 μ m, Sysmex). Targeted GFP cells were subsequently sorted into FACS tubes containing 100 μ L of TRIzol Reagent (Ambion). Tube caps were covered with parafilm and stored at -80 $^{\circ}$ C.

To control whether the sorted cells were the required HmlGFP cells, the sorted cells were further analyzed under inverted microscope (Olympus IX71, Fig. 9C, D and E).

3.9. Isolation of RNA

Samples in TRIzol Reagent were transferred from FACS tubes to eppendorf microtubes, where they were homogenized using DEPC-treated pestle. 900 μ L of TRIzol Reagent and 200 μ L of chloroform was added. Afterwards, each sample was properly mixed by vortexing (at least for 20 - 30 seconds) and left for 10 minutes at room temperature. Samples were then centrifuged (15 min, 4 $^{\circ}$ C, 14 000 RPM). After that, aqueous phase was transferred to a fresh microtube, which was placed on ice and 2 μ L of glycogen was added. This step improved pellet visualization. 500 μ L of 100% isopropanol was added and samples were then kept on ice for 10 minutes. Thereafter, samples were centrifuged (10 min, 4 $^{\circ}$ C, 14 000 RPM), supernatant was removed and 500 μ L of 75 % EtOH (96% EtOH in DEPC H₂O) was added to the pellet. Samples were centrifuged again (5 min, 4 $^{\circ}$ C, 14 000 RPM), supernatant was then carefully removed and pellet was centrifuged (1 min, 4 $^{\circ}$ C, 14 000 RPM). Rest of EtOH was removed and in order to get rid of the final residue, microtubes were left open for approximately 3 minutes in room temperature. Isolated RNA was dissolved in 15 μ L DEPC H₂O. Concentration and purity of isolated RNA was evaluated on *NanoDrop* spectrophotometer (UVS-99 ACTGene).

3.10. Reverse transcription

1 μ L of 50 μ M oligo(dT)₂₀ primer (5'-d(TTTTTTTTTTTTTTTTTTTTTT)-3', KRD), 4 μ L of 20 μ M dNTPs and 2 μ L of DEPC H₂O was added to 7 μ L of each sample. In order to make sure that all components were mixed in one drop, all samples were shortly centrifuged in Eppendorf's MiniSpin. Microtubes were then placed in thermoblock at 65 $^{\circ}$ C for 5 minutes and right after that samples were transferred on ice for 1 minute and then shortly centrifuged again. Afterwards, 1 μ L of 0,1M DTT, 4 μ L of 5x FS III buffer, and 1 μ L of SS III reverse transcriptase (all from Invitrogen) was added to each sample. Samples were then incubated at 50 $^{\circ}$ C for 50 minutes. Final incubation was performed at 75 $^{\circ}$ C for 15 minutes.

3.11. qPCR

To each sample from reverse transcription 230 μ L of dH₂O was added. Afterwards, to 3 μ L of each sample 6 μ L of TP 2x SYBR Master Mix (Top-Bio), 0,25 μ L of 20 μ M forward primer (KRD), 0,25 μ L of 20 μ M reverse primer (KRD) and 2,5 μ L of PCR ultra H₂O (Top-Bio) was added. Each sample was measured in triplicates in 96-well plate (Bio-Rad) covered

with Microseal® 'C' Film (Bio-Rad) and polytetrafluoroethylene sealing mat (Bio-Rad) using CFX 1000 Touch Real-Time Cycler (Bio-Rad). Following qPCR protocol was used:

95°C 3 min	40x
94°C 15 sec denaturation	
54°C 30 sec annealing	
72°C 40 sec elongation	
fluorescence detection	
melting curve analysis 65 – 85°C/step 0,5°C	

qPCR data were analyzed using double delta Ct analysis. Gene expression was standardized relative to gene expression of Rp L32 (Rp49). Expression pattern of Rp L32 was also checked with actin. Sequences of primers used are shown below:

Act	Forward	5'TACCCATTGAGCACGGTAT3'
	Reverse	5'GGTCATCTTCTCACGGTTGG3'
Cis	Forward	5'TTCGATTGACTCCAGCCTGG3'
	Reverse	5'AGCCGGGAACACCTGTCC3'
ImpL2	Forward	5'TTCGCGGTTTCTGGGCACCC3'
	Reverse	5'GCGCGTCCGATCGTCGCATA3'
ImpL3	Forward	5'CAGAGAAGTGGAACGAGCTG3'
	Reverse	5'CATGTTTCGCCAAAACGGAG3'
Eno	Forward	5'CAACATCCAGTCCAACAAGG3'
	Reverse	5'GTTCTTGAAGTCCAGATCGT3'
Gapdh1	Forward	5'TTG TGG ATC TTA CCG TCC GC3'
	Reverse	5'CTCGAACACAGACGAATGGG3'
HexA	Forward	5'ATATCGGGCATGTATATGGG3'
	Reverse	5'CAATTCGCTCACATACTTGG3'

Pfk	Forward	5'AGCTCACATTTCCAAACATCG3'
	Reverse	5'TTGATCACCCAGAATCACTGC3'
Pgi	Forward	5'ACTGTCAATCTGTCTGTCCA3'
	Reverse	5'GATAACAGGAGCATTCTTCTCG3'
Rp49	Forward	5'AAGCTGTTCGCACAAATGGCG3'
	Reverse	5'GCACGTTGTGCACCAGGAAC3'
CG10219	Forward	5'GAGATCTCCGTGAGTGCGC3'
	Reverse	5'CTCCACGCCCCAATGGG3'
Scsα	Forward	5'TCACAAGCGCGGCAAGATC3'
	Reverse	5'TTGATGCCCGAATTGTACTCG3'
Tpi	Forward	5'AGATCAAGGACTGGAAGAACG3'
	Reverse	5'ACCTCCTTGGAGATGTTGTC3'

3.12. NBDG

Infected Hml GFP adults were placed at 24hpi on cornmeal diet with added 200 µL of 2-NBDG (excitation/emission maxima of ~ 465/540 nm, 5 mg/ml stock – used 10 000x diluted, Thermo-Fisher). To analyze the sites of fluorescently labeled deoxyglucose accumulation, after another 24 hours adults were prepared for microscopy (Olympus IX71).

3.13. Confocal microscopy

Infected *Drosophila* adults were dipped in 75% EtOH for one second and the fixation was performed with 4% paraformaldehyde on rotor for 45 minutes at room temperature. Afterwards, samples were washed three times using PBS for 10 minutes per each washing. Eventually, samples were observed using confocal microscopy (Olympus FluoView 1000) and picture analysis was performed using Fiji software.

3.14. Statistics and data processing

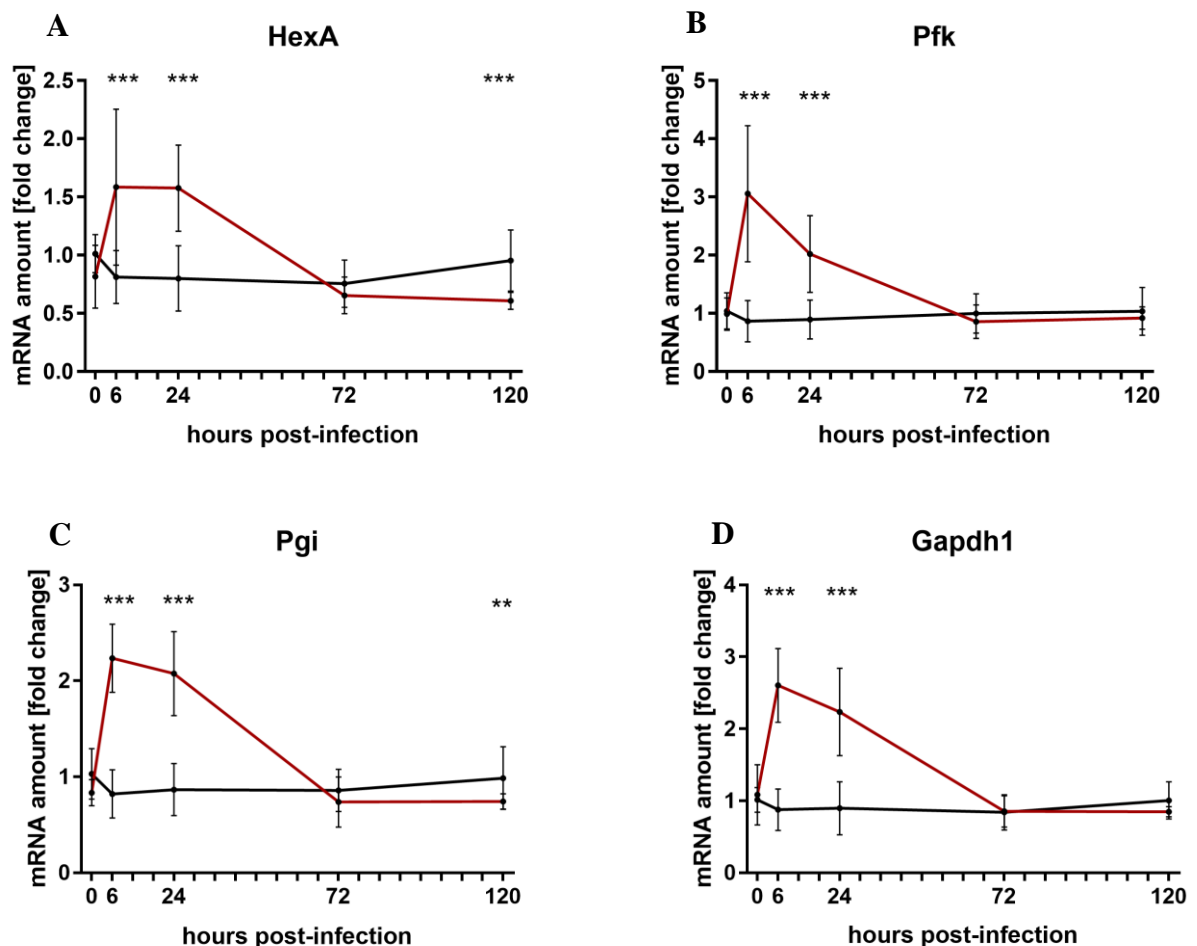
For statistical comparison of various groups and treatments in experiments with quantification of gene expression, metabolites and colony forming units the Two-Way ANOVA with multiple comparisons was used - Tukey multiple comparisons test. Due to the multiple comparisons of the data set the Sidak's multiple comparison correction was made. The normality of the data was tested by both D'Agostino-Pearsons and Sharpio-Wilk tests and the homogeneity was tested by Bartlett's test of homogeneity of variances. The survival analysis was visualized using GraphPad Prism 7. Survival curves were assessed using Gehan-Breslow-Wilcoxon test. Statistical significance is presented in graphs in a following manner: p-value $\leq 0,05$ one asterisk (*), p-value $\leq 0,01$ two asterisks (**), p-value $\leq 0,001$ three asterisks (***). Figure with HRE sequences (Fig. 29) was created using Genius R6 6.1.8 software.

4. RESULTS

4.1. Activated macrophages show temporarily increased expression of glycolytic enzymes

To evaluate the hypothesis, that upon infection, immune cells of *D. melanogaster* show certain metabolic changes, gene expression of glycolytic enzymes and enzymes of the Krebs cycle was measured. Cell sorting technology and UAS-Gal4 system allowed us to measure this expression specifically in hemocytes of HmlGal4>GFP adults.

The data from *Sp* infected adults show that the expression of glycolytic enzymes is increased already at 6hpi. Also at this timepoint some of the glycolytic enzymes peaked (Pfk, Pgi, Gapdh1, Tpi, ImpL3), while the expression at 6hpi of some of the other enzymes was similar as the expression at 24hpi (HexA, Eno). At later timepoints (72hpi and 120hpi) the expression of glycolytic enzymes of infected individuals was already reduced to the level of noninfected flies (Fig. 11). The gene expression of lactate dehydrogenase (ImpL3), which is considered to be the crucial enzyme of increased aerobic glycolysis, was approximately three times increased at 6hpi compared to the noninfected control flies (Fig. 11G).



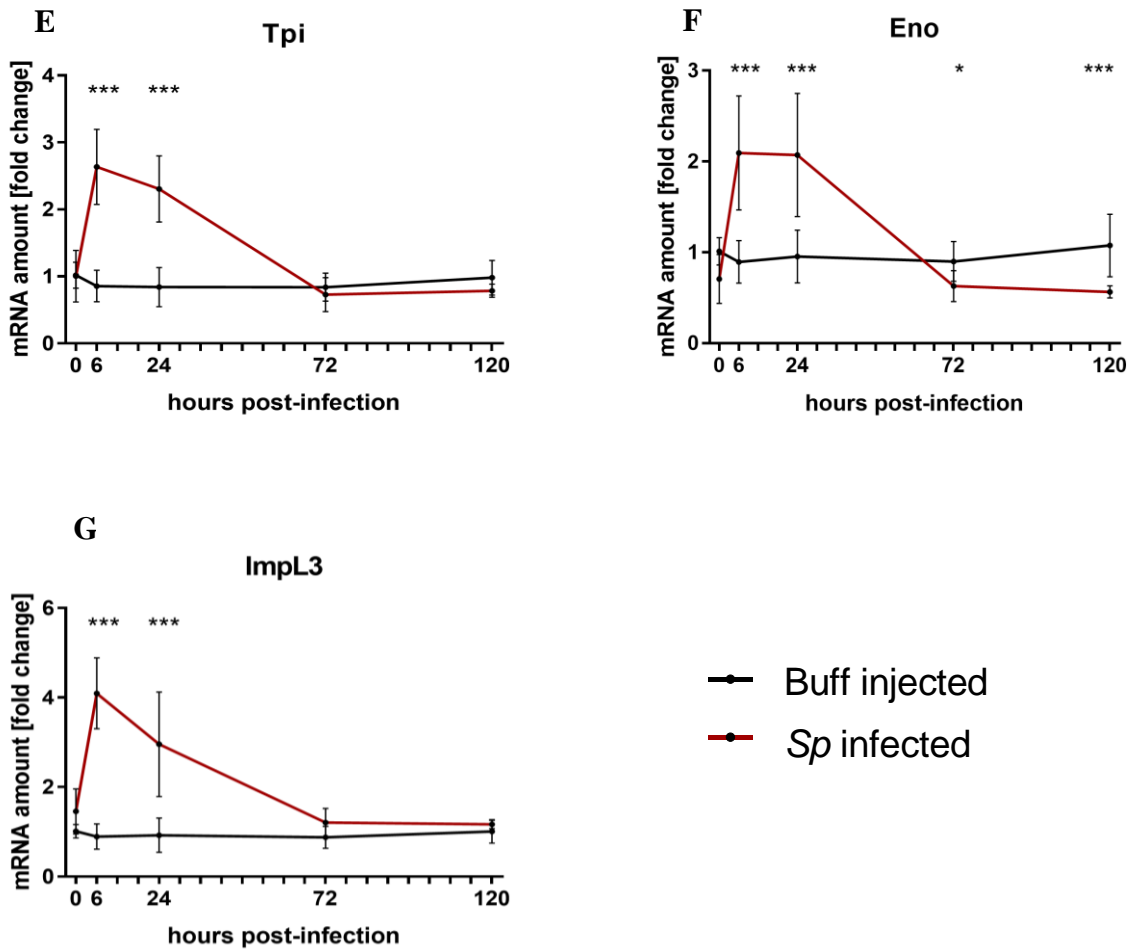


Figure 11: Gene expression of HexA (A), Pfk (B), Pgi (C), Gapdh1 (D), Tpi (E), Eno (F) and ImpL3 (G) of infected adults (red line) at 0, 6, 24, 72 and 120hpi compared to noninfected control flies (black line). The graphs show combined data from three independent experiments. Average number of individuals was approximately 600 per each genotype. Error bars represent standard deviation. P-value was determined using Two-Way ANOVA (Sidak's multiple comparisons test) as follow: P-value for HexA at 120hpi = 0,0003, all other p-values were <0,0001.

We were also interested in the expression of enzymes of the Krebs cycle. There was not observed any changed expression of Cis and CG10219 at 6hpi and 24hpi, nonetheless, the mRNA level of Cis, CG10219 and Scsa was reduced at 72hpi and 120hpi (Fig. 12). mRNA level of Scsa was increased at 6hpi compared to noninfected control flies.

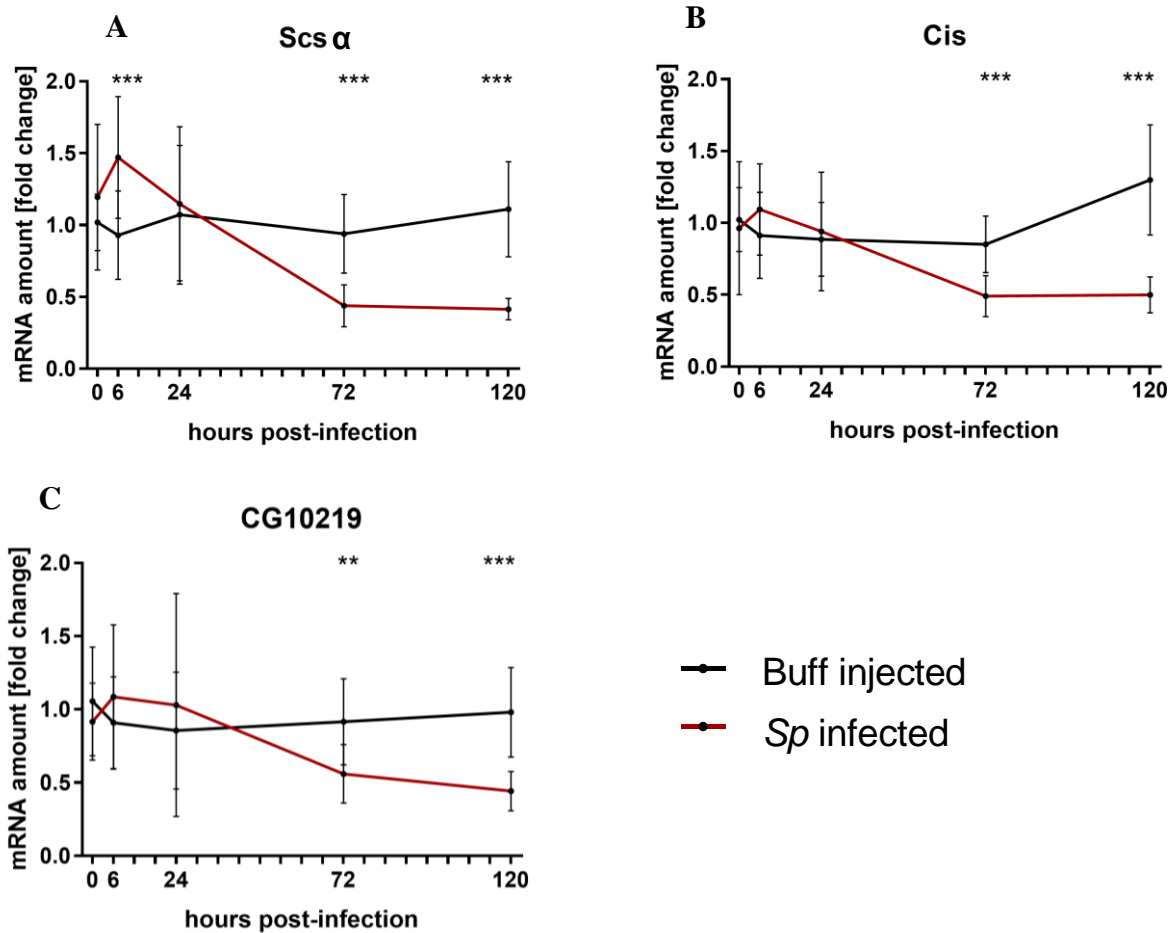


Figure 12: Gene expression of Scs α (A), Cis (B) and CG10219 (C) in infected individuals at 0, 6, 24, 72 and 120hpi compared to noninfected control flies. The graphs show combined data from three independent experiments. Average number of individuals was approximately 600 per each genotype. Error bars represent standard deviation. P-value was determined using Two-Way ANOVA (Sidak's multiple comparisons test) as follow: P-value for CG10219 at 72hpi = 0,0047, all other p-values were <0,0001.

Based on presented data we can claim that expression of glycolytic genes is significantly but transiently increased in response to bacterial infection. The expression of TCA cycle genes is not significantly influenced at early time-points, however, there is obvious decrease in expression of all the TCA genes measured later after infection.

4.2. Metabolic changes of *Drosophila* macrophages *in vivo/in situ*

Since our results have suggested dramatic changes of expression of glycolytic genes in response to infection, we wanted to see whether this increase is also connected with increased glucose consumption. To test if hemocytes of *D. melanogaster* show increased glucose uptake upon infection, fluorescently labeled deoxyglucose 2-NBDG was employed.

Macrophages of infected individuals show an increased accumulation of 2-NBDG, whereas hemocytes of noninfected flies exhibit no significant glucose accumulation (Fig. 13, 14, 15), suggesting that *Sp* infection triggers increased glucose consumption by activated immune cells, which are more competitive in gaining energy sources compared to other tissues.

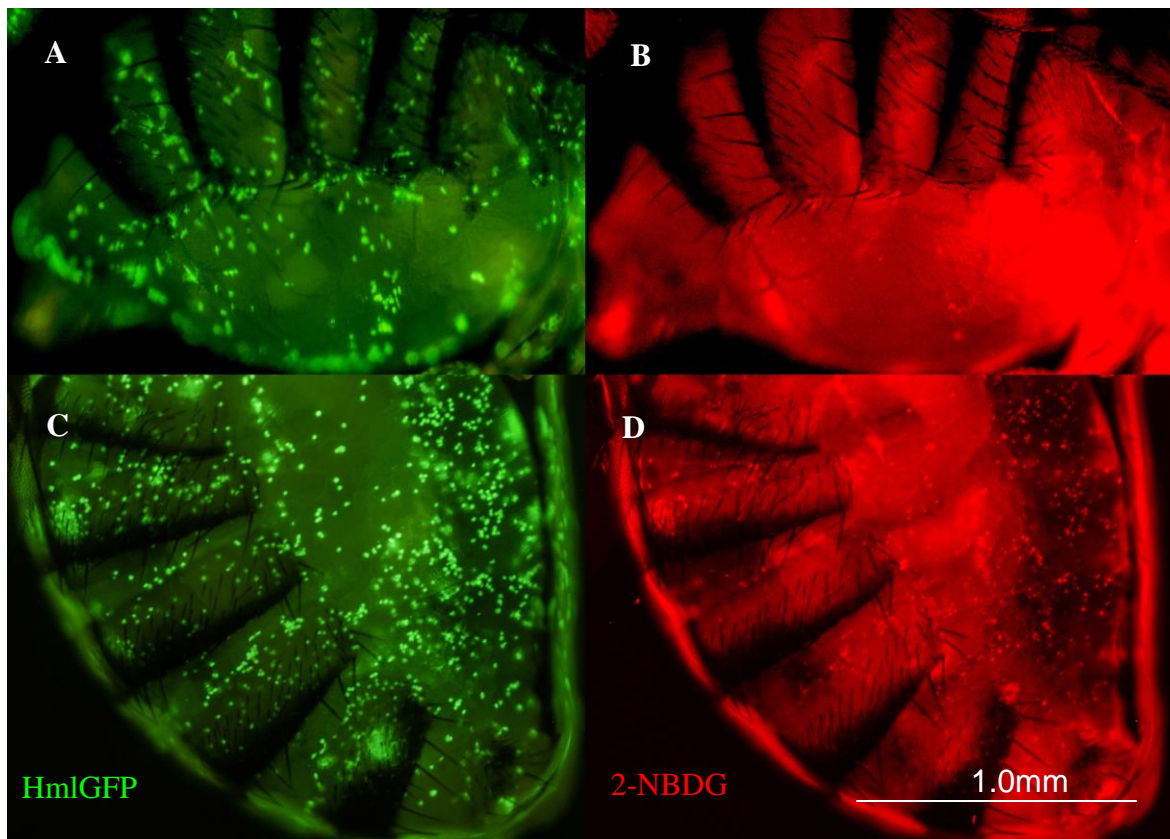


Figure 13: Fluorescent images of hemocytes (HmlGFP) (A, C) and sites with 2-NBDG accumulation (B, D) created using inverted microscope. Images A and B represent abdomen of noninfected control fly and images C and D show abdomen of *Sp* infected *Drosophila*.

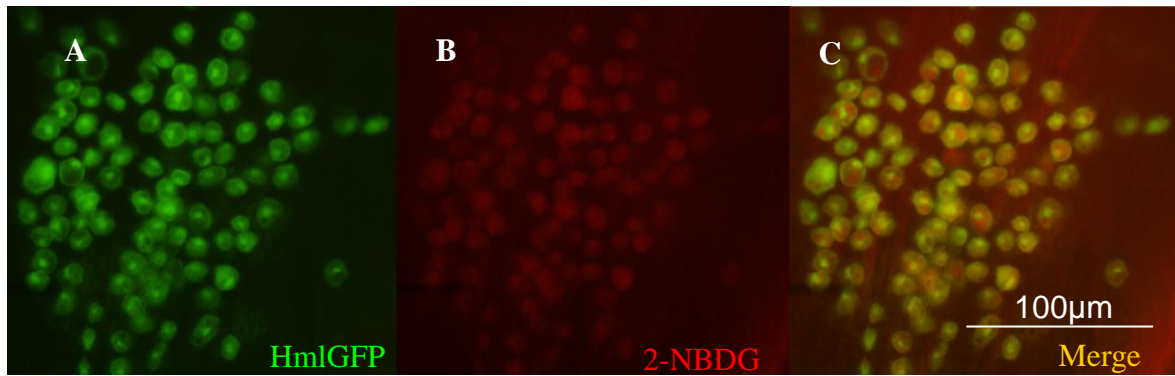


Figure 14: Fluorescent image of hemocytes in infected adults *in vivo* (HmlGFP) (A), sites with 2-NBDG accumulation (B) and merged image (C) created using inverted microscope.

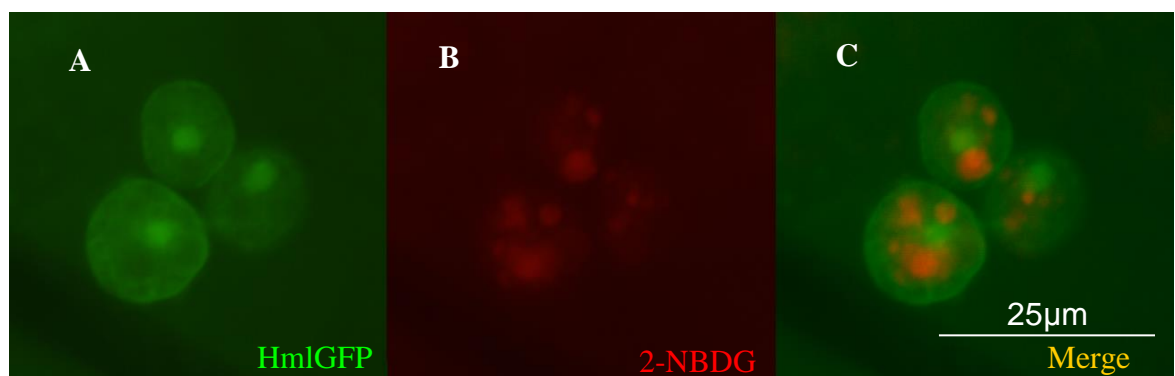


Figure 15: Detailed fluorescent image of hemocytes in infected adults *in vivo* (HmlGFP) (A), sites with 2-NBDG accumulation (B) and merged image (C) created using inverted microscope.

Localization of lactate dehydrogenase expression in adult flies was examined using confocal microscopy to further identify metabolic processes in immune cells. Flies producing LDH fused with red fluorescent protein mCherry and with fluorescently labeled hemocytes (HmlGFP) were used for this experiment (cross no1 in section 3.3. Crosses. Cross-reference to the figure adopted from Jason Tennesen (Fig. 5)). Localization of lactate dehydrogenase expression in adult flies was examined using confocal microscopy. Confocal microscopy revealed that LDH mCherry localization shows a pattern, which is characteristic for localization of hemocytes. Furthermore, there is a high level of colocalization of hemocytes with LDH marker, while no other tissue shows such a strong expression of LDH (Fig. 16 and Fig. 17). There was no obvious increase in fluorescence level upon infection.

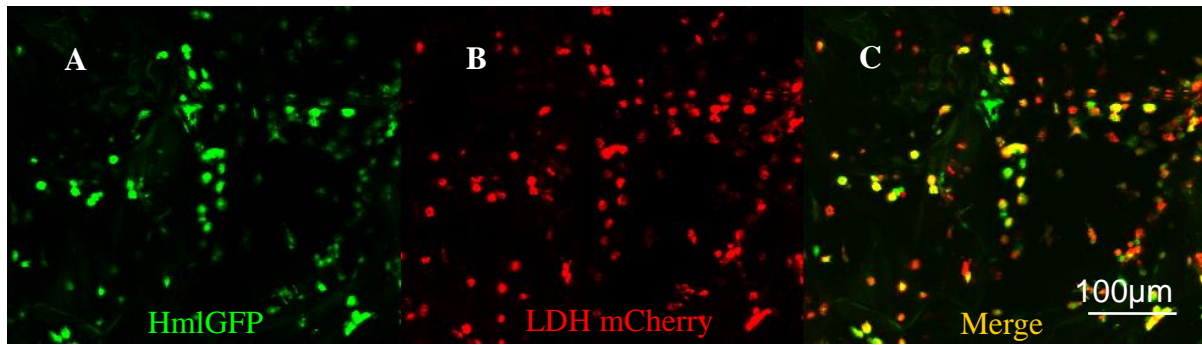


Figure 16: Fluorescent image of hemocytes *in vivo* (HmlGFP) (A), sites with red fluorescent protein LDH mCherry (B) and merged image (C) created using confocal microscopy.

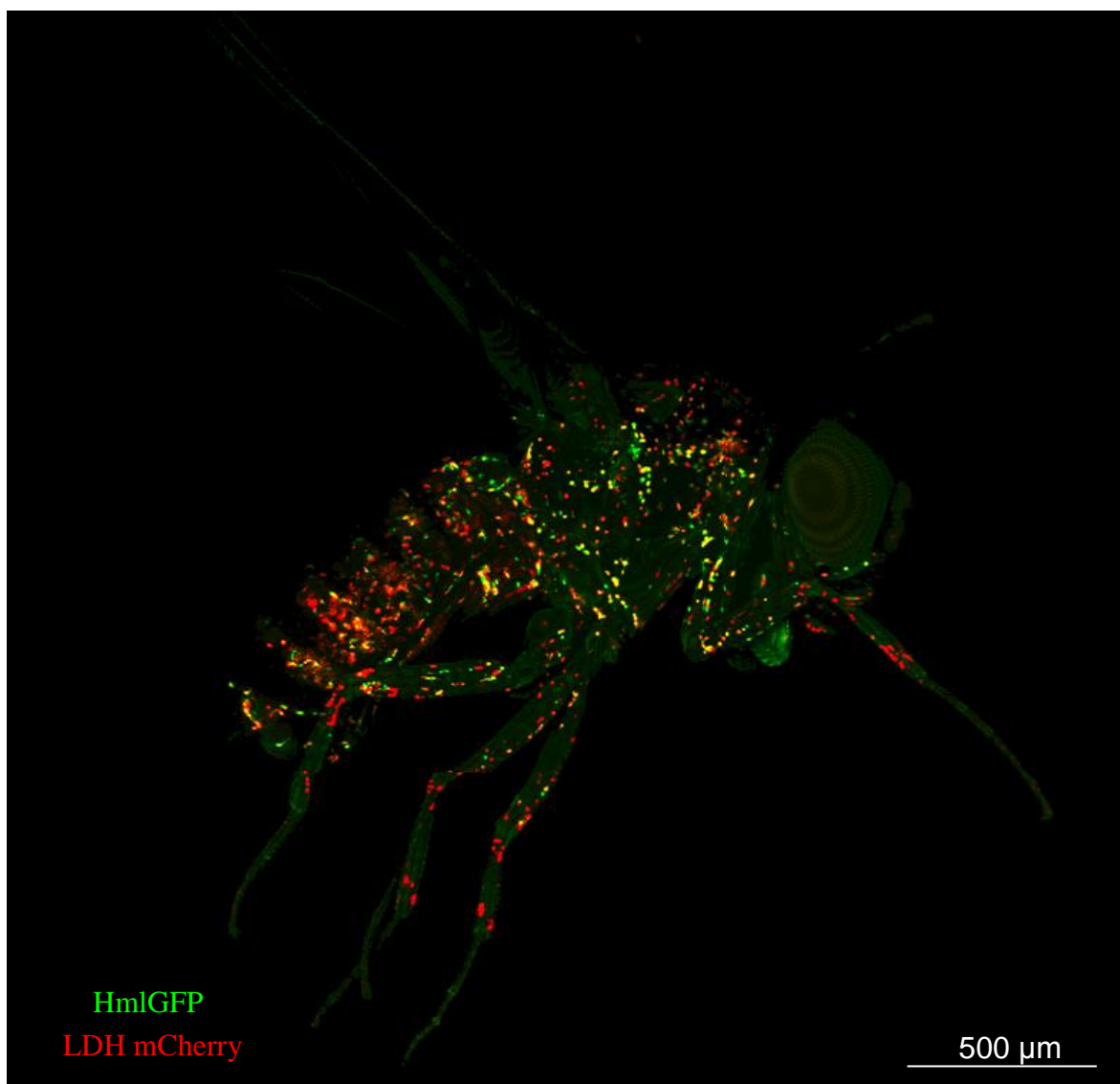


Figure 17: Colocalization of enzyme lactate dehydrogenase (LDH mCherry, red) with immune cells (HmlGFP, green) of *D. melanogaster*. Image captured with confocal microscopy.

The next question was whether the changes in expression of glycolytic genes and LDH, which are known to be HIF1 α target, colocalize with the site of HIF1 α activity. Since HIF1 α is constitutively expressed and degraded in all tissues, expression and immunolocalization techniques often fails to prove its activation. Therefore artificial construct producing LacZ enzyme under HIF1 α specific target domain (hypoxia response element, HRE) was employed. Specific binding of HIF1 α -HRE was described previously (Poon et al., 2009; Maxwell, 2005; Wang et al., 1995). To demonstrate if HRE is activated upon infection, X-gal staining of infected HRE LacZ adults was performed.

Figure 18 shows that cells resembling localization of macrophages of infected individuals were stained blue at 24hpi, whilst hemocytes of noninfected control flies remained unstained, meaning that *Sp* infection triggers activation of HRE in immune cells. This observation clearly shows that HIF1 α is stabilized in activated immune cells and enters nucleus where it binds HRE and activates target genes. Since HRE is present in gene sequence of many metabolic and mainly glycolytic genes we suggest that transcription factor HIF1 α is responsible for increased expression of metabolic genes observed and thus for global metabolic changes in activated immune cells.



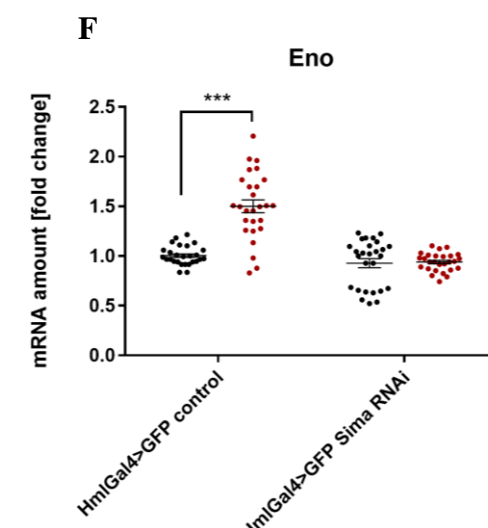
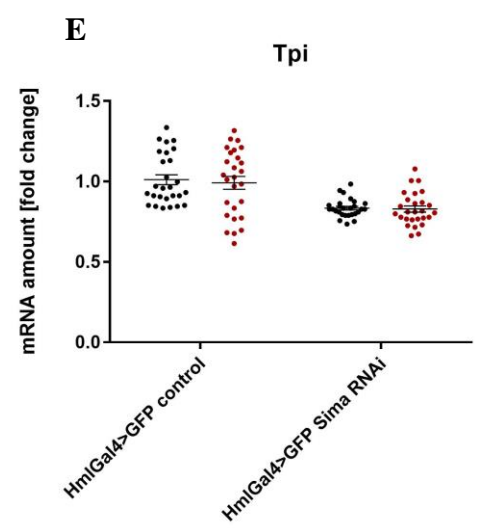
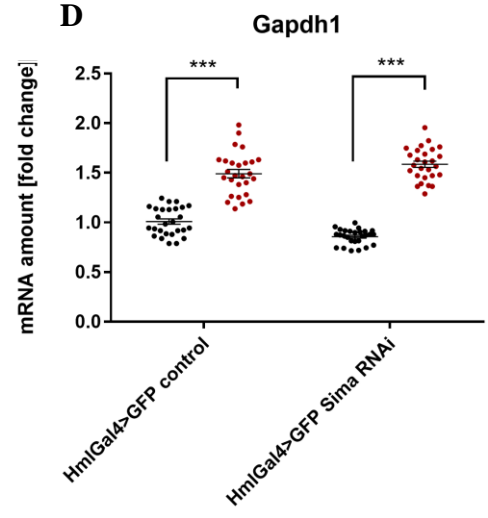
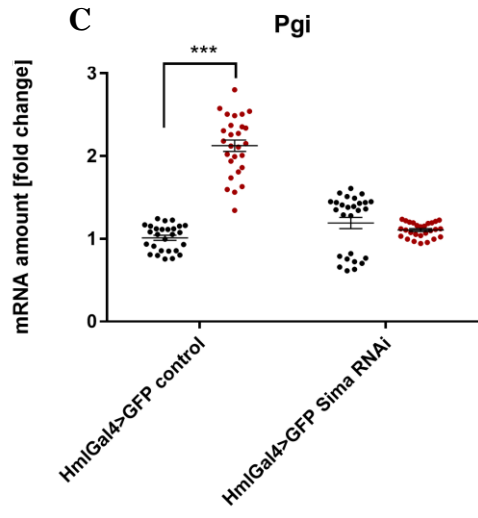
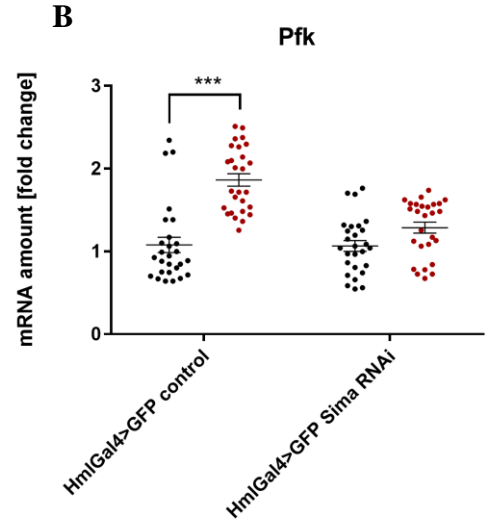
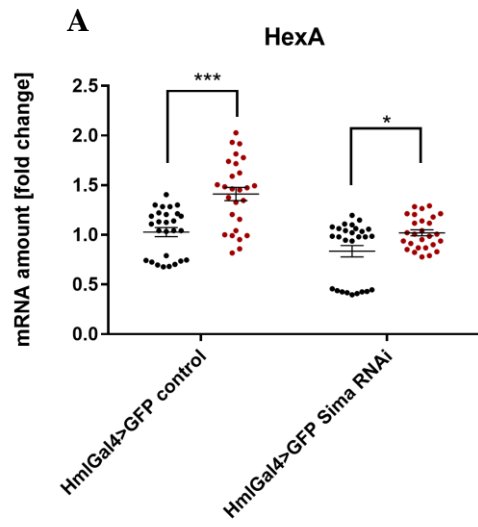
Figure 18: X-gal staining of infected (A) and noninfected (B) individuals containing HRE HRE CRE regulatory sequence in front of the LacZ coding sequence. Two biological replicates for both treatments were performed, N=10.

4.3. Transcription factor HIF1 α plays an important role in macrophage polarization

Since previous experiment clearly showed that HIF1 α is stabilized in activated immune cells, the next step was to knockdown HIF1 α expression and then observe the impact of this treatment on the expression of metabolic enzymes in activated immune cells. Therefore hemocyte specific HIF1 α RNAi was performed as it should prevent the regulatory function of HIF1 α . Gene expression of metabolic enzymes in hemocytes of infected Sima RNAi flies was then measured (cross no2 in section 3.3. Crosses).

The data from qPCR analysis show that infected Sima RNAi adults do not exhibit the rise in mRNA level of Eno, Pgi and Pfk compared to infected control flies. However, HexA and ImpL3 do not show such a strong effect of RNAi since they were partially increased. Nonetheless, compared to infected control flies this increase was much lower. However, not all genes responded the way we expected since Tpi expression was not increased in response

to infection in this set of samples. This observation requires further analyses. Only one glycolytic enzyme measured (Gapdh1) shows the rise in mRNA level which is comparable to the level of infected control adults (Fig. 19), suggesting that Gapdh1 is not regulated via HIF1 α . Taken together, the data suggest that HIF1 α is an important transcription factor responsible for increased expression level of many, however not all, glycolytic genes measured and influence of another factor or more complex mechanism cannot be excluded.



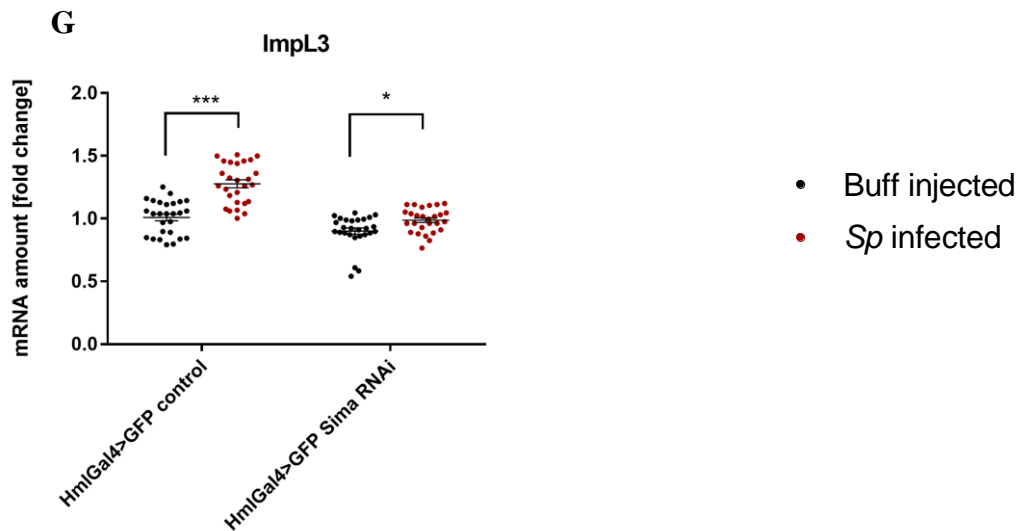


Figure 19: Gene expression of HexA (A), Pfk (B), Pgi (C), Gapdh1 (D), Tpi (E), Eno (F) and ImpL3 (G) of infected Sima RNAi adults at 24hpi compared to control flies. The graphs show combined data from three independent experiments. Average number of individuals was more than 650 per each genotype. The graphs display both biological and technical replicates. Error bars represent standard deviation. P-value was determined using Two-Way ANOVA (Sidak's multiple comparison test) as follow: P-value for HexA <0,0001 (HmlGal4>GFP control) and 0,0272 (HmlGal4>GFP Sima RNAi), p-value for Pfk <0,0001 (HmlGal4>GFP Sima RNAi), p-value for Pgi <0,0001 (HmlGal4>GFP Sima RNAi), p-value for Gapdh1 <0,0001 (both HmlGal4>GFP control and HmlGal4>GFP Sima RNAi), p-value for Eno <0,0001 (HmlGal4>GFP Sima RNAi) and p-value for ImpL3 <0,0001 (HmlGal4>GFP control) and 0,0361 (HmlGal4>GFP Sima RNAi).

Our previous studies showed that the metabolic changes and increased glucose consumption are connected with production of factors responsible for systemic metabolic changes (Bajgar and Dolezal, unpublished). Therefore the effect of Sima RNAi on systemic metabolism during infection was analyzed. To evaluate, whether HIF1 α has an impact also on the level of systemic metabolism, glucose and glycogen concentrations in infected Sima RNAi flies were measured.

While noninfected individuals of both control (cross no7 in section 3.3. Crosses) and experimental RNAi genotype (cross no6 in section 3.3. Crosses) do not change their glucose concentration, the glucose concentration is significantly increased in infected control flies after infection (p-value <0,0001). After 48hpi the concentration levels out to the amount at 0hpi (Fig. 20). This increase in glucose concentration after infection is in accordance with previously published data of our laboratory (Bajgar and Dolezal, accepted). However, this increase was not observed in infected Sima RNAi flies, meaning that downregulated HIF1 α

prevents the flies from hyperglycemia after infection.

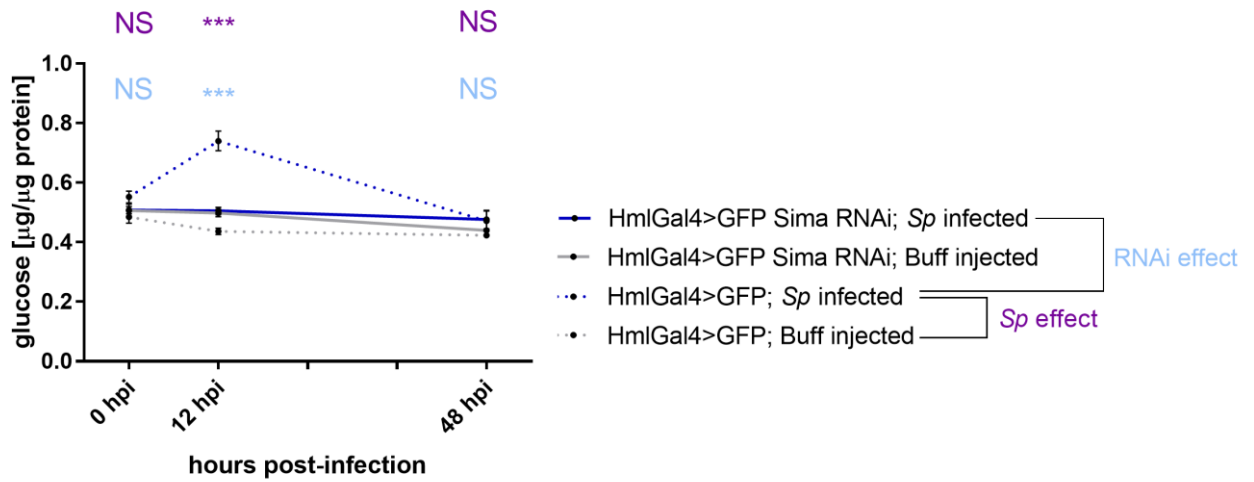


Figure 20: The concentration of free glucose per μg of protein at 0, 12 and 24hpi in adults with Sima knockdown. The graph shows combined data from four independent experiments. The number of individuals was 20 per each genotype. Error bars represent standard deviation. *Sp* effect was determined as a p-value of HmlGal4>GFP; *Sp* infected compared to HmlGal4>GFP; Buff injected and RNAi effect was determined as a p-value of HmlGal4>GFP; *Sp* infected compared to HmlGal4>GFP Sima RNAi; *Sp* infected. P-value <0,0001 for both RNAi and *Sp* effect was determined using Two-Way ANOVA with multiple comparisons (Tukey multiple comparisons test). Solid lines represent RNAi groups and dashed lines represent control genotype. Blue color represents infected individuals and grey color represents flies injected with buffer.

Whilst glucose measurement revealed some interesting facts, glycogen gauging does not exhibit such indisputable data. The glycogen concentration at 0hpi varies between all four groups measured (Fig. 21) even though it should not since the infection cannot have any effect at this timepoint. The glycogen concentration varies between both RNAi groups ($p = 0,0025$) as well as between HmlGFP groups ($p\text{-value} < 0,0001$). Owing to this matter, a graph with normalized concentration of glycogen at 0hpi was created in order to equalize the concentration differences in all four groups (Fig. 22). The data then show that at 12hpi the glycogen concentration is similar between both noninfected genotypes (Sima RNAi as well as the control genotype) and both infected genotypes exhibit decreased glycogen concentration, where the level in Sima RNAi flies seems to be lower compared to control genotype. This data then might suggest that upon infection Sima RNAi flies are not able to metabolize glycogen as efficiently as infected control adults, however, it was not statistically significant ($p\text{-value} = 0,1318$). Nevertheless, this glycogen data should not be used for

deducing any final conclusions about the impact of HIF1 α on the systemic metabolism.

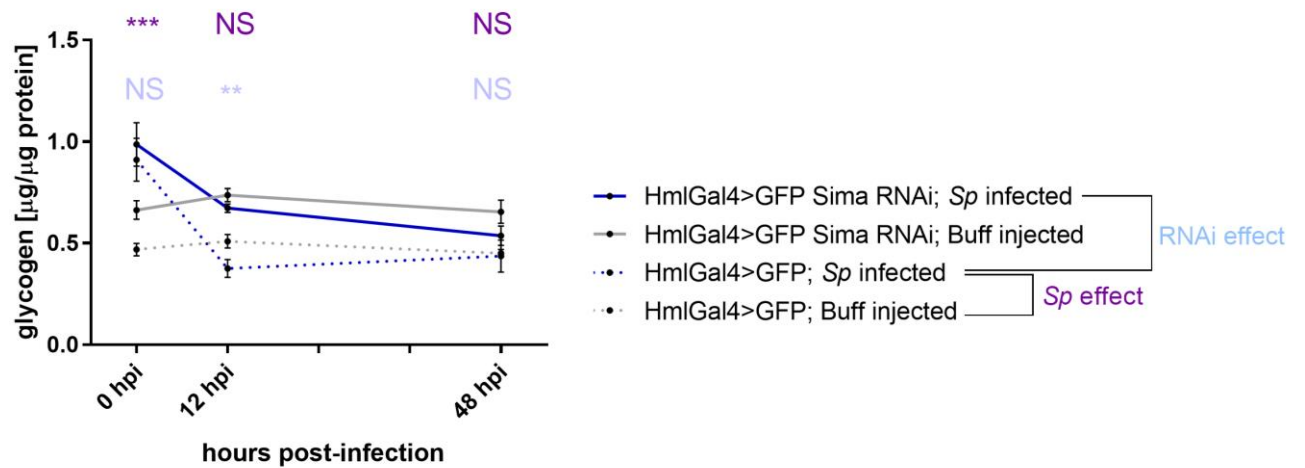


Figure 21: The concentration of glycogen per μg of protein at 0, 12 and 24hpi in adults with Sima knockdown. The graph shows combined data from four independent experiments. The number of individuals was 20 per each genotype. Error bars represent standard deviation. *Sp* effect was determined as a p-value of HmlGal4>GFP; *Sp* infected compared to HmlGal4>GFP; Buff injected and RNAi effect was determined as a p-value of HmlGal4>GFP; *Sp* infected compared to HmlGal4>GFP Sima RNAi; *Sp* infected. P-value <0,0001 for *Sp* effect and p-value = 0,0058 for the effect of RNAi was determined using Two-Way ANOVA with multiple comparisons (Tukey multiple comparisons test). Solid lines represent RNAi groups and dashed lines represent control genotype. Blue color represents infected individuals and grey color represents flies injected with buffer.

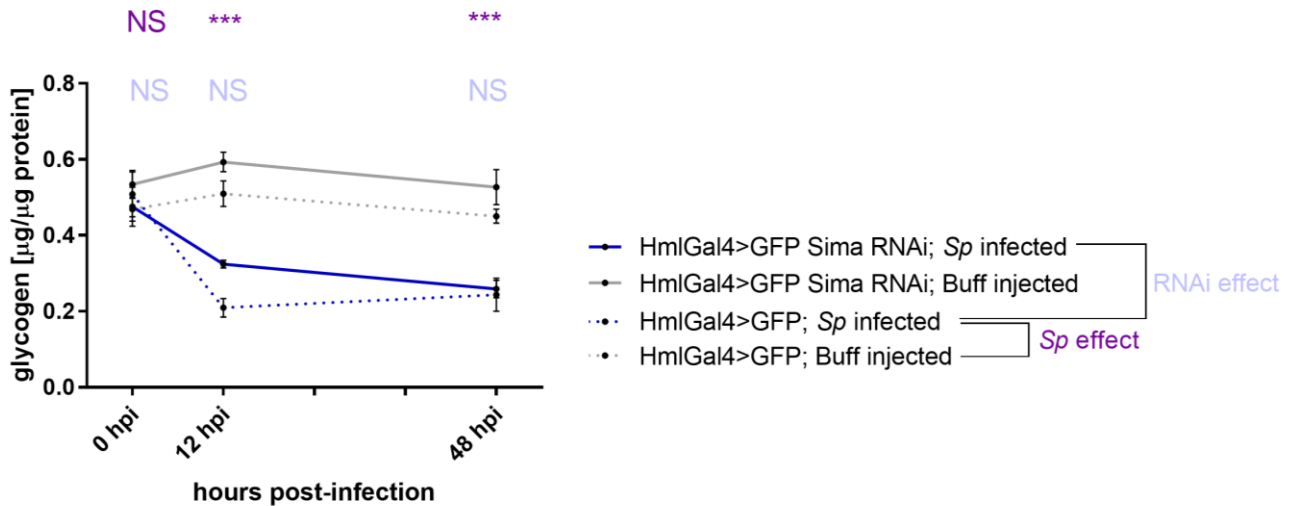


Figure 22: The normalized concentration of glycogen per μg of protein at 0, 12 and 24hpi in adults with Sima knockdown. The graph shows combined data from four independent experiments. The number of individuals was 20 per each genotype. Error bars represent standard deviation. *Sp* effect was determined as a p-value of HmlGal4>GFP; *Sp* infected compared to HmlGal4>GFP; Buff injected and RNAi effect was determined as a p-value of HmlGal4>GFP; *Sp* infected compared to HmlGal4>GFP Sima RNAi; *Sp* infected. P-value <0,0001 at 12hpi and p-value = 0,0015 at 48hpi for *Sp* effect was determined using Two-Way ANOVA with multiple comparisons (Tukey multiple comparisons test). Solid lines represent RNAi groups and dashed lines represent control genotype. Blue color represents infected individuals and grey color represents flies injected with buffer.

4.4. Enzyme lactate dehydrogenase and HIF1 α protein are necessary for effective elimination of bacterial infection

To prove that increased expression of glycolytic enzyme lactate dehydrogenase during infection is essential for effective immune response to bacterial infection, survival of infected flies with knockdowned ImpL3 gene in immune cells (cross no8 in section 3.3. Crosses) was observed (Fig. 23). For this tissue and time specific knockdown UAS-Gal4Gal80 system was used. Fly lines with normal production of ImpL3 gene was used as a control (cross no9 in section 3.3. Crosses).

Flies with ImpL3 RNAi show significantly faster death compared to control genotype (p-value <0,0001). While half of the individuals with ImpL3 RNAi is already dead at eighth day after infection, control flies experienced the medium time to death at seventeenth day after infection and this dying slowly proceeds until the end of the experiment.

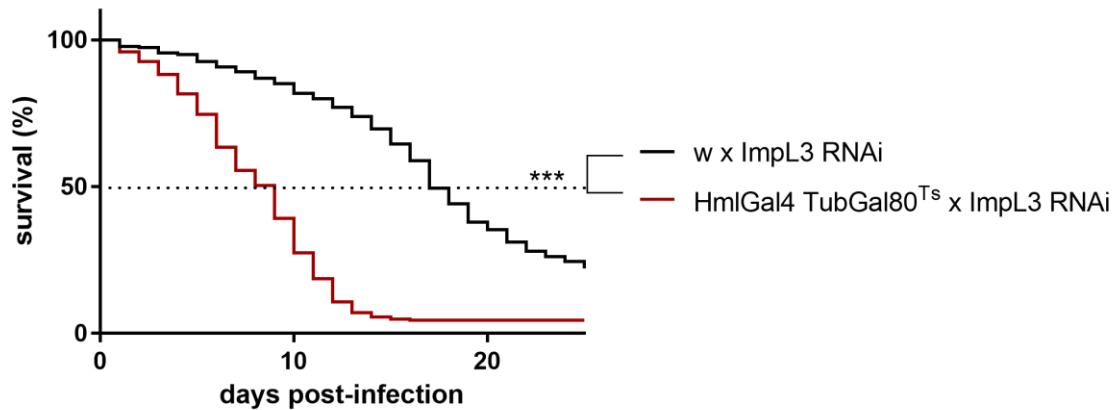


Figure 23: Survival of ImpL3 RNAi flies after *Sp* infection compared to infected control flies. Survival curves show combined data from three independent experiments. Average number of individuals was more than 500 per each genotype. Gehan-Breslow-Wilcoxon test has been run to obtain p-value <0,0001.

Similarly, survival of infected flies with knockdowned HIF1 α gene in immune cells (fly line HmlGal4Gal80 x UAS Sima RNAi KK line and TRiP line, cross no4 and cross no6 in section 3.3. Crosses) was also observed. Flies with HIF1 α RNAi show significantly faster death compared to control genotype (p<0,0001 for both KK and TRiP line). The medium time to death for individuals with HIF1 α RNAi was the fifth day (TRiP line) and ninth day (KK line) after infection, while for control flies it was the twenty-first (TRiP line) and twenty-third (KK line) day, which was the last day of the experiment (Fig. 24).

These survival data clearly identified that both LDH and Sima are essential for proper immune response to pathogenic bacteria.

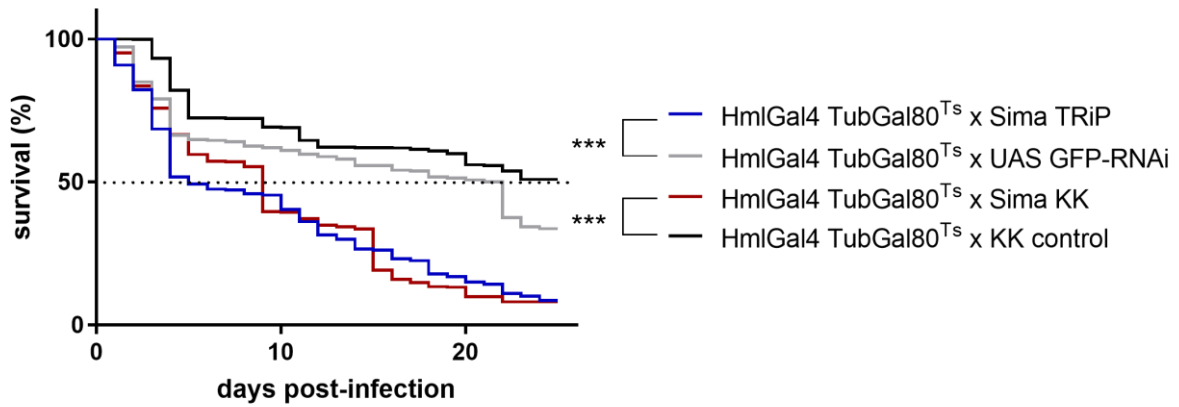


Figure 24: Survival of HIF1 α RNAi flies after *Sp* infection compared to infected control flies. Survival curves show combined data from three independent experiments. Average number of individuals was more than 600 per each genotype. Gehan-Breslow-Wilcoxon test has been run to obtain p-value <0,0001 for both KK and TRiP line.

To determine, whether the infected flies died due to low tolerance or due to low resistance to the infection and to evaluate the effectiveness of phagocytosis, CFUs (see 2.5 Colony forming units (CFUs)) were performed for both survival experiments at 0, 18, 24 and 48hpi.

Concerning the CFUs for the experiment with knockdowned ImpL3, no difference between the experimental and control genotype was observed at 18hpi (T1), however at 24hpi (T2), a statistically significant difference (p-value = 0,0463) occurred and got even stronger at 48hpi (T3) (p-value = 0,0062) (Fig. 25).

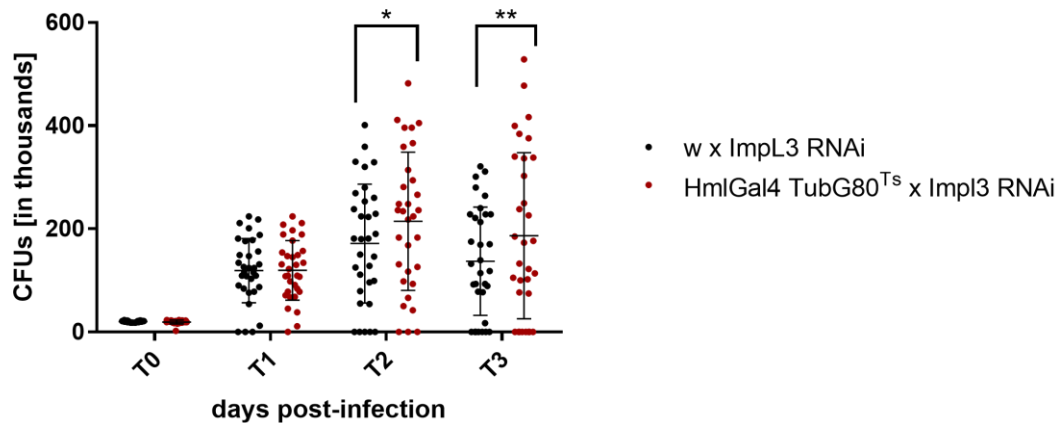


Figure 25: Growth rate of bacterial colonies in infected ImpL3 RNAi individuals compared to infected control flies. Resulting graph shows combined data from three independent experiments. The overall number of individuals equaled 32 per each genotype. P-value = 0,0463 for T2 and p-value = 0,0062 for T3 was determined using Two-Way ANOVA with multiple comparisons (Tukey multiple comparisons test).

Concerning the CFUs for the experiment with Sima knockdown, no significant difference between the experimental and control genotype was observed at 0, 18 and 24hpi, however at 48hpi (T3) the number of bacteria per fly (CFUs) was significantly higher in individuals with Sima KK (p-value = 0,0071) (Fig. 26).

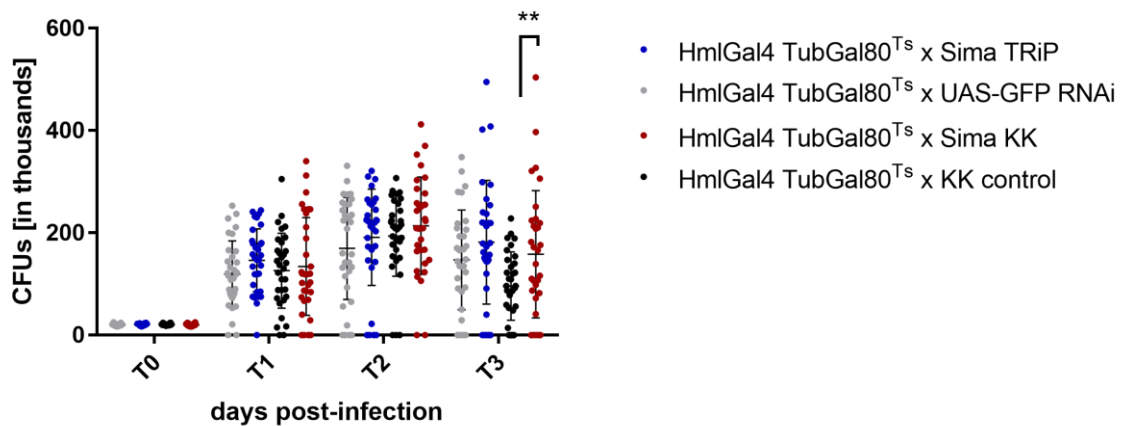


Figure 26: Growth rate of bacterial colonies in infected Sima RNAi individuals compared to infected control flies. Resulting graph shows combined data from three independent experiments. The overall number of individuals equaled 36 per each genotype. P-value = 0,0071 was determined using Two-Way ANOVA with multiple comparisons (Tukey multiple comparisons test).

Even though the CFUs data do not show a very strong difference between the flies with hemocyte specific downregulation of Sima or ImpL3 compared to control genotypes, we still believe that they exhibit impaired phagocytosis and they are dying due to deteriorated ability of bacterial killing rather than due to demanding immune response based on the raw data from the graphs. Another strategy and increased number of replicates is needed to solve this issue.

4.5. The regulation of ImpL2 gene in immune response in *D. melanogaster*

Despite the main focus of this thesis being the characterization of metabolic changes in hemocytes of infected *D. melanogaster*, the impact of the infection on systemic metabolism was evaluated as well (Fig. 20, 21 and 22). Metabolites measurement led to the consideration about what is responsible for the changes in systemic metabolites concentration during immune response. Previous experiments of our laboratory showed that ImpL2 gene is upregulated in hemocytes upon infection and that ImpL2 is a signaling molecule inducing systemic metabolic changes, which are characteristic for immune response to bacterial infection (Sokcevicova, MSc. thesis 2017 [in Czech]). ImpL2 is also known for insulin signaling regulation (Sloth Andersen et al., 2000), regulation of trehalose (Figueroa-Clarevaga and Bilder, 2016) and glucose (Kwon et al., 2015) in the context of cancer. Since HIF1 α -HRE signaling cascade is responsible for regulation of expression of large number of genes, one of them being ImpL2 during hypoxia (Allee, 2011; Li et al., 2013), we suggested, that ImpL2 gene might be regulated via HIF1 α -HRE cascade also during infection. To evaluate this theory, mRNA level of ImpL2 in Sima RNAi flies was measured (cross no2 in section 3.3. Crosses).

The data show that upon infection, mRNA level of ImpL2 in HmlGal4>GFP adults is significantly increased at 24hpi and remains upregulated all the way up to 120hpi (Fig. 27).

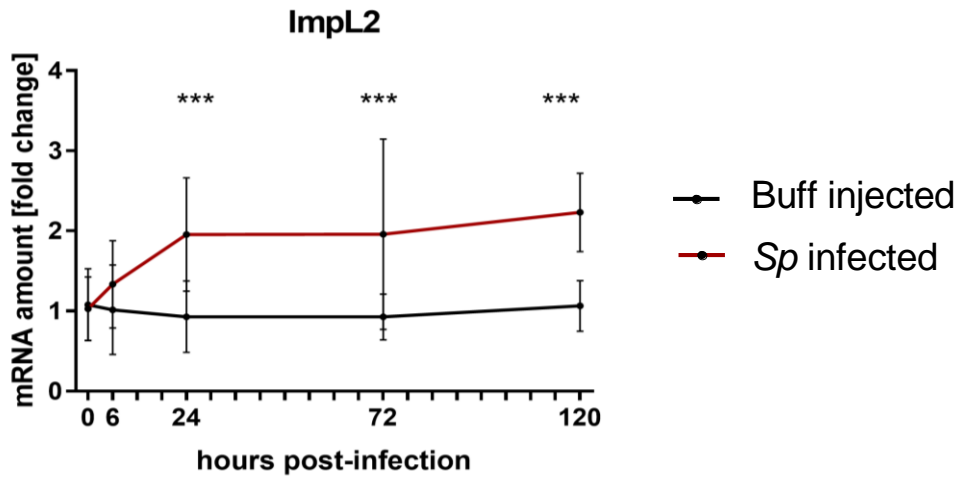


Figure 27: Gene expression of ImpL2 of infected HmlGal4>GFP adults at 0, 6, 24, 72 and 120hpi compared to noninfected control flies. The graph shows combined data from three independent experiments. Average number of individuals was approximately 600 per each genotype. Error bars represent standard deviation. P-value <0,0001 for 24, 72 and 120hpi was determined using Two-Way ANOVA (Sidak’s multiple comparisons test).

This infection induced upregulation was observed also in the second qPCR experiment in infected control genotype (Fig. 28). Nonetheless, in flies with hemocyte specific HIF1 α knockdown the expression level remained the same as it was before infection (Fig. 28).

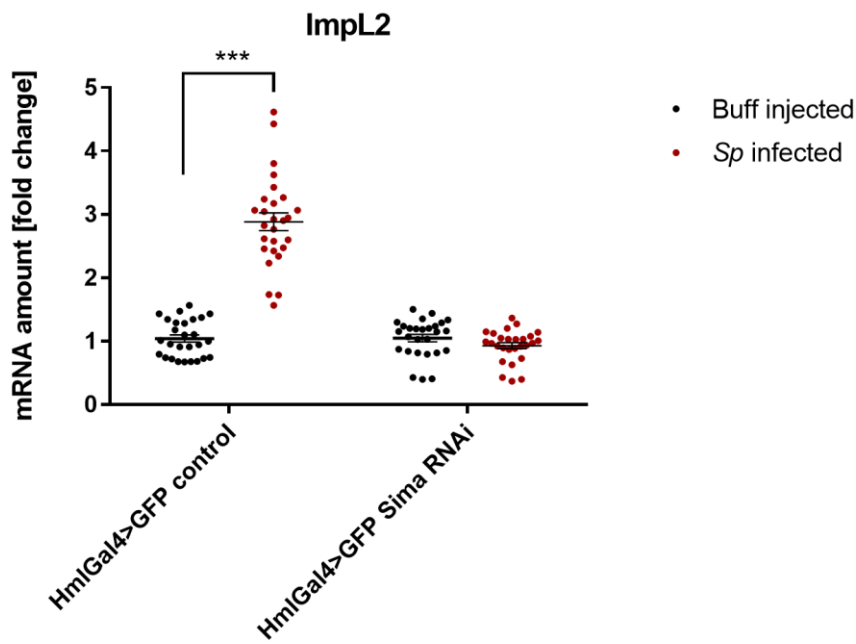


Figure 28: Gene expression of ImpL2 gene of infected Sima RNAi adults at 24hpi compared to control flies. The graph shows combined data from three independent experiments. Average number of individuals was more than 650 per each genotype. The graph displays both biological and technical replicates. Error bars represent standard deviation. P-value <0,0001 was determined using Two-Way ANOVA.

These data suggest that ImpL2 gene is a target gene of the transcription factor HIF1 α and that its upregulation in response to bacterial infection and systemic metabolic effects are interconnected with the level of activation of macrophages.

5. DISCUSSION

Adequate immune response and control of pathogen growth requires a fast activation of immune system. Bacterial killing is a very complex process requiring adaptation of many cellular processes, one of them being remodeling of cellular metabolism (Frauwirth and Thompson, 2004). It was shown that in order to be activated mammalian immune cells undergo metabolic reprogramming (Vats et al., 2006). We showed in this thesis that immune cells of *Sp* infected flies increase the expression of glycolytic enzymes suggesting increased glycolytic flux (Fig. 11). This observation is in accordance with old publications from Newsholme or Hard, who claimed, that activated macrophages increase the expression of hexokinase and glucose-6-phosphate dehydrogenase (Newsholme, 1986; Hard, 1970). One of the key enzyme of increased glycolysis is lactate dehydrogenase which expression is 3-fold increased after infection (Fig. 11G). Lactate dehydrogenase was also showed to be localized primarily in immune cells (Fig. 16 and 17). Our experiments also showed that knockdown of lactate dehydrogenase leads to an impaired survival of infected flies (Fig. 23), suggesting that the effective immune response depends on increased glycolysis and production of lactate. Inasmuch as the cell metabolism is altered, it is to be expected that the immune system requires different amount of energy. Metabolic changes in activated immune cells make the immune response energetically costly (Straub et al., 2010), thus a systemic metabolic adaptation of the whole organism is necessary. The energy is therefore reallocated from storage towards the immune system. This theory corresponds with our data showing a transiently increased level of free glucose in infected flies (Fig. 20). We also observed highly increased glucose consumption by immune cells of infected individuals (Fig. 13, 14 and 15). We suggest, that the increased amount of glucose is then consumed by immune cells to feed the increased glycolysis.

It was described that HIF1 α signaling cascade plays an important role in activated mammalian macrophages under normoxic conditions (Blouin, 2003). This thesis showed activation of HRE in hemocytes upon infection (Fig. 18), suggesting that HIF1 α is stabilized and translocated into the nucleus. This statement also corresponds with increased expression of glycolytic enzymes (Fig. 11) since they were described as HIF1 α target genes (Greijer et al., 2005). Knockdown of HIF1 α in immune cells resulted in the inability of these flies to increase the mRNA level of glycolytic genes (Fig. 19) as well as mRNA level of ImpL2 gene (Fig. 28). Therefore, we suggest that ImpL2 is under control of HIF1 α transcription factor as well. ImpL2 was shown to have a significant effect on regulation of glucose metabolism

during infection (Sokcevicova, MSc. thesis 2017 [in Czech]) and we thus propose that flies with HIF1 α knockdown failed to increase the concentration of free glucose (Fig. 20) since they were not able to increase the expression of ImpL2 (Fig. 28). Figueroa-Clarevega and Bilder suggested that the tumor-secreted IGFBP (ImpL2 homolog) creates insulin resistance in distant tissues and therefore we think that ImpL2 causes insulin resistance of nonimmune tissues to ensure enough glucose for hemocytes (Figueroa-Clarevega and Bilder, 2015).

5.1. Activated macrophages show temporarily increased expression of glycolytic enzymes

Under hypoxic conditions cells preferentially produce ATP by the breakdown of glucose via glycolysis and the resulting molecule - pyruvate is being converted to lactate rather than acetyl-CoA. In some cases as a matter of priority cells use glycolysis for ATP generation even when oxygen is not limiting. This process is known as aerobic glycolysis or Warburg effect, which was described as a metabolism characteristic for tumor cells (Warburg et al., 1927) and also as a metabolism of activated mammalian immune cells (Hard, 1970; Newsholme, 1986). Aerobic glycolysis is also a necessary requirement for polarization of macrophages triggered by Toll signalization to M1 phenotype and establishment of their bactericidal function (Galván-Peña and O'Neill, 2014). M1 macrophages are accumulated in sites of wounds. The increase in number of M1 macrophages is typical for systemic infection called sepsis (Wang et al., 2014).

The data from analysis of mRNA levels of metabolic genes (Fig. 11), which are presented in this thesis, suggest that M1 type of metabolism, increased glycolysis and production of lactate, is utilized also by immune cells of *Sp* infected *D. melanogaster*. Infection-triggered increase in glycolytic enzymes expression was observed also in larvae (Bajgar et al., 2015). What leads the immune cells to increase the glycolytic pathway? Are they limited by oxygen? Glycolysis represents a metabolic pathway which produces only limited amount of ATP (2 ATP molecules per one molecule of glucose), however, this production is very fast and speed is a crucial attribute for successful elimination of bacterial infection. The conversion of glyceraldehyde-3-phosphate into 1,2-bisphosphoglycerate requires NAD⁺ which originates by conversion of pyruvate to lactate via lactate dehydrogenase. Upregulated ImpL3 gene may contribute to the theory that activated hemocytes show signs of pseudohypoxia (increased cytosolic ratio of free NAD⁺ to NADH).

The expression of enzymes of the TCA cycle do not seem to be as unequivocal as the expression data of the glycolytic enzymes. The mRNA level of the TCA cycle genes of

infected adults showed that at early timepoints after infection there is no change of the Krebs cycle enzymes, however, the decrease was observed at later timepoints (Fig. 12). Bajgar et al. measured the expression of citrate cycle enzymes at 6 and 18hpi in *Drosophila* larvae and no change was observed (Bajgar et al., 2015). It was shown that high NAD⁺/NADH ratio leads to decreased mitochondrial content, mitochondrial fragmentation and activation of mitophagy (Jang et al., 2012), which may represent a negative feedback to attenuate the TCA cycle. Upon infection, mitochondria of immune cells exhibit high rate of ROS production (Matsuzawa, 2005). ROS are then transferred to phagolysosomes in order to kill the phagocytosed bacteria (West et al., 2011). Phagolysosome acidification thus might be the main purpose of mitochondria during bacterial infection. This leads us to the consideration whether these observations might be the reason why at later timepoints after the infection the function of the TCA cycle enzymes is decreased. This decrease was observed not only in Krebs cycle enzymes, but in some glycolytic enzymes as well (HexA, Eno) (Fig. 11) which may suggest that at this point the macrophages are already exhausted and after the elimination of the infection they enter the quiescent state. These results thus raise very interesting questions. Do the macrophages die after the phase of resolution? Could the high rate of ROS production lead to the death of such a cell? There are several tools which would allow to study this issue. One of them is simple counting of the number of circulating hemocytes before and during the infection, during the phase of resolution and at the time when there are no longer any bacteria. Nonetheless, would this approach answer our question? Does the number of hemocytes change during the lifetime of the fly? The proliferative capacity of hemocytes has been a matter of debate. It is generally believed that the adults lack a hematopoietic organ and survive on the contribution of both embryonic and larval hematopoiesis. However, a report from 2015 claims *de novo* production of hemocytes in the adult fly in the dorsal abdominal four hemocyte clusters (hematopoietic hubs). Upon *E. coli* infection they seem to proliferate and furthermore, they are capable of phagocytosis and are referred to as a simple version of the vertebrate bone marrow (Ghosh et al., 2015). Nonetheless, the majority of studies have not been able to obtain any evidence of proliferation in adult hemocyte populations (Rizki, 1978; Van de Bor et al., 2015; Lanot et al., 2001) even under an immune challenge (Gold and Brückner, 2015). However, immunosenescence which involves a decline in both hemocyte number and phagocytic function, has been documented as adult flies grow older (Mackenzie et al., 2011; Horn et al., 2014) and evidence of homeostatic hemocyte maintenance has been obtained (Horn et al., 2014). Another way how to elucidate whether the macrophages die is to use the sensor called

Apoliner, that involves two fused fluorescent protein which become separated by caspase activity, which is typical for apoptotic cells (Lanot et al., 2001).

To elucidate the importance of the TCA cycle metabolism during infection hemocyte specific RNAi of one of the ETC subunit could be performed and the survival of these flies could be observed.

We were also interested whether the mitochondria of hemocytes of infected flies undergo some structural changes that could explain expression pattern of TCA cycle genes. However, confocal microscopy is not sufficient for this study and therefore we suggest to perform it using electron microscopy.

Although the proteomic and metabolomic data showed that the gene expression of the glycolytic enzymes strongly correlates with the amount of the functional protein (Lee et al., 2017), we are aware that the data from qPCR analysis are only a supporting evidence, not a conclusive proof. To further support the occurrence of metabolic switch in activated immune cells, we present here *in vivo/in situ* observations as well.

5.2. Metabolic changes of *Drosophila* macrophages *in vivo/in situ*

In the next part of this project, *in vivo* reporters and tracers were employed to further document several typical features of M1 macrophages, such as high level of glucose accumulation (typical for M1 macrophages as well as for cancer tissues), active role of HIF1 α transcription factor and high expression level of lactate dehydrogenase as a crucial enzyme of increased glycolysis.

Clear difference in 2-deoxyglucose accumulation in activated immune cells compared to resting immune cells as well as non-immune tissues was observed (Fig. 13, 14 and 15). This important *in vivo* experiment proves the capacity of activated immune cells to gain more glucose in competition with other tissues and thus supporting the theory of "selfish immune system" (Peters et al., 2004). Similar experiments were carried out also in larval immune response model. Bajgar and col. showed that immune cells increase the accumulation of ¹⁴C labeled glucose almost three times compared to noninfected controls in response to parasitic wasp infection (Bajgar et al. 2015). To further follow the destiny of consumed glucose by activated macrophages, ¹³C glucose could be employed and its incorporation into various molecules could be measured using mass spectroscopy. However, we assume that quantity of the material which is needed for such analysis is limiting for us since we might not be able to obtain enough material from FACS.

Activated immune cells show striking activity of HIF1 α , hallmark of M1 polarization. Stabilization of HIF1 α and its nuclear transport is a typical characteristic of hypoxic and pseudohypoxic state (Mohlin et al., 2017). The next experiment showed significantly increased activity of transcription factors activating HRE (Fig. 18) and we thus suggest that HIF1 α is activated in hemocytes upon infection. We are planning to perform X-gal staining and the experiment with 2-NBDG also at later timepoints after infection (120hpi) to observe, whether the hemocytes accumulate the glucose also in the phase of resolution of inflammation and whether HIF1 α is still stabilized or not.

We also confirmed that immune cells of *D. melanogaster* strongly express the enzyme lactate dehydrogenase, a key enzyme of increased glycolysis. Furthermore, no other tissue shows such a strong expression of LDH (Fig. 16 and 17). Unfortunately, the LDH enzyme which is fused with red fluorescent mCherry protein in immune cells shines so potently in control (uninfected) state that it is nearly impossible to observe any upregulation in response to infection even when the flies are heterozygous for this construct. However, we know from the expression data that the LDH expression is increased three times in HmlGFP cells (Fig. 11G). The experiment with LDH visualization may suggest that the macrophages are prepared for the utilization of increased glycolysis in advance. Another explanation why we observe such a strong expression of LDH might be a fact that the LDH mCherry protein persists longer than its transcript (Fig. 5).

5.3. Transcription factor HIF1 α plays an important role in macrophage polarization

Under normoxic conditions HIF α is constitutively produced, but it is bound by VHL via ODD domain, ubiquitinated and thus degraded by the proteasome. Since molecular oxygen serves for PHDs (*Drosophila* homolog Fga) as a co-substrate of the reaction, in hypoxia activity of PHDs is inhibited and HIF1 α is thus stabilized and accumulates. Subsequently, HIF1 α is translocated to the nucleus, dimerizes with HIF β (*Drosophila* homolog Tgo), where they bind to HRE and the expression of target genes is promoted (Semenza, 2014). On that account we were considering whether HIF1 α plays a similar role also in pseudohypoxic conditions in activated macrophages. X-gal staining experiment already showed that HRE is activated (Fig. 18) suggesting stabilization and translocation of HIF1 α . To reveal the effect of this stabilization, we decided to perform hemocyte specific Sima knockdown. Our expression data clearly show a trend that upon infection Sima RNAi flies are not able to increase the mRNA level of several glycolytic genes (Fig. 19), suggesting that HIF1 α regulates the expression of glycolytic genes in activated hemocytes.

This statement is supported with a research conducted by Wappner group who revealed that LDH is a direct Sima target (Lavista-Llanos, 2002).

The RNAi line that was used for this experiment (KK line) targets only one mRNA transcript (Sima-RD) out of four possible ones (Sima-RA, Sima-RB, Sima-RC, Sima-RD), meaning that the downregulation of Sima was only partial. Nonetheless, the effect on the expression level of glycolytic genes is still obvious. Although this survey might suggest that this RD transcript is the important one, these issues were further analyzed. Theoretically, out of four different Sima isoforms only two (Sima-RA and Sima-RD) seem to have all the necessary domains for entering the nucleus, binding of DNA and thus influence the expression of target genes (see 7. Supplementary data for more detail). However, Sima RNAi TRiP line (BL-26207, FBst0026207) should be used in the future as it targets all four mRNA transcripts (RSVP RNAi Validation & Phenotypes, www.flyrnai.org/cgi-bin/RSVP_search.pl).

Upon infection systemic metabolic changes are mainly represented by increased level of free glucose and decreased level of glycogen (Govind, 2008). In figure 20 a tendency of the infected control line to increase the level of free glucose can be observed. This glucose serves as a energy resource for immune cells. We further showed that infected individuals with Sima knockdown are not able to increase the level of free glucose (Fig. 20). This measurement is in accordance with a paper from Jantsch et al., who showed, that knockdown of HIF1 α significantly reduced glucose use in dendritic cells (Jantsch et al., 2008). These data also corresponds with the theory that activated immune cells alter their systemic metabolism in order to fulfil different requirements. Since the proper activation of immune cells is blocked via HIF1 α RNAi, those demands do not change and thus the signals for changing the systemic metabolism are not released. Simultaneously, the level of glycogen should decrease since glycogen represents the main glucose storage in fly's body. This metabolic changes are realized via glycogen phosphorylase (Reyes-DelaTorre et al., 2012). Consequently, hemocytes trigger insulin resistance of other tissues and thus glucose can not enter the cells and stays in hemolymph available for hemocytes (Bajgar et al., 2015). Nonetheless, the data from glycogen measurement are complicated. Since glycogen concentration at 0hpi varies between all four genotypes measured (Fig. 21), it may suggest that the way of glycogen gauging used is not reliable enough. One explanation could be the fact that while 45 μ L of sample for glucose measurement was used, for glycogen measurement only 25 μ L was added according to the protocol. From the reason that

glycogen concentration did not make much sense, graph with normalized concentration of glycogen was created (Fig. 22). The data then showed that the glycogen level in infected control genotype is lower than in Sima RNAi flies, suggesting, that flies with Sima knockdown do not metabolize glycogen as extensively as infected controls are, however, this difference was not significant. As it was already mentioned, the data from glycogen measurement should not be used for deducing any final conclusions about the impact of HIF1 α on the systemic metabolism.

5.4. Enzyme lactate dehydrogenase and HIF1 α protein are necessary for effective elimination of bacterial infection

It can be assumed from the data above that transcription factor HIF1 α and enzyme LDH are important players in polarization of *Drosophila* macrophages. Lactate dehydrogenase is regulated via HIF1 α -HRE signaling cascade since hypoxia response elements contained in gene promoter contain essential binding sites for HIF1 α (Semenza et al., 1996).

Hemocyte specific knockdown of HIF1 α (Fig. 24) and LDH (Fig. 23) genes in infected individuals was performed in order to bring a convincing evidence about the importance of the macrophage polarization for effective immune response. The extracellular bacterial infection used needs to be eliminated via phagocytosis because otherwise the fly dies. Survival analyses showed that HIF1 α and LDH knockdown is lethal for most of the experimental individuals compared to control genotypes. This observation is in agreement with the mice experiments performed by Peyssonnaud and col., who showed that HIF1 α -null macrophages have decreased bactericidal activity and that they were not capable of restricting systemic spread of infection from an initial tissue focus (Peyssonnaud et al., 2005). To evaluate the efficiency of RNAi, the relative expression of ImpL3 and Sima was measured in both control and experimental genotype (see Fig. S9 and Fig. S10 in section 7. Supplementary data).

As it was already shown above, knockdown of HIF1 α results in inefficient regulation of glucose metabolism during infection (Fig. 20). This may then result in higher mortality rate (Fig. 24) and this observation can be explained by two possible reasons, the first one being the actual immune reaction, which is very demanding, and the second one being poor activation of hemocytes resulting in insufficient response to pathogenic bacteria. To verify these hypotheses the number of colony forming units in control and TRiP as well as KK line was measured (Fig. 26). CFUs data show a statistically significant result only at T3.

However, we still tend to prefer the second hypothesis, that the immune cells are insufficiently activated and thus the immune response is not effective enough, resulting in higher reproduction of the bacteria compared to infected control flies. These results would be in accordance with the changes of glucose level during infection (Govind, 2008). Glucose represents the energy for immune cells activation and if an increase in free glucose is prevented, insufficiently activated hemocytes are not able to thwart the bacterial proliferation. Even though the impaired survival of TRiP line was statistically significant compared to the control flies, the control genotype for KK line showed slower dying than the control genotype for TRiP line used (Fig. 24). This may be caused by a different genetic background, meaning, that the control genotype for TRiP line was more susceptible to the *Sp* infection than the KK control. From this reason the dose of injected bacteria should have been lowered or the genotype of KK line should have been converted to our white fly background.

Concerning the knockdown of LDH, flies with ImpL3 RNAi showed significantly faster dying compared to the control genotype (Fig. 23). According to the theory, knockdown of lactate dehydrogenase results in decreased production of lactate and increased accumulation of pyruvate, which may result in abrogation of further activity of glycolysis. Since mRNA levels of glycolytic enzymes measured in this thesis (Fig. 11) suggested that the glycolytic pathway is exploited by activated macrophages in an increased extent, the impairment of glycolysis is thus fatal. The number of CFUs in individuals with ImpL3 RNAi was significantly higher at T2 and T3 (Fig. 25), suggesting lower ability to phagocyte. These experiments showed that the LDH and HIF1 α expression is essential for bactericidal role of macrophages.

5.5. The regulation of ImpL2 gene in immune response in *D. melanogaster*

ImpL2 has been identified as a signal molecule inducing systemic metabolic changes characteristic for bacterial infection and that it is produced by hemocytes (Sokcevicova, MSc. thesis 2017 [in Czech]). Mechanism of ImpL2 function is its extracellular bond with Dilp2 (Drosophila Insulin-Like Peptid 2), which is synthesized in insulin producing cells. This bond then downregulates insulin signaling (Sloth Andersen et al., 2000). Consequently, the level of circulating glucose rises, the level of glycogen decreases and insulin resistance and tissue kachexia occurs (Figuroa-Clarevaga and Bilder, 2015). ImpL2 has its homologous gene IGFBP7 (Insulin-like Growth Factor Binding Protein) in humans (Sloth Andersen et al., 2000).

We showed that ImpL2 is upregulated in response to infection (Fig. 27) and this rise in ImpL2 expression is inhibited in flies with HIF1 α knockdown (Fig. 28). Similarly as LDH or Eno promoter contains hypoxia response element sequences (Semenza et al., 1996), ImpL2 contains them as well. Figure 29 shows that we found six HRE sequences in genomic and coding sequence of ImpL2, suggesting that ImpL2 is HIF target gene.

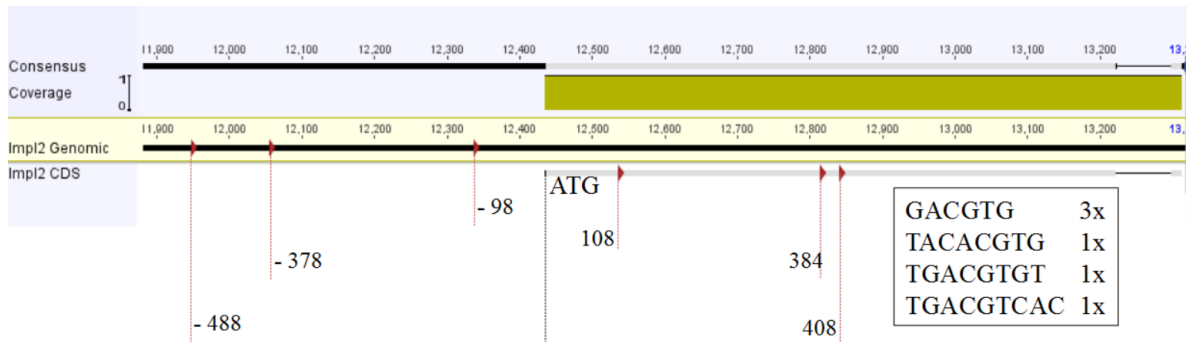


Figure 29: ImpL2 genomic and coding sequence containing six hypoxia response element sequences.

This finding is in accordance with a claim that ImpL2 is bound by HIF1 α upon hypoxic conditions (Allee, 2011; Li et al., 2013), which led us to the consideration that ImpL2 gene might be regulated via HIF1 α -HRE cascade also during infection. This theory was supported by our results from qPCR analyses showing that strikingly, the upregulation of ImpL2 in response to bacterial infection and the systemic metabolic effects are linked with the macrophage activation. HIF1 α -HRE-ImpL2 thus represents the interconnection between cellular and systemic metabolic rearrangement. An interesting question rose here: Is this HIF1 α -HRE-ImpL2 cascade immune specific or can it be adopted also by other tissues?

6. CONCLUSION

Our data clearly show that upon infection hemocytes of model organism *D. melanogaster* undergo significant remodeling of metabolic pathways. We showed that these cells accumulate glucose, contain significant amount of LDH enzyme and their HIF1 α is stabilized and thus translocated to the nucleus, which results in expression changes of glycolytic enzymes. Activated immune cells of *D. melanogaster* exhibit increased expression of glycolytic genes including LDH, a key enzyme of increased glycolysis. Moreover, the expression of LDH and HIF1 α in hemocytes is essential for effective resistance to bacterial infection. Activated immune cells also have a significant effect on regulation of systemic glucose metabolism. We suggest that HIF1 α -HRE-Impl2 axis is employed upon infection in activated hemocytes in order to induce infection-triggered transient hyperglycemia to ensure enough glucose for immune cells (Fig. 30).

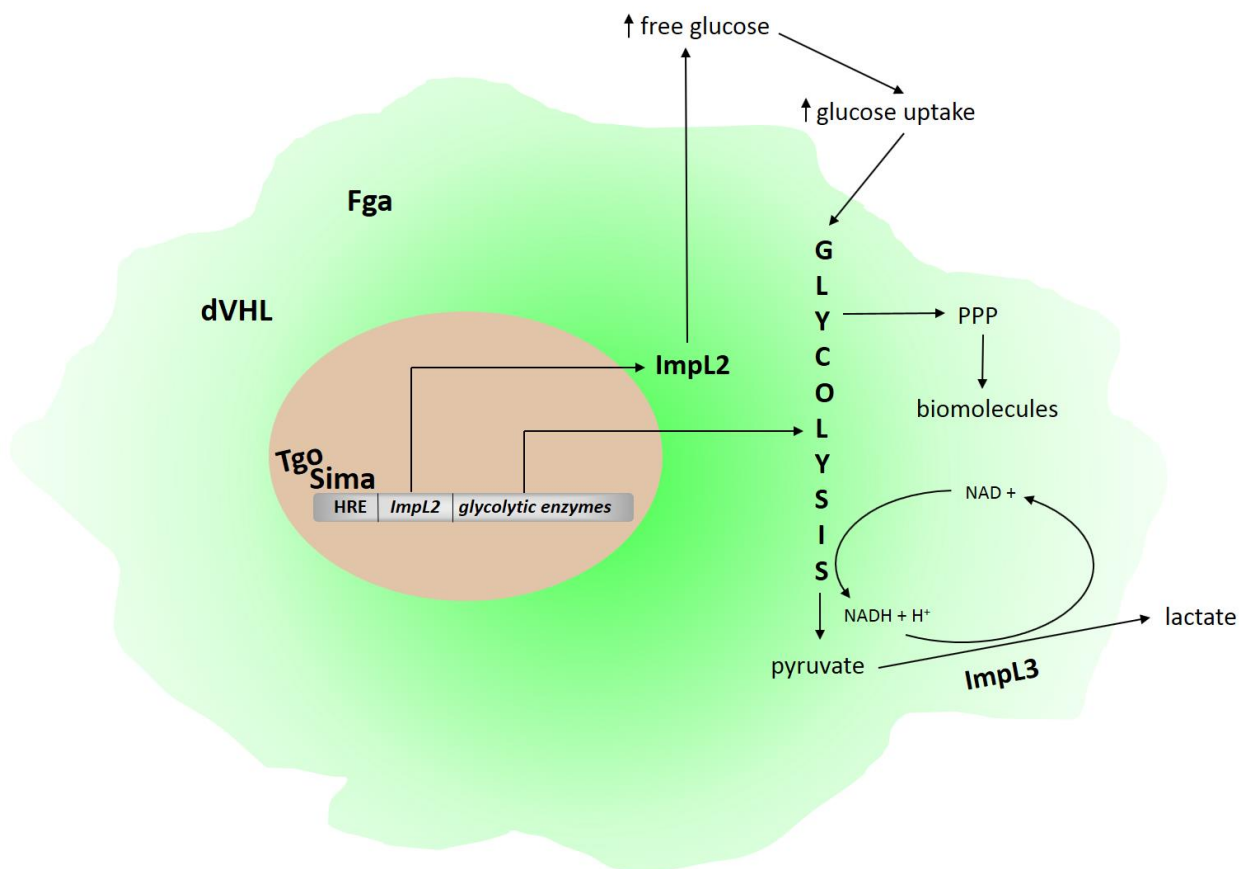


Figure 30: Suggested concluding model of activated macrophage of *D. melanogaster*.

7.1. Introduction

During our research concerning HIF1 α playing a role of important transcription factor of metabolic switch in activated macrophages in *D. melanogaster* we found out that Sima (*Drosophila* homolog of HIF1 α) has four different transcripts (Sima-RA, RB, RC and RD). However, our Sima RNAi line that was used for the experiment where gene expression of glycolytic enzymes was measured (KK line) targets only RD transcript. This led us to the question which transcript plays an important role in immune response of *D. melanogaster*.

Gorr et al. showed that under hypoxic conditions Sima is expressed in full-length (fl) and splice variant (sv) isoforms in cultures of SL2 cells and a role of flSima as functional HIF1 α protein was shown as well. Eventhough the expression of svSima increased linearly throughout the hypoxic time course, the relative mRNA amount never exceeded 13% of flSima mRNA even at its peak abundance (Gorr et al., 2004). From figure 4a in this paper (Fig. S1) we concluded that fl isoform represents RA transcript and sv isoform RB transcript, meaning, that Sima-RB lacks ODD sequence, which is necessary for HIF1 α degradation, and it also lacks the polyglutamine repeats and the sequence required for translocation to the nucleus. svSima was more abundant under hypoxic than normoxic conditions despite it lacks the ODD sequence and one would expect constitutive stabilization. However, svSima localizes in the cytosol and binds with Tgo creating an unproductive cytosolic heterodimer at the expense of flSima/Tgo complexes, meaning it controls access of Tgo to flSima under hypoxic conditions. Sima gene thus express its own agonistic and antagonistic protein products and splice variant isoform displays a potential to regulate HIF function (Gorr et al., 2004).

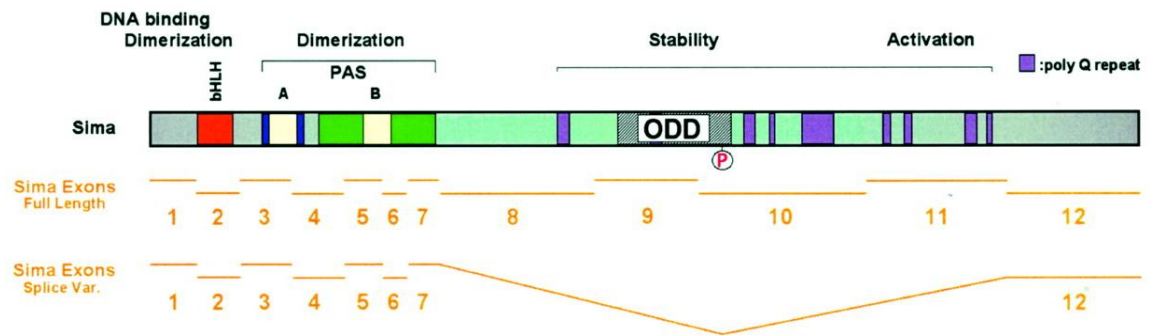


Figure S1: Functionally relevant regions (*i.e.* bHLH, PAS, ODD and polyglutamine repeats (*poly Q*)) of Sima protein and exon composition of its full-length (fl) and splice variant (sv) isoforms. Adopted from Gorr et al., 2004.

The coding sequence of Sima consists of fourteen exons. Exon composition of each transcript is shown in figure S2. A note should be made that in figure S1 there are only twelve exons portrayed since exons 2 and 9 were omitted because only RA and RB transcripts were compared.

7.2. Materials and methods

Cell sorting, isolation of RNA, reverse transcription and qPCR were performed according to section 3. Materials and methods. Sequences of primers used are shown below:

Rp49	Forward	5'AAGCTGTCGCACAAATGGCG3'
	Reverse	5'GCACGTTGTGCACCAGGAAC3'
Sima-RA, B	Forward	5'CCAAAGGAGAAAAGAAGGAAC3'
	Reverse	5'GAA TCT TGA GGA AAG CGA TG3'
Sima-RA, B, D	Forward	5'TCGTATAAGGTCATTCACATC3'
	Reverse	5'AAGAGGTGTCAAGTAGATCC3'
Sima-RB	Forward	5'CATAAGGATGACGAT TCCGAA3'
	Reverse	5'CGGGTTGTTATGATAGTCC3'

Sima-RC	Forward	5'CTAAGTTCAAAAAGTAATCTTGAG3'
	Reverse	5'TCCTTGGTTTCCTGAGCG3'

Sima-RD	Forward	5'TCGAGGATTTTCATGAACAATG3'
	Reverse	5'TTCAATGTCCTGCTTGATGTC3'

Gel electrophoresis was performed with 10 μ L of samples from qPCR reaction, to which 2 μ L of loading dye (0,09 % bromphenol blue, 0,09 % xylene cyanol, 60 % glycerol, 60mM EDTA) was added. 1 μ L of Ethidium bromide (Sigma) was added to 40 mL of 1,5% agarose gel. 3 μ L of 100 bp DNA Ladder with added Gel loading dye purple (6x) (New England Biolabs) was used. Electrophoresis was ran at 60, then 90V. Picture (Fig. S7) of the resulting gel was made afterwards using White/UV Transilluminator (UVP).

Data were statistically evaluated according to section 3.14. Statistics and data processing. Figures with Sima transcripts (Fig. S2) were created using Genious R6 6.1.8 software.

7.3. Results

7.3.1. Gene expression of HIF1 α isoforms in macrophages of *D. melanogaster*. Efficiency of Sima KK RNAi.

Since our results showed that HIF1 α plays a role of important transcription factor in hemocytes of infected fly, we were interested wheather its expression changes in response to infection, even though it is known that HIF1 α is regulated via its degradation or stabilization (Masoud and Li, 2015).

Since there are four possible Sima trascripts, specific primers had to be used. In order to obtain them, sequence of Sima mRNA molecules, which was downloaded from FlyBase, a database of *Drosophila* genes & genomes (flybase.org), was mapped to the Sima genomic sequence (Fig. S2).

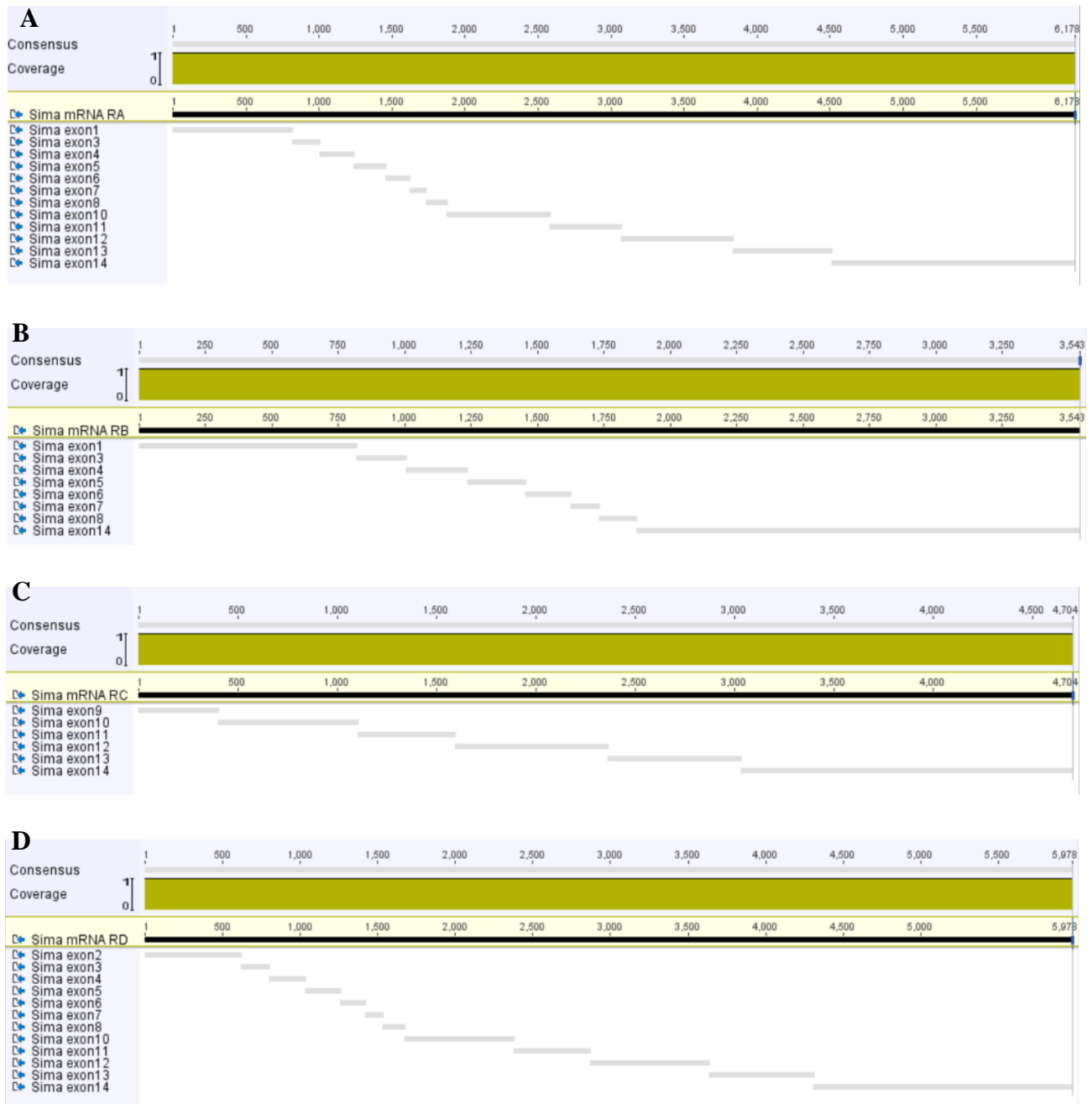


Figure S2: Sima-RA (A), Sima-RB (B), Sima-RC (C) and Sima-RD (D) transcripts mapped on Sima genomic sequence.

The regions where the primers were designed are shown in figure S3 and table S4, their melting temperatures and assumed product sizes are shown in table S1. Since it was not possible to design a specific primer for Sima-RA only, primer for both Sima-RA and Sima-RB isoforms was created (Sima-RA, B). To measure the expression of all Sima transcripts one collective pair of primers should have been created. However, it was not possible and since Sima-RC transcript lacks the functional domains a pair of primers for Sima-RA, B, D

was created. The primer combinations were designed to amplify exclusively from cDNA in order to avoid amplification from possible gDNA contamination.

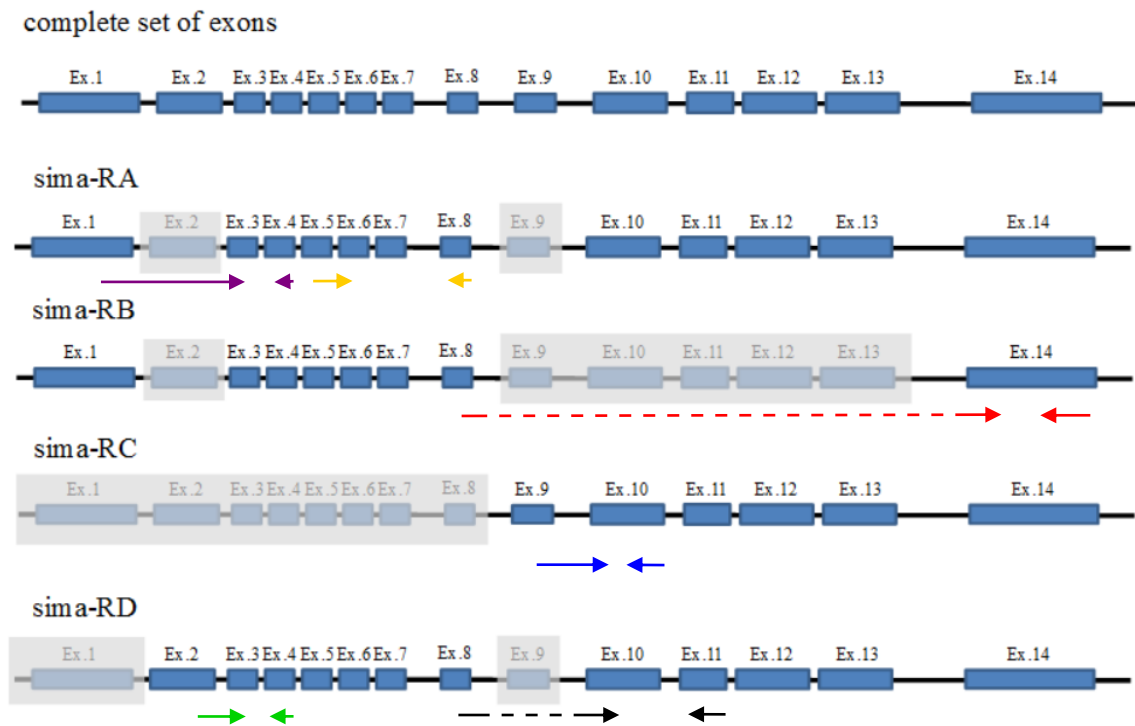


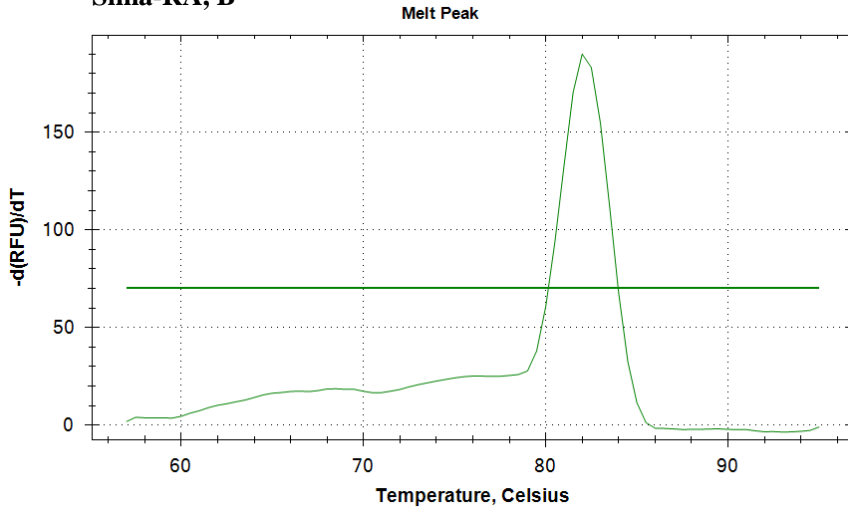
Figure S3: Schematic representation of exons contained in Sima-RA, RB, RC and RD transcripts. Exons covered with grey boxed are spliced. Colourful arrows (full line) represent the position of designed Sima primers (Sima-RB red, Sima-RC blue, Sima-RD green, Sima-RA,B purple, Sima-RA,D black and Sima-RA,B,D yellow). Sima-RB and Sima-RA,D primers were exon skipping (represented by dashed part of the arrow).

Table S1: Position on genomic DNA of Sima primers, melting temperature and size of the resulting product. In the third column the color with which the primer pair is represented in Fig. S3 is stated.

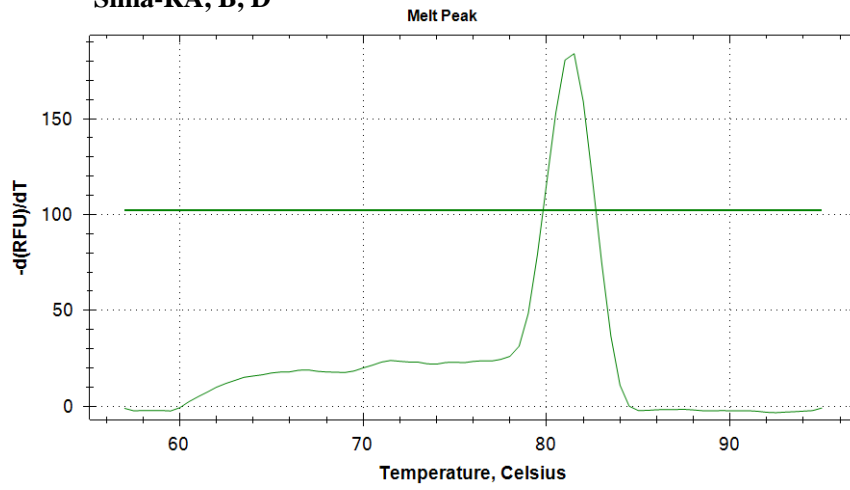
primer name	position color used in Fig. 26	melting temperature (°C)	Product size (bps)
Sima-RA,B Fwd	border ex. 1-3 purple	57	187
Sima-RA,B Rev	ex. 4 purple	56	
Sima-RB Fwd	border ex. 8-14 red	57	142
Sima-RB Rev	ex. 14 red	55	
Sima-RC Fwd	border ex. 9-10 blue	55	160
Sima-RC Rev	ex. 10 blue	55	
Sima-RD Fwd	border ex. 2-3 green	56	248
Sima-RD Rev	ex. 4 green	57	
Sima-RA,B,D Fwd	border ex. 5-6 yellow	56	226
Sima-RA,B,D Rev	ex. 8 yellow	56	

From the melting curves we deduced that from the designed Sima primers only one specific product is formed (Fig. S6), which was also tested using gel electrophoresis, which served also for the evaluation of the assumed size of the resulting products. Figure S7 shows that the size of the products corresponds with the assumed ones.

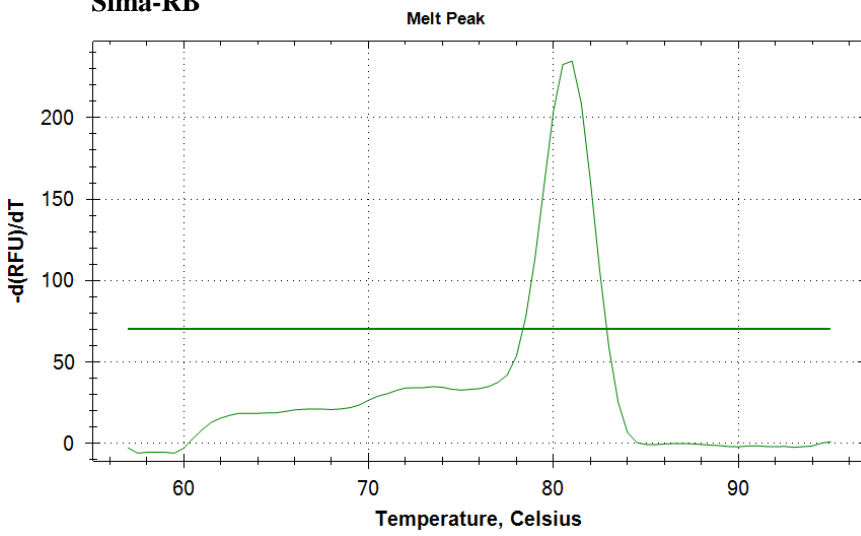
Sima-RA, B



Sima-RA, B, D



Sima-RB



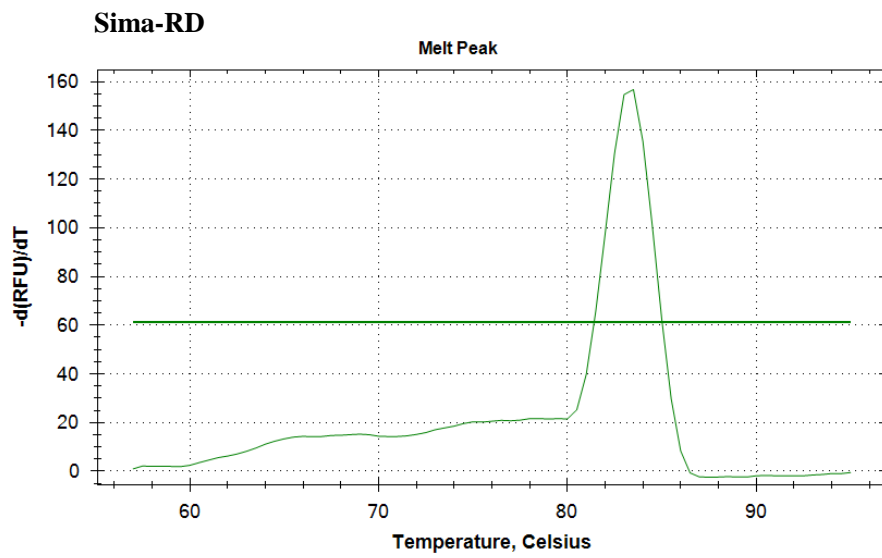
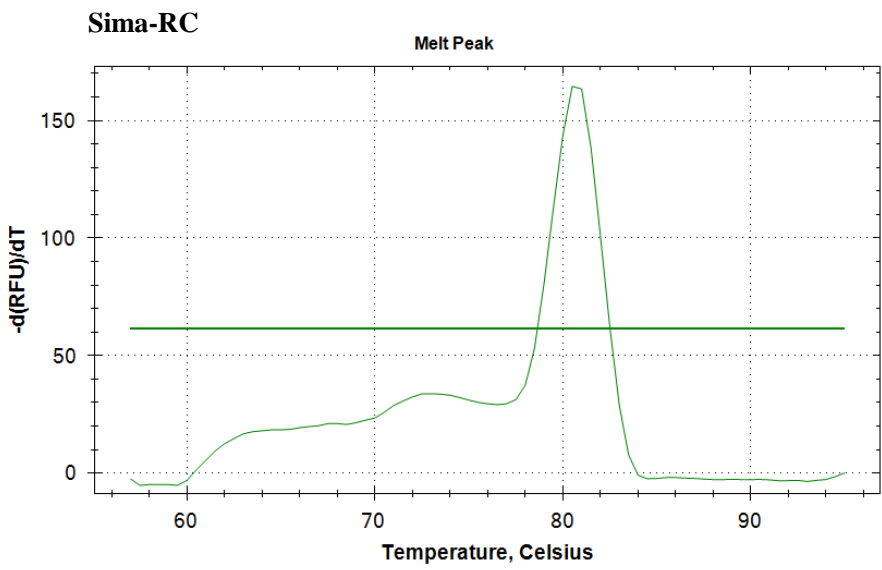


Figure S6: Melting curves of Sima transcripts.

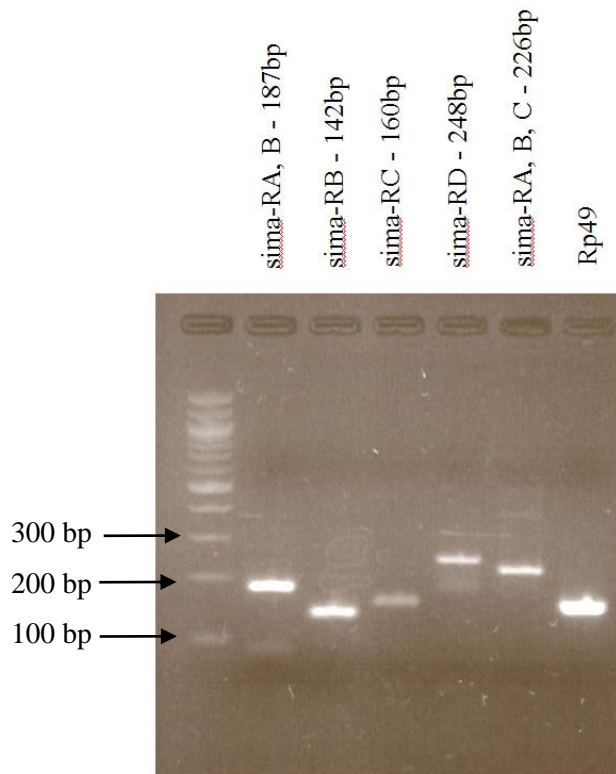


Figure S7: Agarose gel electrophoresis of Sima transcripts. Lane 1 = 100 bp molecular marker, lane 2 = Sima-RA, B, lane 3 = Sima-RB, lane 4 = Sima-RC, lane 5 = Sima-RD, lane 6 = Sima-RA, B, D and lane 7 = ribosomal protein L32.

Figure S8 shows the expression of Sima transcripts in hemocytes at 24hpi. Sima-RD transcript was strongly decreased after infection in Sima RNAi adults compared to control genotype (p-value <0,0001), suggesting that the RNAi interference was effective. Strikingly, despite the fact that the RNAi targeted only Sima-RD transcript, infected Sima RNAi flies were not able to increase the expression of Sima-RA, B, D compared to infected control genotype (p-value <0,0001). Similar trend showed also Sima-RA, B. Sima-RB showed strong effect of RNAi even in noninfected individuals (p-value <0,0001). Sima-RC does not seem to respond to the RNA interference the way that the other transcripts do since it was slightly increased in RNAi flies compared to control genotype after infection (p-value = 0,015) (Fig. S8).

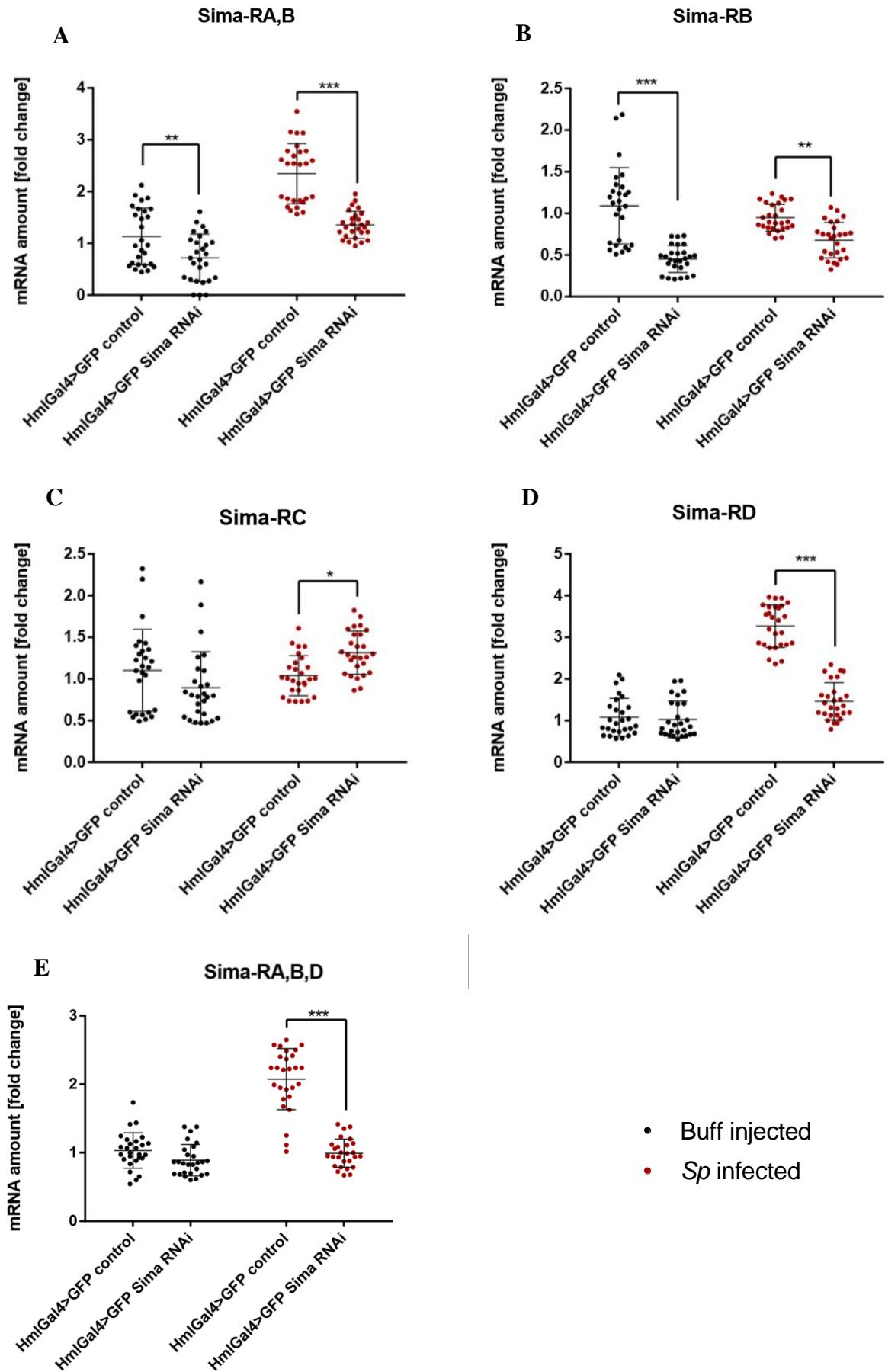


Figure S8: Gene expression of Sima-RA, B (A), Sima-RB (B), Sima-RC (C), Sima-RB (D), Sima-RA, B, D (E) of infected control and Sima RNAi adults at 24hpi. Average number of individuals was more than

200 per each genotype. The graphs display technical replicates. Error bars represent standard deviation. P-value was determined using Two-Way ANOVA (Sidak's multiple comparison test) as follow: P-value for Sima-RA, B = 0,004 (Buff injected) and <0,0001 (*Sp* infected), p-value for Sima-RB <0,0001 (Buff injected) and = 0,001 (*Sp* infected), p-value for Sima-RC = 0,015, p-value for Sima-RD <0,0001, p-value for Sima-RA, B, D <0,0001.

Furthermore, according to FlyBase, a database of *Drosophila* genes & genomes (flybase.org) all four Sima transcripts give rise to one polypeptide (one from each transcript - Sima-PA, Sima-PB, Sima-PC and Sima-PD polypeptide). Their molecular weight and functional domains stated in FlyBase are shown in table S2.

Table S2: Molecular weight and functional domains of Sima polypeptides.

polypeptide	molecular weight (kDa)	functional domains
PA	165,8 kDa	bHLH, PAS (2 repeats), PAS-fold, PAS-fold-3, PAC
PB	47,6 kDa	bHLH, PAS (2 repeats), PAS-fold, PAS-fold-3
PC	95,4 kDa	none predicted
PD	176,3 kDa	bHLH, PAS (2 repeats), PAS-fold, PAS-fold-3, PAC

From the information about exons contained in Sima mRNA and from Sima polypeptide domains we may deduce that Sima-RB probably does not give rise to a fully functional transcription factor Sima since it does not contain ODD sequence and nuclear localization signals (Gorr et al., 2004). Gorr et al., also showed that overexpressed Sima-RB failed to transactivate reporter genes (Gorr et al., 2004). Furthermore, Sima-PC polypeptide does not contain the domain necessary for dimerization with Tgo and it also lacks PAS domain and PAC motif so it may not play an important role in HIF1 α -HRE signaling cascade as well. This suggests that only from RA and RD transcript a properly functional Sima protein might be formed and since our RNAi line targeted only RD transcript, the observed impact of hemocyte specific Sima RNAi that downregulates also RA transcript or even all of them could be even stronger. To prove this theory the measurement of glycolytic genes expression in Sima RNAi flies should be repeated with Sima TRiP line (BL-26207).

Based on our observations, all of the Sima splice variants are present in macrophages of *D. melanogaster*, suggesting, that there is probably some reason to express all four transcripts. We were interested whether some of the isoforms are connected specifically to

infection induced stabilization. Our data show that the expression of Sima-RA, B, Sima-RD and Sima-RA, B, D increased in response to infection in immune cells (p-value <0,0001 for Sima-RA, B, Sima-RD as well as Sima-RA, B, D; p-value not displayed in the graphs) (Fig. S8). Sima-RA and Sima-RD thus seem to play an important role upon infection, whilst Sima-RB and Sima-RC may play only marginal role in this process since their expression was not changed in response to infection. The data suggest that our RNAi line may downregulate also other transcripts, not only Sima-RD, which leads us to the speculation that the transcripts may be mutually regulated and that there might be some kind of negative feedback loop. However, this is just a mere speculation and further analysis in this field is needed.

7.3.2. Efficiency of Sima TRiP RNAi and Impl3 RNAi

In order to evaluate the efficiency of Impl3 RNAi and Sima TRiP RNAi, which were used for survival experiments (and in case of Sima TRiP RNAi for metabolites measurement), expression of Impl3 and Sima genes was measured in Impl3 RNAi (cross no8 in section 3.3. Crosses) and Sima TRiP flies (cross no6 in section 3.3. Crosses) compared to their control genotypes (cross no9 and cross no7 in section 3.3. Crosses) (Fig. S9).

Sima TRiP line downregulates the expression of Sima-RA, B, D even in noninfected flies (p-value <0,0001) (Fig. S9) compared to Sima KK line, which shows the effect on Sima-RA, B, D transcript only upon infection (Fig. S8). This data showed that the RNA interference was effective. Gene expression of Sima-RA, B and Sima-RB was decreased in noninfected individuals as well as in infected flies (all p-values <0,0001). Sima-RD was strongly downregulated after infection in Sima RNAi genotype (p-value <0,0001). Sima-RC transcript shows similar behaviour as in Sima KK RNAi line, meaning that it was upregulated in Sima RNAi flies in response to infection (p-value <0,0001).

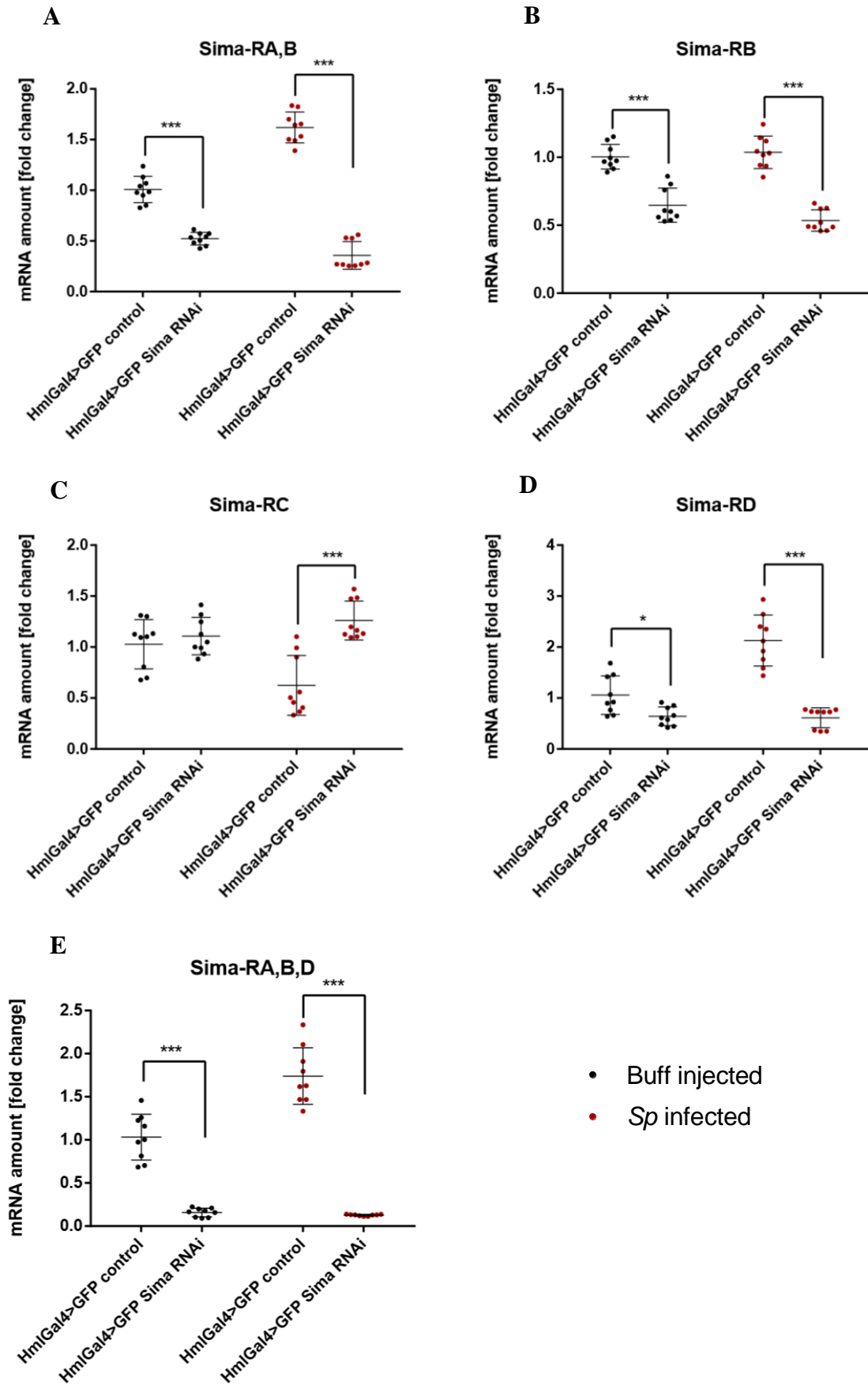


Figure S9: Gene expression of Sima-RA, B (A), Sima-RB (B), Sima-RC (C), Sima-RD (D), Sima-RA, B, D (E) of infected and noninfected control and Sima RNAi adults at 24hpi. Average number of individuals

was more than 200 per each genotype. The graphs display both technical replicates. Error bars represent standard deviation. P-value was determined using Two-Way ANOVA (Sidak's multiple comparison test) as follow: P-value for Sima-RA, B <0,0001 (Buff injected) and <0,0001 (*Sp* infected), p-value for Sima-RB <0,0001 (Buff injected) and <0,0001 (*Sp* infected), p-value for Sima-RC <0,0001, p-value for Sima-RD = 0,0284 (Buff injected) and <0,0001 (*Sp* infected), p-value for Sima-RA, B, D <0,0001 (Buff injected) and <0,0001 (*Sp* infected).

Gene expression of *ImpL3* gene was downregulated in RNAi line compared to control genotype in noninfected (p-value <0,0001) as well as in infected (p-value <0,0001) individuals, meaning that the RNA interference was effective (Fig. S10).

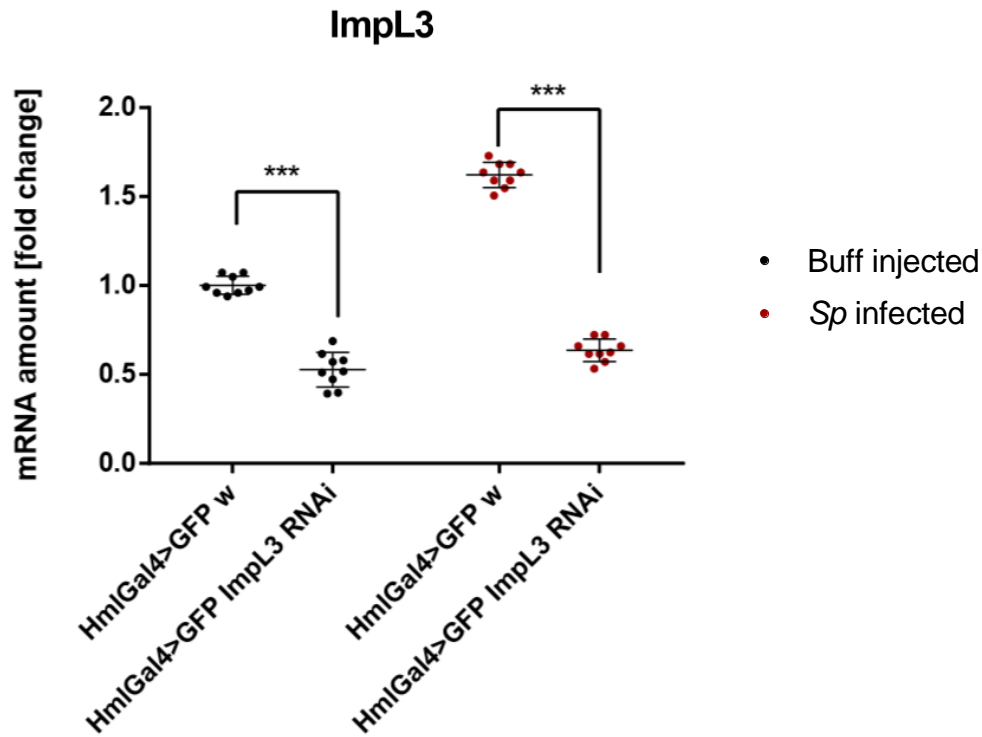


Figure S10: Gene expression of *ImpL3* of infected and noninfected control and *ImpL3* RNAi adults at 24hpi. Average number of individuals was more than 200 per each genotype. The graph displays technical replicates. Error bars represent standard deviation. P-value <0,0001 for both Buff injected and *Sp* infected was determined using Two-Way ANOVA (Sidak's multiple comparison test).

8. REFERENCES

- Adamo, S. A. (2006). Comparative Psychoneuroimmunology: Evidence From the Insects. *Behavioral and Cognitive Neuroscience Reviews*, 5(3), 128–140. <https://doi.org/10.1177/1534582306289580>
- Agaisse, H., Petersen, U. M., Boutros, M., Mathey-Prevot, B., & Perrimon, N. (2003). Signaling role of hemocytes in *Drosophila* JAK/STAT-dependent response to septic injury. *Developmental Cell*, 5(3), 441–450. Retrieved from <http://www.ncbi.nlm.nih.gov/pubmed/12967563>
- Aktan, F. (2004). iNOS-mediated nitric oxide production and its regulation. *Life Sciences*, 75(6), 639–653. <https://doi.org/10.1016/j.lfs.2003.10.042>
- Albina, J. E., Mills, C. D., Henry, W. L., & Caldwell, M. D. (1990). Temporal expression of different pathways of 1-arginine metabolism in healing wounds. *Journal of Immunology (Baltimore, Md. : 1950)*, 144(10), 3877–3880. Retrieved from <http://www.ncbi.nlm.nih.gov/pubmed/2332635>
- Allavena, P., Peccatori, F., Maggioni, D., Erroi, A., Sironi, M., Colombo, N., ... Mangioni, C. (1990). Intraperitoneal recombinant gamma-interferon in patients with recurrent ascitic ovarian carcinoma: modulation of cytotoxicity and cytokine production in tumor-associated effectors and of major histocompatibility antigen expression on tumor cells. *Cancer Research*, 50(22), 7318–7323. Retrieved from <http://www.ncbi.nlm.nih.gov/pubmed/2121337>
- Allee, J. (2011). Impl2 represses insulin signalling in response to hypoxia. Dissertation thesis. University of Oregon. Retrieved from <http://www.scholarsbank.uoregon.edu>
- Andersen, S. K., Gjedsted, J., Christiansen, C., & Tønnesen, E. (2004). The roles of insulin and hyperglycemia in sepsis pathogenesis. *Journal of Leukocyte Biology*, 75(3), 413–421. <https://doi.org/10.1189/jlb.0503195>
- Arrese, E. L., & Soulages, J. L. (2010). Insect Fat Body: Energy, Metabolism, and Regulation. *Annual Review of Entomology*, 55(1), 207–225. <https://doi.org/10.1146/annurev-ento-112408-085356>
- Avraham-Davidi, I., Yona, S., Grunewald, M., Landsman, L., Cochain, C., Silvestre, J. S., ... Keshet, E. (2013). On-site education of VEGF-recruited monocytes improves their performance as angiogenic and arteriogenic accessory cells. *The Journal of Experimental Medicine*, 210(12), 2611–2625. <https://doi.org/10.1084/jem.20120690>
- Ayres, J. S., & Schneider, D. S. (2012). Tolerance of Infections. *Annual Review of Immunology*, 30(1), 271–294. <https://doi.org/10.1146/annurev-immunol-020711-075030>
- Baardman, J., Licht, I., de Winther, M. P., & Van den Bossche, J. (2015). Metabolic–epigenetic crosstalk in macrophage activation. *Epigenomics*, 7(7), 1155–1164. <https://doi.org/10.2217/epi.15.71>
- Bajgar, A., Kucerova, K., Jonatova, L., Tomcala, A., Schneedorferova, I., Okrouhlik, J., & Dolezal, T. (2015). Extracellular Adenosine Mediates a Systemic Metabolic Switch during Immune Response. *PLOS Biology*, 13(4), e1002135. <https://doi.org/10.1371/journal.pbio.1002135>

- Beatty, G. L., Chiorean, E. G., Fishman, M. P., Saboury, B., Teitelbaum, U. R., Sun, W., ... Vonderheide, R. H. (2011). CD40 Agonists Alter Tumor Stroma and Show Efficacy Against Pancreatic Carcinoma in Mice and Humans. *Science*, *331*(6024), 1612–1616. <https://doi.org/10.1126/science.1198443>
- Bedard, K., & Krause, K.-H. (2007). The NOX Family of ROS-Generating NADPH Oxidases: Physiology and Pathophysiology. *Physiological Reviews*, *87*(1), 245–313. <https://doi.org/10.1152/physrev.00044.2005>
- Bendtzen, K., Mandrup-Poulsen, T., Nerup, J., Nielsen, J. H., Dinarello, C. A., & Svenson, M. (1986). Cytotoxicity of human pI 7 interleukin-1 for pancreatic islets of Langerhans. *Science (New York, N.Y.)*, *232*(4757), 1545–1547. Retrieved from <http://www.ncbi.nlm.nih.gov/pubmed/3086977>
- Blouin, C. C. (2003). Hypoxic gene activation by lipopolysaccharide in macrophages: implication of hypoxia-inducible factor 1. *Blood*, *103*(3), 1124–1130. <https://doi.org/10.1182/blood-2003-07-2427>
- Borregaard, N., & Herlin, T. (1982). Energy Metabolism of Human Neutrophils during Phagocytosis. *Journal of Clinical Investigation*, *70*(3), 550–557. <https://doi.org/10.1172/JCI110647>
- Brand, A. H., & Perrimon, N. (1993). Targeted gene expression as a means of altering cell fates and generating dominant phenotypes. *Development (Cambridge, England)*, *118*(2), 401–415. Retrieved from <http://www.ncbi.nlm.nih.gov/pubmed/8223268>
- Brenot, A., Knolhoff, B. L., DeNardo, D. G., & Longmore, G. D. (2018). SNAIL1 action in tumor cells influences macrophage polarization and metastasis in breast cancer through altered GM-CSF secretion. *Oncogenesis*, *7*(3), 32. <https://doi.org/10.1038/s41389-018-0042-x>
- Burns, J., & Manda, G. (2017). Metabolic Pathways of the Warburg Effect in Health and Disease: Perspectives of Choice, Chain or Chance. *International Journal of Molecular Sciences*, *18*(12), 2755. <https://doi.org/10.3390/ijms18122755>
- Buttgereit, F., Burmester, G. R., & Brand, M. D. (2000). Bioenergetics of immune functions: fundamental and therapeutic aspects. *Immunology Today*, *21*(4), 192–199. Retrieved from <http://www.ncbi.nlm.nih.gov/pubmed/10740243>
- Byles, V., Covarrubias, A. J., Ben-Sahra, I., Lamming, D. W., Sabatini, D. M., Manning, B. D., & Horng, T. (2013). The TSC-mTOR pathway regulates macrophage polarization. *Nature Communications*, *4*. <https://doi.org/10.1038/ncomms3834>
- Chaudhuri, A. (2014). Regulation of Macrophage Polarization by RON Receptor Tyrosine Kinase Signaling. *Frontiers in Immunology*, *5*. <https://doi.org/10.3389/fimmu.2014.00546>
- Chettri, J. K., Raida, M. K., Holten-Andersen, L., Kania, P. W., & Buchmann, K. (2011). PAMP induced expression of immune relevant genes in head kidney leukocytes of rainbow trout (*Oncorhynchus mykiss*). *Developmental & Comparative Immunology*, *35*(4), 476–482. <https://doi.org/10.1016/j.dci.2010.12.001>
- Colegio, O. R., Chu, N.-Q., Szabo, A. L., Chu, T., Rhebergen, A. M., Jairam, V., ... Medzhitov, R. (2014). Functional polarization of tumour-associated macrophages by tumour-derived lactic acid. *Nature*, *513*(7519), 559–563.

<https://doi.org/10.1038/nature13490>

- Collier, B., Dossett, L. A., May, A. K., & Diaz, J. J. (2008). Glucose control and the inflammatory response. *Nutrition in Clinical Practice : Official Publication of the American Society for Parenteral and Enteral Nutrition*, 23(1), 3–15. Retrieved from <http://www.ncbi.nlm.nih.gov/pubmed/18203960>
- Colombo, N., Peccatori, F., Paganin, C., Bini, S., Brandely, M., Mangioni, C., ... Allavena, P. (1992). Anti-tumor and immunomodulatory activity of intraperitoneal IFN- γ in ovarian carcinoma patients with minimal residual tumor after chemotherapy. *International Journal of Cancer*, 51(1), 42–46. <https://doi.org/10.1002/ijc.2910510109>
- Crabtree, H. G. (1929). Observations on the carbohydrate metabolism of tumours. *The Biochemical Journal*, 23(3), 536–545. Retrieved from <http://www.ncbi.nlm.nih.gov/pubmed/16744238>
- Dandona, P., Aljada, A., & Bandyopadhyay, A. (2004). Inflammation: the link between insulin resistance, obesity and diabetes. *Trends in Immunology*, 25(1), 4–7. Retrieved from <http://www.ncbi.nlm.nih.gov/pubmed/14698276>
- Davies, L. C., Jenkins, S. J., Allen, J. E., & Taylor, P. R. (2013). Tissue-resident macrophages. *Nature Immunology*, 14(10), 986–995. <https://doi.org/10.1038/ni.2705>
- De Lella Ezcurra, A. L., Bertolin, A. P., Kim, K., Katz, M. J., Gándara, L., Misra, T., ... Wappner, P. (2016). miR-190 Enhances HIF-Dependent Responses to Hypoxia in *Drosophila* by Inhibiting the Prolyl-4-hydroxylase Fga. *PLOS Genetics*, 12(5), e1006073. <https://doi.org/10.1371/journal.pgen.1006073>
- Donath, M. Y. (2014). Targeting inflammation in the treatment of type 2 diabetes: time to start. *Nature Reviews Drug Discovery*, 13(6), 465–476. <https://doi.org/10.1038/nrd4275>
- Doughty, C. A. (2006). Antigen receptor-mediated changes in glucose metabolism in B lymphocytes: role of phosphatidylinositol 3-kinase signaling in the glycolytic control of growth. *Blood*, 107(11), 4458–4465. <https://doi.org/10.1182/blood-2005-12-4788>
- Doulias, P.-T., Tenopoulou, M., Greene, J. L., Raju, K., & Ischiropoulos, H. (2013). Nitric Oxide Regulates Mitochondrial Fatty Acid Metabolism Through Reversible Protein S-Nitrosylation. *Science Signaling*, 6(256), rs1-rs1. <https://doi.org/10.1126/scisignal.2003252>
- Dzik, J. M. (2010). The ancestry and cumulative evolution of immune reactions. *Acta Biochimica Polonica*, 57(4), 443–466. Retrieved from <http://www.ncbi.nlm.nih.gov/pubmed/21046016>
- Dzik, J. M. (2014). Evolutionary roots of arginase expression and regulation. *Frontiers in Immunology*, 5, 544. <https://doi.org/10.3389/fimmu.2014.00544>
- Everts, B., Amiel, E., van der Windt, G. J. W., Freitas, T. C., Chott, R., Yarasheski, K. E., ... Pearce, E. J. (2012). Commitment to glycolysis sustains survival of NO-producing inflammatory dendritic cells. *Blood*, 120(7), 1422–1431. <https://doi.org/10.1182/blood-2012-03-419747>
- Ferrandon, D. (1998). A drosomycin-GFP reporter transgene reveals a local immune response in *Drosophila* that is not dependent on the Toll pathway. *The EMBO Journal*, 17(5), 1217–1227. <https://doi.org/10.1093/emboj/17.5.1217>

- Figuroa-Clarevega, A., & Bilder, D. (2015). Malignant *Drosophila* Tumors Interrupt Insulin Signaling to Induce Cachexia-like Wasting. *Developmental Cell*, *33*(1), 47–55. <https://doi.org/10.1016/j.devcel.2015.03.001>
- Foley, E., & O'Farrell, P. H. (2003). Nitric oxide contributes to induction of innate immune responses to gram-negative bacteria in *Drosophila*. *Genes & Development*, *17*(1), 115–125. <https://doi.org/10.1101/gad.1018503>
- Fong, Y. M., Marano, M. A., Moldawer, L. L., Wei, H., Calvano, S. E., Kenney, J. S., ... Lowry, S. F. (1990). The acute splanchnic and peripheral tissue metabolic response to endotoxin in humans. *Journal of Clinical Investigation*, *85*(6), 1896–1904. <https://doi.org/10.1172/JCI114651>
- Frauwirth, K. A., & Thompson, C. B. (2004). Regulation of T Lymphocyte Metabolism. *The Journal of Immunology*, *172*(8), 4661–4665. <https://doi.org/10.4049/jimmunol.172.8.4661>
- Galván-Peña, S., & O'Neill, L. A. J. (2014). Metabolic Reprogramming in Macrophage Polarization. *Frontiers in Immunology*, *5*. <https://doi.org/10.3389/fimmu.2014.00420>
- Ganeshan, K., & Chawla, A. (2014). Metabolic Regulation of Immune Responses. *Annual Review of Immunology*, *32*(1), 609–634. <https://doi.org/10.1146/annurev-immunol-032713-120236>
- Ganz, T. (2012). Macrophages and Systemic Iron Homeostasis. *Journal of Innate Immunity*, *4*(5–6), 446–453. <https://doi.org/10.1159/000336423>
- Garcia-Alvarez, M., Marik, P., & Bellomo, R. (2014). Sepsis-associated hyperlactatemia. *Critical Care*, *18*(5), 503. <https://doi.org/10.1186/s13054-014-0503-3>
- Geissmann, F., Manz, M. G., Jung, S., Sieweke, M. H., Merad, M., & Ley, K. (2010). Development of Monocytes, Macrophages, and Dendritic Cells. *Science*, *327*(5966), 656–661. <https://doi.org/10.1126/science.1178331>
- Gendrin, M., Welchman, D. P., Poidevin, M., Hervé, M., & Lemaitre, B. (2009). Long-Range Activation of Systemic Immunity through Peptidoglycan Diffusion in *Drosophila*. *PLoS Pathogens*, *5*(12), e1000694. <https://doi.org/10.1371/journal.ppat.1000694>
- Ghosh, D. K., Wu, C., Pitters, E., Moloney, M., Werner, E. R., Mayer, B., & Stuehr, D. J. (1997). Characterization of the Inducible Nitric Oxide Synthase Oxygenase Domain Identifies a 49 Amino Acid Segment Required for Subunit Dimerization and Tetrahydrobiopterin Interaction. *Biochemistry*, *36*(35), 10609–10619. <https://doi.org/10.1021/bi9702290>
- Ghosh, S., Singh, A., Mandal, S., & Mandal, L. (2015). Active Hematopoietic Hubs in *Drosophila* Adults Generate Hemocytes and Contribute to Immune Response. *Developmental Cell*, *33*(4), 478–488. <https://doi.org/10.1016/j.devcel.2015.03.014>
- Gold, K. S., & Brückner, K. (2015). Macrophages and cellular immunity in *Drosophila melanogaster*. *Seminars in Immunology*, *27*(6), 357–368. <https://doi.org/10.1016/j.smim.2016.03.010>
- Gorr, T. A., Tomita, T., Wappner, P., & Bunn, H. F. (2004). Regulation of *Drosophila* Hypoxia-inducible Factor (HIF) Activity in SL2 Cells. *Journal of Biological Chemistry*, *279*(34), 36048–36058. <https://doi.org/10.1074/jbc.M405077200>

- Govind, S. (2008). Innate immunity in *Drosophila*: Pathogens and pathways. *Insect Science*, 15(1), 29–43. <https://doi.org/10.1111/j.1744-7917.2008.00185.x>
- Greenberg, S., & Grinstein, S. (2002). Phagocytosis and innate immunity. *Current Opinion in Immunology*, 14(1), 136–145. Retrieved from <http://www.ncbi.nlm.nih.gov/pubmed/11790544>
- Greijer, A., van der Groep, P., Kemming, D., Shvarts, A., Semenza, G., Meijer, G., ... van der Wall, E. (2005). Up-regulation of gene expression by hypoxia is mediated predominantly by hypoxia-inducible factor 1 (HIF-1). *The Journal of Pathology*, 206(3), 291–304. <https://doi.org/10.1002/path.1778>
- Ha, E.-M. (2005). A Direct Role for Dual Oxidase in *Drosophila* Gut Immunity. *Science*, 310(5749), 847–850. <https://doi.org/10.1126/science.1117311>
- Hamilton, T. A., Zhao, C., Pavicic, P. G., & Datta, S. (2014). Myeloid Colony-Stimulating Factors as Regulators of Macrophage Polarization. *Frontiers in Immunology*, 5. <https://doi.org/10.3389/fimmu.2014.00554>
- Hard, G. C. (1970). Some biochemical aspects of the immune macrophage. *British Journal of Experimental Pathology*, 51(1), 97–105. Retrieved from <http://www.ncbi.nlm.nih.gov/pubmed/5434449>
- Haschemi, A., Kosma, P., Gille, L., Evans, C. R., Burant, C. F., Starkl, P., ... Wagner, O. (2012). The Sedoheptulose Kinase CARKL Directs Macrophage Polarization through Control of Glucose Metabolism. *Cell Metabolism*, 15(6), 813–826. <https://doi.org/10.1016/j.cmet.2012.04.023>
- Horn, L., Leips, J., & Starz-Gaiano, M. (2014). Phagocytic ability declines with age in adult *Drosophila* hemocytes. *Aging Cell*, 13(4), 719–728. <https://doi.org/10.1111/ace1.12227>
- Howell, J. J., & Manning, B. D. (2011). mTOR couples cellular nutrient sensing to organismal metabolic homeostasis. *Trends in Endocrinology & Metabolism*, 22(3), 94–102. <https://doi.org/10.1016/j.tem.2010.12.003>
- Ignarro, L. J. (1990). Biosynthesis and Metabolism of Endothelium-Derived Nitric Oxide. *Annual Review of Pharmacology and Toxicology*, 30(1), 535–560. <https://doi.org/10.1146/annurev.pa.30.040190.002535>
- Imtiyaz, H. Z., & Simon, M. C. (2010). Hypoxia-Inducible Factors as Essential Regulators of Inflammation (pp. 105–120). https://doi.org/10.1007/82_2010_74
- Jacobs, S. R., Herman, C. E., Maciver, N. J., Wofford, J. A., Wieman, H. L., Hammen, J. J., & Rathmell, J. C. (2008). Glucose uptake is limiting in T cell activation and requires CD28-mediated Akt-dependent and independent pathways. *Journal of Immunology (Baltimore, Md. : 1950)*, 180(7), 4476–4486. Retrieved from <http://www.ncbi.nlm.nih.gov/pubmed/18354169>
- Janeway, C. A., & Medzhitov, R. (2002). Innate immune recognition. *Annual Review of Immunology*, 20, 197–216. <https://doi.org/10.1146/annurev.immunol.20.083001.084359>
- Janeway, C.A. Jr., Travers, P., Walport, M., et al. Immunobiology: The Immune System in Health and Disease. 5th edition. New York: Garland Science; 2001. Principles of innate and adaptive immunity. Available from: <https://www.ncbi.nlm.nih.gov/books/NBK27090/>

- Jang, S., Kang, H. T., & Hwang, E. S. (2012). Nicotinamide-induced Mitophagy. *Journal of Biological Chemistry*, 287(23), 19304–19314. <https://doi.org/10.1074/jbc.M112.363747>
- Jantsch, J., Chakravorty, D., Turza, N., Prechtel, A. T., Buchholz, B., Gerlach, R. G., ... Willam, C. (2008). Hypoxia and hypoxia-inducible factor-1 alpha modulate lipopolysaccharide-induced dendritic cell activation and function. *Journal of Immunology (Baltimore, Md. : 1950)*, 180(7), 4697–4705. Retrieved from <http://www.ncbi.nlm.nih.gov/pubmed/18354193>
- Jha, A. K., Huang, S. C.-C., Sergushichev, A., Lampropoulou, V., Ivanova, Y., Loginicheva, E., ... Artyomov, M. N. (2015). Network Integration of Parallel Metabolic and Transcriptional Data Reveals Metabolic Modules that Regulate Macrophage Polarization. *Immunity*, 42(3), 419–430. <https://doi.org/10.1016/j.immuni.2015.02.005>
- Kawai, T., & Akira, S. (2007). Signaling to NF-κB by Toll-like receptors. *Trends in Molecular Medicine*, 13(11), 460–469. <https://doi.org/10.1016/j.molmed.2007.09.002>
- Kellett, D. N. (1966). 2-Deoxyglucose and inflammation. *The Journal of Pharmacy and Pharmacology*, 18(3), 199–200. Retrieved from <http://www.ncbi.nlm.nih.gov/pubmed/4381222>
- Kelly, B., & O'Neill, L. A. J. (2015). Metabolic reprogramming in macrophages and dendritic cells in innate immunity. *Cell Research*, 25(7), 771–784. <https://doi.org/10.1038/cr.2015.68>
- Kitowska, K., Zakrzewicz, D., Königshoff, M., Chrobak, I., Grimminger, F., Seeger, W., ... Eickelberg, O. (2008). Functional role and species-specific contribution of arginases in pulmonary fibrosis. *American Journal of Physiology-Lung Cellular and Molecular Physiology*, 294(1), L34–L45. <https://doi.org/10.1152/ajplung.00007.2007>
- Komohara, Y., Jinushi, M., & Takeya, M. (2014). Clinical significance of macrophage heterogeneity in human malignant tumors. *Cancer Science*, 105(1), 1–8. <https://doi.org/10.1111/cas.12314>
- Kraakman, M. J., Murphy, A. J., Jandeleit-Dahm, K., & Kammoun, H. L. (2014). Macrophage Polarization in Obesity and Type 2 Diabetes: Weighing Down Our Understanding of Macrophage Function? *Frontiers in Immunology*, 5. <https://doi.org/10.3389/fimmu.2014.00470>
- Krauss, S., Brand, M. D., & Buttgerit, F. (2001). Signaling takes a breath--new quantitative perspectives on bioenergetics and signal transduction. *Immunity*, 15(4), 497–502. Retrieved from <http://www.ncbi.nlm.nih.gov/pubmed/11672532>
- Kuzin, B., Roberts, I., Peunova, N., & Enikolopov, G. (1996). Nitric Oxide Regulates Cell Proliferation during Drosophila Development. *Cell*, 87(4), 639–649. [https://doi.org/10.1016/S0092-8674\(00\)81384-7](https://doi.org/10.1016/S0092-8674(00)81384-7)
- Kwon, Y., Song, W., Droujinine, I. A., Hu, Y., Asara, J. M., & Perrimon, N. (2015). Systemic Organ Wasting Induced by Localized Expression of the Secreted Insulin/IGF Antagonist ImpL2. *Developmental Cell*, 33(1), 36–46. <https://doi.org/10.1016/j.devcel.2015.02.012>
- Lanot, R., Zachary, D., Holder, F., & Meister, M. (2001). Postembryonic Hematopoiesis in Drosophila. *Developmental Biology*, 230(2), 243–257. <https://doi.org/10.1006/dbio.2000.0123>

- Larsen, C. M., Faulenbach, M., Vaag, A., Vølund, A., Ehses, J. A., Seifert, B., ... Donath, M. Y. (2007). Interleukin-1–Receptor Antagonist in Type 2 Diabetes Mellitus. *New England Journal of Medicine*, 356(15), 1517–1526. <https://doi.org/10.1056/NEJMoa065213>
- Larson, S. J., & Dunn, A. J. (2001). Behavioral Effects of Cytokines. *Brain, Behavior, and Immunity*, 15(4), 371–387. <https://doi.org/10.1006/brbi.2001.0643>
- Lavista-Llanos, S., Centanin, L., Irisarri, M., Russo, D. M., Gleadle, J. M., Bocca, S. N., ... Wappner, P. (2002). Control of the Hypoxic Response in *Drosophila melanogaster* by the Basic Helix-Loop-Helix PAS Protein Similar. *Molecular and Cellular Biology*, 22(19), 6842–6853. <https://doi.org/10.1128/MCB.22.19.6842-6853.2002>
- Lee, H.-J., Jedrychowski, M. P., Vinayagam, A., Wu, N., Shyh-Chang, N., Hu, Y., ... Kirschner, M. W. (2017). Proteomic and Metabolomic Characterization of a Mammalian Cellular Transition from Quiescence to Proliferation. *Cell Reports*, 20(3), 721–736. <https://doi.org/10.1016/j.celrep.2017.06.074>
- Lemaitre, B., & Hoffmann, J. (2007). The Host Defense of *Drosophila melanogaster*. *Annual Review of Immunology*, 25(1), 697–743. <https://doi.org/10.1146/annurev.immunol.25.022106.141615>
- Lemaitre, B., Kromer-Metzger, E., Michaut, L., Nicolas, E., Meister, M., Georgel, P., ... Hoffmann, J. A. (1995). A recessive mutation, immune deficiency (imd), defines two distinct control pathways in the *Drosophila* host defense. *Proceedings of the National Academy of Sciences of the United States of America*, 92(21), 9465–9469. Retrieved from <http://www.ncbi.nlm.nih.gov/pubmed/7568155>
- Lemaitre, B., Reichhart, J. M., & Hoffmann, J. A. (1997). *Drosophila* host defense: differential induction of antimicrobial peptide genes after infection by various classes of microorganisms. *Proceedings of the National Academy of Sciences of the United States of America*, 94(26), 14614–14619. <https://doi.org/9405661>
- Ley, K., Laudanna, C., Cybulsky, M. I., & Nourshargh, S. (2007). Getting to the site of inflammation: the leukocyte adhesion cascade updated. *Nature Reviews Immunology*, 7(9), 678–689. <https://doi.org/10.1038/nri2156>
- Li, Y., Padmanabha, D., Gentile, L. B., Dumur, C. I., Beckstead, R. B., & Baker, K. D. (2013). HIF- and Non-HIF-Regulated Hypoxic Responses Require the Estrogen-Related Receptor in *Drosophila melanogaster*. *PLoS Genetics*, 9(1), e1003230. <https://doi.org/10.1371/journal.pgen.1003230>
- Linford, N. J., Bilgir, C., Ro, J., & Pletcher, S. D. (2013). Measurement of Lifespan in *Drosophila melanogaster*. *Journal of Visualized Experiments*, (71). <https://doi.org/10.3791/50068>
- Litman, G. W., & Cooper, M. D. (2007). Why study the evolution of immunity? *Nature Immunology*, 8(6), 547–548. <https://doi.org/10.1038/ni0607-547>
- Locasale, J. W., & Cantley, L. C. (2011). Metabolic Flux and the Regulation of Mammalian Cell Growth. *Cell Metabolism*, 14(4), 443–451. <https://doi.org/10.1016/j.cmet.2011.07.014>
- Maarsingh, H., Dekkers, B. G. J., Zuidhof, A. B., Bos, I. S. T., Menzen, M. H., Klein, T., ... Meurs, H. (2011). Increased arginase activity contributes to airway remodelling in

- chronic allergic asthma. *European Respiratory Journal*, 38(2), 318–328.
<https://doi.org/10.1183/09031936.00057710>
- Mackenzie, D. K., Bussière, L. F., & Tinsley, M. C. (2011). Senescence of the cellular immune response in *Drosophila melanogaster*. *Experimental Gerontology*, 46(11), 853–859. <https://doi.org/10.1016/j.exger.2011.07.004>
- MacMicking, J., Xie, Q., & Nathan, C. (1997). NITRIC OXIDE AND MACROPHAGE FUNCTION. *Annual Review of Immunology*, 15(1), 323–350.
<https://doi.org/10.1146/annurev.immunol.15.1.323>
- Maderna, P., & Godson, C. (2003). Phagocytosis of apoptotic cells and the resolution of inflammation. *Biochimica et Biophysica Acta (BBA) - Molecular Basis of Disease*, 1639(3), 141–151. <https://doi.org/10.1016/j.bbadis.2003.09.004>
- Masoud, G. N., & Li, W. (2015). HIF-1 α pathway: role, regulation and intervention for cancer therapy. *Acta Pharmaceutica Sinica B*, 5(5), 378–389.
<https://doi.org/10.1016/j.apsb.2015.05.007>
- Matsuzawa, A., Saegusa, K., Noguchi, T., Sadamitsu, C., Nishitoh, H., Nagai, S., ... Ichijo, H. (2005). ROS-dependent activation of the TRAF6-ASK1-p38 pathway is selectively required for TLR4-mediated innate immunity. *Nature Immunology*, 6(6), 587–592.
<https://doi.org/10.1038/ni1200>
- Maxwell, P. H. (2005). The HIF pathway in cancer. *Seminars in Cell & Developmental Biology*, 16(4–5), 523–530. <https://doi.org/10.1016/j.semcdb.2005.03.001>
- McKean, K. A., Yourth, C. P., Lazzaro, B. P., & Clark, A. G. (2008). The evolutionary costs of immunological maintenance and deployment. *BMC Evolutionary Biology*, 8(1), 76.
<https://doi.org/10.1186/1471-2148-8-76>
- Medzhitov, R. (2007). Recognition of microorganisms and activation of the immune response. *Nature*, 449(7164), 819–826. <https://doi.org/10.1038/nature06246>
- Michelucci, A., Cordes, T., Ghelfi, J., Pailot, A., Reiling, N., Goldmann, O., ... Hiller, K. (2013). Immune-responsive gene 1 protein links metabolism to immunity by catalyzing itaconic acid production. *Proceedings of the National Academy of Sciences*, 110(19), 7820–7825. <https://doi.org/10.1073/pnas.1218599110>
- Mills, C. D. (2001). Macrophage Arginine Metabolism to Ornithine/Urea or Nitric Oxide/Citrulline: A Life or Death Issue. *Critical ReviewsTM in Immunology*, 21(5), 28.
<https://doi.org/10.1615/CritRevImmunol.v21.i5.10>
- Mills, C. D. (2012). M1 and M2 Macrophages: Oracles of Health and Disease. *Critical Reviews in Immunology*, 32(6), 463–488. Retrieved from
<http://www.ncbi.nlm.nih.gov/pubmed/23428224>
- Mills, C. D., Lenz, L. L., & Ley, K. (2015). Macrophages at the Fork in the Road to Health or Disease. *Frontiers in Immunology*, 6. <https://doi.org/10.3389/fimmu.2015.00059>
- Mills, C. D., & Ley, K. (2014). M1 and M2 Macrophages: The Chicken and the Egg of Immunity. *Journal of Innate Immunity*, 6(6), 716–726.
<https://doi.org/10.1159/000364945>
- Mills, C. D., Shearer, J., Evans, R., & Caldwell, M. D. (1992). Macrophage arginine metabolism and the inhibition or stimulation of cancer. *Journal of Immunology*

- (*Baltimore, Md. : 1950*), 149(8), 2709–2714. Retrieved from <http://www.ncbi.nlm.nih.gov/pubmed/1401910>
- Mills, C. D., Thomas, A. C., Lenz, L. L., & Munder, M. (2014). Macrophage: SHIP of Immunity. *Frontiers in Immunology*, 5. <https://doi.org/10.3389/fimmu.2014.00620>
- Modolell, M., Corraliza, I. M., Link, F., Soler, G., & Eichmann, K. (1995). Reciprocal regulation of the nitric oxide synthase/arginase balance in mouse bone marrow-derived macrophages by TH 1 and TH 2 cytokines. *European Journal of Immunology*, 25(4), 1101–1104. <https://doi.org/10.1002/eji.1830250436>
- Mohlin, S., Wigerup, C., Jögi, A., & Pålman, S. (2017). Hypoxia, pseudohypoxia and cellular differentiation. *Experimental Cell Research*, 356(2), 192–196. <https://doi.org/10.1016/j.yexcr.2017.03.007>
- Mosser, D. M., & Edwards, J. P. (2008). Exploring the full spectrum of macrophage activation. *Nature Reviews Immunology*, 8(12), 958–969. <https://doi.org/10.1038/nri2448>
- Murray, P. J., Allen, J. E., Biswas, S. K., Fisher, E. A., Gilroy, D. W., Goerdt, S., ... Wynn, T. A. (2014). Macrophage Activation and Polarization: Nomenclature and Experimental Guidelines. *Immunity*, 41(1), 14–20. <https://doi.org/10.1016/j.immuni.2014.06.008>
- Nathan, C. (2002). Points of control in inflammation. *Nature*, 420(6917), 846–852. <https://doi.org/10.1038/nature01320>
- Nathan, C. F., & Hibbs, J. B. (1991). Role of nitric oxide synthesis in macrophage antimicrobial activity. *Current Opinion in Immunology*, 3(1), 65–70. Retrieved from <http://www.ncbi.nlm.nih.gov/pubmed/1711326>
- Netea, M. G., Joosten, L. A. B., Latz, E., Mills, K. H. G., Natoli, G., Stunnenberg, H. G., ... Xavier, R. J. (2016). Trained immunity: A program of innate immune memory in health and disease. *Science*, 352(6284), aaf1098–aaf1098. <https://doi.org/10.1126/science.aaf1098>
- Newsholme, P., Curi, R., Gordon, S., & Newsholme, E. A. (1986). Metabolism of glucose, glutamine, long-chain fatty acids and ketone bodies by murine macrophages. *The Biochemical Journal*, 239(1), 121–125. Retrieved from <http://www.ncbi.nlm.nih.gov/pubmed/3800971>
- Newsholme, P., Gordon, S., & Newsholme, E. A. (1987). Rates of utilization and fates of glucose, glutamine, pyruvate, fatty acids and ketone bodies by mouse macrophages. *The Biochemical Journal*, 242(3), 631–636. Retrieved from <http://www.ncbi.nlm.nih.gov/pubmed/3593269>
- Neyen, C., Bretscher, A. J., Binggeli, O., & Lemaitre, B. (2014). Methods to study *Drosophila* immunity. *Methods*, 68(1), 116–128. <https://doi.org/10.1016/j.ymeth.2014.02.023>
- Novak, M. L., & Koh, T. J. (2013). Macrophage phenotypes during tissue repair. *Journal of Leukocyte Biology*, 93(6), 875–881. <https://doi.org/10.1189/jlb.1012512>
- O'Neill, L. A. J. (2015). A Broken Krebs Cycle in Macrophages. *Immunity*, 42(3), 393–394. <https://doi.org/10.1016/j.immuni.2015.02.017>
- Padmanabha, D., & Baker, K. D. (2014). *Drosophila* gains traction as a repurposed tool to

- investigate metabolism. *Trends in Endocrinology & Metabolism*, 25(10), 518–527.
<https://doi.org/10.1016/j.tem.2014.03.011>
- Pauleau, A.-L., Rutschman, R., Lang, R., Pernis, A., Watowich, S. S., & Murray, P. J. (2004). Enhancer-Mediated Control of Macrophage-Specific Arginase I Expression. *The Journal of Immunology*, 172(12), 7565–7573.
<https://doi.org/10.4049/jimmunol.172.12.7565>
- Pearce, E. L., & Pearce, E. J. (2013). Metabolic Pathways in Immune Cell Activation and Quiescence. *Immunity*, 38(4), 633–643. <https://doi.org/10.1016/j.immuni.2013.04.005>
- Pegg, A. E. (2009). Mammalian polyamine metabolism and function. *IUBMB Life*, 61(9), 880–894. <https://doi.org/10.1002/iub.230>
- Peled, M., & Fisher, E. A. (2014). Dynamic Aspects of Macrophage Polarization during Atherosclerosis Progression and Regression. *Frontiers in Immunology*, 5.
<https://doi.org/10.3389/fimmu.2014.00579>
- Peters, A., Schweiger, U., Pellerin, L., Hubold, C., Oltmanns, K. M., Conrad, M., ... Fehm, H. L. (2004). The selfish brain: competition for energy resources. *Neuroscience & Biobehavioral Reviews*, 28(2), 143–180.
<https://doi.org/10.1016/j.neubiorev.2004.03.002>
- Peyssonaux, C., Datta, V., Cramer, T., Doedens, A., Theodorakis, E. A., Gallo, R. L., ... Johnson, R. S. (2005). HIF-1 α expression regulates the bactericidal capacity of phagocytes. *Journal of Clinical Investigation*, 115(7), 1806–1815.
<https://doi.org/10.1172/JCI23865>
- Poon, E., Harris, A. L., & Ashcroft, M. (2009). Targeting the hypoxia-inducible factor (HIF) pathway in cancer. *Expert Reviews in Molecular Medicine*, 11, e26.
<https://doi.org/10.1017/S1462399409001173>
- Ratner, S., & Vinson, S. B. (1983). Phagocytosis and Encapsulation: Cellular Immune Responses in Arthropoda. *American Zoologist*, 23(1), 185–194.
<https://doi.org/10.1093/icb/23.1.185>
- Reales-Calderón, J. A., Aguilera-Montilla, N., Corbí, Á. L., Molero, G., & Gil, C. (2014). Proteomic characterization of human proinflammatory M1 and anti-inflammatory M2 macrophages and their response to *Candida albicans*. *PROTEOMICS*, 14(12), 1503–1518. <https://doi.org/10.1002/pmic.201300508>
- Regan, J. C., Brandão, A. S., Leitão, A. B., Mantas Dias, Â. R., Sucena, É., Jacinto, A., & Zaidman-Rémy, A. (2013). Steroid Hormone Signaling Is Essential to Regulate Innate Immune Cells and Fight Bacterial Infection in *Drosophila*. *PLoS Pathogens*, 9(10), e1003720. <https://doi.org/10.1371/journal.ppat.1003720>
- Regulski, M., & Tully, T. (1995). Molecular and biochemical characterization of dNOS: a *Drosophila* Ca²⁺/calmodulin-dependent nitric oxide synthase. *Proceedings of the National Academy of Sciences of the United States of America*, 92(20), 9072–9076. Retrieved from <http://www.ncbi.nlm.nih.gov/pubmed/7568075>
- Reyes-DelaTorre, A., Teresa, M., & Rafael, J. (2012). Carbohydrate Metabolism in *Drosophila*: Reliance on the Disaccharide Trehalose. In *Carbohydrates - Comprehensive Studies on Glycobiology and Glycotechnology*. InTech.
<https://doi.org/10.5772/50633>

- Rizki, T. M. (1978). The circulatory system and associated cells and tissues. In *The Genetics and Biology of Drosophila*, Vol 2B (ed. M. Ashburner and T. R. F. Wright), pp 397-452. London, New York: Academic Press.
- Rodriguez-Prados, J.-C., Traves, P. G., Cuenca, J., Rico, D., Aragones, J., Martin-Sanz, P., ... Bosca, L. (2010). Substrate Fate in Activated Macrophages: A Comparison between Innate, Classic, and Alternative Activation. *The Journal of Immunology*, *185*(1), 605–614. <https://doi.org/10.4049/jimmunol.0901698>
- Roote, J., & Prokop, A. (2013). How to Design a Genetic Mating Scheme: A Basic Training Package for Drosophila Genetics. *G3 & Genes/Genomes/Genetics*, *3*(2), 353–358. <https://doi.org/10.1534/g3.112.004820>
- Rosenthal, M. D., & Moore, F. A. (2015). Persistent inflammatory, immunosuppressed, catabolic syndrome (PICS): A new phenotype of multiple organ failure. *Journal of Advanced Nutritional and Human Metabolism*, *1*(1). <https://doi.org/10.14800/janhm.784>
- Rus, F., Flatt, T., Tong, M., Aggarwal, K., Okuda, K., Kleino, A., ... Silverman, N. (2013). Ecdysone triggered PGRP-LC expression controls Drosophila innate immunity. *The EMBO Journal*, *32*(11), 1626–1638. <https://doi.org/10.1038/emboj.2013.100>
- Sbarra, A. J., & Karnovsky, M. L. (1959). The biochemical basis of phagocytosis. I. Metabolic changes during the ingestion of particles by polymorphonuclear leukocytes. *The Journal of Biological Chemistry*, *234*(6), 1355–1362. Retrieved from <http://www.ncbi.nlm.nih.gov/pubmed/13654378>
- Semenza, G. L. (2014). Oxygen Sensing, Hypoxia-Inducible Factors, and Disease Pathophysiology. *Annual Review of Pathology: Mechanisms of Disease*, *9*(1), 47–71. <https://doi.org/10.1146/annurev-pathol-012513-104720>
- Semenza, G. L., Jiang, B. H., Leung, S. W., Passantino, R., Concordet, J. P., Maire, P., & Giallongo, A. (1996). Hypoxia response elements in the aldolase A, enolase 1, and lactate dehydrogenase A gene promoters contain essential binding sites for hypoxia-inducible factor 1. *The Journal of Biological Chemistry*, *271*(51), 32529–32537. Retrieved from <http://www.ncbi.nlm.nih.gov/pubmed/8955077>
- Sengupta, R., Sahoo, R., Mukherjee, S., Regulski, M., Tully, T., Stuehr, D. J., & Ghosh, S. (2003). Characterization of Drosophila nitric oxide synthase: a biochemical study. *Biochemical and Biophysical Research Communications*, *306*(2), 590–597. Retrieved from <http://www.ncbi.nlm.nih.gov/pubmed/12804606>
- Serbina, N. V., Jia, T., Hohl, T. M., & Pamer, E. G. (2008). Monocyte-Mediated Defense Against Microbial Pathogens. *Annual Review of Immunology*, *26*(1), 421–452. <https://doi.org/10.1146/annurev.immunol.26.021607.090326>
- Short, S. M., & Lazzaro, B. P. (2013). Reproductive Status Alters Transcriptomic Response to Infection in Female Drosophila melanogaster. *G3 & Genes/Genomes/Genetics*, *3*(5), 827–840. <https://doi.org/10.1534/g3.112.005306>
- Schulz, C., Perdiguero, E. G., Chorro, L., Szabo-Rogers, H., Cagnard, N., Kierdorf, K., ... Geissmann, F. (2012). A Lineage of Myeloid Cells Independent of Myb and Hematopoietic Stem Cells. *Science*, *336*(6077), 86–90. <https://doi.org/10.1126/science.1219179>

- Sigh, J., Lindenstrom, T., & Buchmann, K. (2004). The parasitic ciliate *Ichthyophthirius multifiliis* induces expression of immune relevant genes in rainbow trout, *Oncorhynchus mykiss* (Walbaum). *Journal of Fish Diseases*, 27(7), 409–417. <https://doi.org/10.1111/j.1365-2761.2004.00558.x>
- Sindrilaru, A., Peters, T., Wieschalka, S., Baican, C., Baican, A., Peter, H., ... Scharffetter-Kochanek, K. (2011). An unrestrained proinflammatory M1 macrophage population induced by iron impairs wound healing in humans and mice. *Journal of Clinical Investigation*, 121(3), 985–997. <https://doi.org/10.1172/JCI44490>
- Singer, M., Deutschman, C. S., Seymour, C. W., Shankar-Hari, M., Annane, D., Bauer, M., ... Angus, D. C. (2016). The Third International Consensus Definitions for Sepsis and Septic Shock (Sepsis-3). *JAMA*, 315(8), 801. <https://doi.org/10.1001/jama.2016.0287>
- Skugor, S., Glover, K., Nilsen, F., & Krasnov, A. (2008). Local and systemic gene expression responses of Atlantic salmon (*Salmo salar* L.) to infection with the salmon louse (*Lepeophtheirus salmonis*). *BMC Genomics*, 9(1), 498. <https://doi.org/10.1186/1471-2164-9-498>
- Sloth Andersen, A., Hertz Hansen, P., Schäffer, L., & Kristensen, C. (2000). A New Secreted Insect Protein Belonging to the Immunoglobulin Superfamily Binds Insulin and Related Peptides and Inhibits Their Activities. *Journal of Biological Chemistry*, 275(22), 16948–16953. <https://doi.org/10.1074/jbc.M001578200>
- Sokcevicova, H. (2017): The role of *Impl2* gene in the regulation of immune response to bacterial infection in *Drosophila melanogaster*. MSc. thesis, in Czech. University of South Bohemia in České Budějovice
- Straub, R. H. (2014). Insulin resistance, selfish brain, and selfish immune system: an evolutionarily positively selected program used in chronic inflammatory diseases. *Arthritis Research & Therapy*, 16 Suppl 2, S4. <https://doi.org/10.1186/ar4688>
- Straub, R. H., Cutolo, M., Buttgereit, F., & Pongratz, G. (2010). Review: Energy regulation and neuroendocrine-immune control in chronic inflammatory diseases. *Journal of Internal Medicine*, 267(6), 543–560. <https://doi.org/10.1111/j.1365-2796.2010.02218.x>
- Takeda, N., O’Dea, E. L., Doedens, A., Kim, J. -w., Weidemann, A., Stockmann, C., ... Johnson, R. S. (2010). Differential activation and antagonistic function of HIF-isoforms in macrophages are essential for NO homeostasis. *Genes & Development*, 24(5), 491–501. <https://doi.org/10.1101/gad.1881410>
- Takeuchi, O., & Akira, S. (2010). Pattern Recognition Receptors and Inflammation. *Cell*, 140(6), 805–820. <https://doi.org/10.1016/j.cell.2010.01.022>
- Tannahill, G. M., Curtis, A. M., Adamik, J., Palsson-McDermott, E. M., McGettrick, A. F., Goel, G., ... O’Neill, L. A. J. (2013). Succinate is an inflammatory signal that induces IL-1 β through HIF-1 α . *Nature*, 496(7444), 238–242. <https://doi.org/10.1038/nature11986>
- Taylor, P. R., & Gordon, S. (2003). Monocyte Heterogeneity and Innate Immunity. *Immunity*, 19(1), 2–4. [https://doi.org/10.1016/S1074-7613\(03\)00178-X](https://doi.org/10.1016/S1074-7613(03)00178-X)
- Thomas, A. C., & Mattila, J. T. (2014). “Of mice and men”: arginine metabolism in macrophages. *Frontiers in Immunology*, 5, 479. <https://doi.org/10.3389/fimmu.2014.00479>

- Thompson, C. B. (1995). New insights into V(D)J recombination and its role in the evolution of the immune system. *Immunity*, 3(5), 531–539. Retrieved from <http://www.ncbi.nlm.nih.gov/pubmed/7584143>
- Tsou, C.-L., Peters, W., Si, Y., Slaymaker, S., Aslanian, A. M., Weisberg, S. P., ... Charo, I. F. (2007). Critical roles for CCR2 and MCP-3 in monocyte mobilization from bone marrow and recruitment to inflammatory sites. *Journal of Clinical Investigation*, 117(4), 902–909. <https://doi.org/10.1172/JCI29919>
- Tzou, P., De Gregorio, E., & Lemaitre, B. (2002). How *Drosophila* combats microbial infection: a model to study innate immunity and host-pathogen interactions. *Current Opinion in Microbiology*, 5(1), 102–110. Retrieved from <http://www.ncbi.nlm.nih.gov/pubmed/11834378>
- Van De Bor, V., Zimniak, G., Papone, L., Cerezo, D., Malbouyres, M., Juan, T., ... Noselli, S. (2015). Companion Blood Cells Control Ovarian Stem Cell Niche Microenvironment and Homeostasis. *Cell Reports*, 13(3), 546–560. <https://doi.org/10.1016/j.celrep.2015.09.008>
- Vats, D., Mukundan, L., Odegaard, J. I., Zhang, L., Smith, K. L., Morel, C. R., ... Chawla, A. (2006). Oxidative metabolism and PGC-1 β attenuate macrophage-mediated inflammation. *Cell Metabolism*, 4(3), 255. <https://doi.org/10.1016/j.cmet.2006.08.006>
- Vlahos, R. (2014). Role of alveolar macrophages in chronic obstructive pulmonary disease. *Frontiers in Immunology*, 5. <https://doi.org/10.3389/fimmu.2014.00435>
- Wang, G. L., & Semenza, G. L. (1995). Purification and characterization of hypoxia-inducible factor 1. *The Journal of Biological Chemistry*, 270(3), 1230–1237. Retrieved from <http://www.ncbi.nlm.nih.gov/pubmed/7836384>
- Wang, N., Liang, H., & Zen, K. (2014). Molecular Mechanisms That Influence the Macrophage M1 \leftrightarrow M2 Polarization Balance. *Frontiers in Immunology*, 5. <https://doi.org/10.3389/fimmu.2014.00614>
- Warburg, O., Wind, F., & Negelein, E. (1927). THE METABOLISM OF TUMORS IN THE BODY. *The Journal of General Physiology*, 8(6), 519–530. Retrieved from <http://www.ncbi.nlm.nih.gov/pubmed/19872213>
- Weigert, A., & Brüne, B. (2008). Nitric oxide, apoptosis and macrophage polarization during tumor progression. *Nitric Oxide*, 19(2), 95–102. <https://doi.org/10.1016/j.niox.2008.04.021>
- Weinhouse, S. (1951). Studies on the fate of isotopically labeled metabolites in the oxidative metabolism of tumors. *Cancer Research*, 11(8), 585–591. Retrieved from <http://www.ncbi.nlm.nih.gov/pubmed/14859221>
- West, A. P., Brodsky, I. E., Rahner, C., Woo, D. K., Erdjument-Bromage, H., Tempst, P., ... Ghosh, S. (2011). TLR signalling augments macrophage bactericidal activity through mitochondrial ROS. *Nature*, 472(7344), 476–480. <https://doi.org/10.1038/nature09973>
- Westwell-Roper, C. Y., Ehses, J. A., & Verchere, C. B. (2014). Resident Macrophages Mediate Islet Amyloid Polypeptide-Induced Islet IL-1 β Production and β -Cell Dysfunction. *Diabetes*, 63(5), 1698–1711. <https://doi.org/10.2337/db13-0863>

- What is Hypoxia? How is it relevant to life sciences? *Antibodies, Kits, Proteins and Research Reagents: Novus Biologicals*. Retrieved April 07, 2018, from www.novusbio.com/support/hypoxia-and-hif-faqsF
- Wigglesworth, V. B. (1974). The Circulatory System and Associated Tissues. In *Insect Physiology* (pp. 33–45). Boston, MA: Springer US. https://doi.org/10.1007/978-1-4899-3202-0_3
- Wilson, H. M. (2014). SOCS Proteins in Macrophage Polarization and Function. *Frontiers in Immunology*, 5. <https://doi.org/10.3389/fimmu.2014.00357>
- Wingrove, J. A., & O'Farrell, P. H. (1999). Nitric Oxide Contributes to Behavioral, Cellular, and Developmental Responses to Low Oxygen in *Drosophila*. *Cell*, 98(1), 105–114. [https://doi.org/10.1016/S0092-8674\(00\)80610-8](https://doi.org/10.1016/S0092-8674(00)80610-8)
- Wolowczuk, I., Verwaerde, C., Viltart, O., Delanoye, A., Delacre, M., Pot, B., & Grangette, C. (2008). Feeding Our Immune System: Impact on Metabolism. *Clinical and Developmental Immunology*, 2008, 1–19. <https://doi.org/10.1155/2008/639803>
- Xue, J., Schmidt, S. V., Sander, J., Draffehn, A., Krebs, W., Quester, I., ... Schultze, J. L. (2014). Transcriptome-Based Network Analysis Reveals a Spectrum Model of Human Macrophage Activation. *Immunity*, 40(2), 274–288. <https://doi.org/10.1016/j.immuni.2014.01.006>
- Yona, S., Kim, K.-W., Wolf, Y., Mildner, A., Varol, D., Breker, M., ... Jung, S. (2013). Fate Mapping Reveals Origins and Dynamics of Monocytes and Tissue Macrophages under Homeostasis. *Immunity*, 38(1), 79–91. <https://doi.org/10.1016/j.immuni.2012.12.001>
- Zhu, L., Zhao, Q., Yang, T., Ding, W., & Zhao, Y. (2015). Cellular Metabolism and Macrophage Functional Polarization. *International Reviews of Immunology*, 34(1), 82–100. <https://doi.org/10.3109/08830185.2014.969421>
- Zimmermann, N., King, N. E., Laporte, J., Yang, M., Mishra, A., Pope, S. M., ... Rothenberg, M. E. (2003). Dissection of experimental asthma with DNA microarray analysis identifies arginase in asthma pathogenesis. *Journal of Clinical Investigation*, 111(12), 1863–1874. <https://doi.org/10.1172/JCI17912>